



Offshore Wind Turbines Situated in Areas with Strong Currents

Jensen, Morten S.; Juul Larsen, Brian; Frigaard, Peter; DeVos, Leen; Christensen, Erik D.; Asp Hansen, Erik; Solberg, Tron; Hjertager, Bjørn H.; Bove, Stefano

Publication date:
2006

Document Version
Publisher's PDF, also known as Version of record

[Link to publication from Aalborg University](#)

Citation for published version (APA):

Jensen, M. S., Juul Larsen, B., Frigaard, P., DeVos, L., Christensen, E. D., Asp Hansen, E., Solberg, T., Hjertager, B. H., & Bove, S. (2006). *Offshore Wind Turbines Situated in Areas with Strong Currents*. Offshore Center Denmark. <http://www.offshorecenter.dk/log/filer/6004RE01ER4.pdf>

General rights

Copyright and moral rights for the publications made accessible in the public portal are retained by the authors and/or other copyright owners and it is a condition of accessing publications that users recognise and abide by the legal requirements associated with these rights.

- Users may download and print one copy of any publication from the public portal for the purpose of private study or research.
- You may not further distribute the material or use it for any profit-making activity or commercial gain
- You may freely distribute the URL identifying the publication in the public portal -

Take down policy

If you believe that this document breaches copyright please contact us at vbn@aub.aau.dk providing details, and we will remove access to the work immediately and investigate your claim.



Offshore Center Denmark

Offshore Wind Turbines situated in Areas with Strong Currents

Report financed by

**Rambøll,
Aalborg Universitet,
Offshore Center Denmark**

Aalborg Universitet Esbjerg
and A2SEA

RAMBOLL

DHI
WATER & ENVIRONMENT

AALBORG UNIVERSITY



Vestas

A2SEA
Taking Windpower Offshore

Offshore Center Danmark
Offshore Wind Turbines situated in Areas with Strong Currents

DOC. NO. 6004RE01ER1

February 2006

TITLE : Offshore Wind Turbines situated in Areas with Strong Currents
Morten Sand Jensen, Rambøll
Brian Juul Larsen, Aalborg University
Peter Frigaard, Aalborg University
Leen De Vos, Aalborg University

AUTHORS : Erik D. Christensen, DHI - Water & Environment
Erik Asp Hansen, DHI - Water & Environment
Tron Solberg, Aalborg University Esbjerg
Bjørn H. Hjertager, Aalborg University Esbjerg
Stefano Bove, Aalborg University Esbjerg

SYNOPSIS : Prediction of local scour caused by offshore wind turbine foundations using empirical formulae or numerical models.

EDITOR : Morten Sand Jensen, RAMBØLL

CONTROLLED BY : Morten Holmager, Offshore Center Danmark

APPROVED BY : Peter Blach, Offshore Center Danmark

VERSION : REV. NO. DATE REMARKS

1	01-02-2006	
---	------------	--

DISTRIBUTION : Participants of conference, February 9th 2006

This is an unpublished work, the copyright of which vests by Offshore Center Danmark and the consortium participants. All rights reserved.

The information contained herein is the property of above parties and is supplied without liability for errors or omissions.

No part may be reproduced or used except as authorised by contract or other written permission.

Table of contents

1.	Introduction	4
1.1	Objective of the study	4
1.2	Project organisation	5
2.	Focus of the study	6
3.	Reporting of the study	7
REPORT 1 - Prediction of scour - recommendations		8
REPORT 2 - Review of monopile scour		23
REPORT 3 - Experimental study of scour around offshore wind turbines in areas with strong currents		79
REPORT 4 - Influence of breaking waves on scour processes around circular offshore wind turbine foundations		107
REPORT 5 - CFD modelling of scour around offshore wind turbines in areas with strong currents		127

1. Introduction

The wind farm industry has moved offshore and recently a number of large offshore wind farms have been built. A significant part of the costs developing these wind farms is related to the foundation of the structure. A large number of the foundations are based on a circular steel cylinder piled 20-30 m into the soil. Such a cylinder will hereafter be referred to as a monopile or simply a pile. Large erosion holes have been observed associated in relation to a monopile, especially a monopile located where there is a strong current as often is the case in estuaries and tidal plateaus. Scour is the engineering term for the erosion caused by water of the soil surrounding a coastal structure a pier, monopile or abutments and will hereafter be used. Such scour holes around a monopile can jeopardise the stability of the whole structure and will require deeper piling or local armouring of the seabed. Securing the bed is most often done by rock infill. Both methods are relative costly and therefore it is of great importance to predict the correct scour development for the given scenario.

All offshore work is in general associated with large cost therefore it is important to be able to predict the expected scour.

Considerable efforts have in the past been directed towards the study of scour in unidirectional flows, but the effects produced by tidal conditions have not previously been quantified. In present study there is a special focus on an offshore environment influenced by a significant dominating current due to tidal effects as such a scenario is common in present and future offshore wind farms. In addition, the effect of breaking waves is studied, as there seem to be uncertainty whether breaking waves can induce scour depths larger than a strong uniform current alone. Both tidal currents and breaking waves are reproduced in the hydraulic laboratory during this study in order to compare the results with existing equations for prediction of scour depths. Analytical methods as well as the capabilities of numerical methods are reviewed.

1.1. Objective of the study

The objective of this study is to summarize and provide latest knowledge and methods used in order to estimate local scour depths at monopiles located offshore. Furthermore, it is the aim to provide recommendations for prediction of the scour depth in a tidal environment.

1.2. Project organisation

The project is lead by Offshore Center Danmark (OCD) and financed by The Ministry of Science, Technology and Innovation with 1 million DKK. A significant part of the work is self-financed by the companies involved.

The companies involved are:

- Aalborg University (Aalborg and Esbjerg departments)
- Rambøll
- DHI - Water & Environment
- Vestas
- A2SEA

Aalborg University and DHI has significant experience in experimental testing in their hydraulic laboratories and numerous foundation designs with special focus on the scouring and protection of the foundations have been studied in their laboratories. Rambøll has provided the design of several offshore wind farms. Vestas are one of the leading wind turbine manufacturers in the world and are behind some of the largest established wind farms. A2SEA has been involved in the installation of several offshore wind farms.

The project ran from February 2004 until February 2006.

2. Focus of the study

Scour or erosion associated offshore structures is very complex and involves many parameters such as structure shape, hydraulic environment, type of soils etc. In order to limit the study it has been decided to focus on the parameters in order to reflect realistic present and future scenarios of offshore wind turbine farms. This focus is described in the following.

It is mentioned in the introduction that the stability of the monopile can be jeopardized if a large scour hole occur. This is correct, but there are other problems related to the scouring such as especially fatigue problems of the monopile. Changing the support of the pile changes the eigenfrequency of the structure. The eigenfrequency is again related to the endurance of the structure or the fatigue resistance of the structure. The band of the allowed eigenfrequency is very narrow for these monopile foundations and therefore it is very important to estimate the scour correctly.

The focus of the study will be on large, circular monopiles dominated by a tidal current system. A typical range of cylinders between 3 to 5 m seems to be the preferred size. The water depths are typical in the same order as the diameter of the monopile. Often there exist a significant tidal range, which creates strong currents. It is these currents alone, which are capable of creating scour holes. The presence of waves tends to minimize the scour holes. Also the effect of breaking waves and a combination of breaking waves and a strong current is included in present study.

Only scour in non-cohesive soils is considered. Scour around monopiles placed in cohesive soils can also become relative significant but the scouring process is closely related to the soil parameters. The development of scour in cohesive soils can take months or many years where scour in non-cohesive soils can happen within hours.

The study is focused on existing equations predicting scour depths. These equations are all empirical fitted to experimental data. All the equations will be evaluated and compared to prototype data as well as experimental data.

The scour phenomena around a monopile have in present study also been investigated with the use of numerical tools. DHI has tested the scour under breaking waves with their commercial model. Aalborg University (the department in Esbjerg) has tested the scour around a monopile in a steady current using a commercial Computational Fluid Dynamic program (CFD). The objective testing the numerical models is to study the capabilities of the state-of-art numerical tools. If such tools are found effective it can be used when alternative shapes (from circular) or structural details as J-tubes, ice cones or other appurtenances are introduced.

3. Reporting of the study

The study is reported by a number of independent reports. A brief description is given in the following.

REPORT 1 - Prediction of scour - recommendations

Candidate analytic equations are chosen and tested to available data. The objective is to provide recommendations for prediction of scour depth.

REPORT 2 - Review of monopile scour

This is a literature review regarding estimating local scour depths at wide monopiles located in shallow waters subject to significant current velocities.

REPORT 3 - Experimental study of scour around offshore wind turbines in areas with strong currents

The tests performed in the hydraulic laboratory are described and reported. The scour around a monopile is measured under different conditions. Important parameters are tested.

REPORT 4 - Influence of breaking waves on scour processes around circular offshore wind turbine foundations

This report includes an experimental study of scour processes in physical model as well as an experimental study using particle image velocimetry (PIV) technique and numerical modelling of bed velocities. The objective is to investigate the influence of breaking waves on scour processes around a monopile.

REPORT 5 - CFD modelling of scour around offshore wind turbines in areas with strong currents

This report covers computational fluid dynamic (CFD) modelling of scour around a monopile. The objective is to show the capabilities of the model. The commercial model FLUENT is used.

OFFSHORE WIND TURBINES SITUATED IN AREAS WITH STRONG CURRENTS

REPORT 1

Prediction of scour - recommendations

Author

Morten Sand Jensen, Rambøll

Work Group

Peter Frigaard, Aalborg University

Michael Høgedal, Vestas

Morten Sand Jensen, Rambøll

Table of contents

1.	Summary	10
2.	Introduction	11
3.	Candidate local scour formulae	12
4.	Experimental tests in the hydraulic laboratory	13
4.1	Description of the tests	13
4.2	Summary of test results	13
5.	Existing local scour data	15
6.	Evaluation of candidate scour formulae	16
7.	Recommendations for prediction of scour	16
8.	References	16

1. Summary

Four candidate formulae for the prediction of local scour around circular monopiles have been chosen. These formulae are the often-referred formulae by Breusers et al. (1977) and Sumer et al. (1992). Also, the more recent and more comprehensive formulae by Richardson & Davis "CSU/HEC-18/CEM" (2001) and Sheppard (2003) have been chosen.

In order to verify the candidate scour equations these have been tested against full-scale data as well as small-scale data. Because full-scale tests are without the influence of scale effects and other limitations the importance of these tests are significant.

The scale tests performed in the laboratory shows that it is difficult to verify a significant difference between scour developed in a uniform current compared to scour developed during tidal cycles.

The evaluation of the candidate equation shows that all formulae turns out to be useful with the exception of the formula proposed by Sheppard. The formula proposed by Breusers et al. is chosen as the recommended formula because the equation seems sounder than the CSU/HEC-18/CEM equation, especially at higher current velocities. The formula by Sumer may over predict the scour depths at shallow water depths, ie when the water depth is 1-2 times the pile diameter.

Breusers et al. proposed a formula using a coefficient $k=1.5$ (in design $k=2.0$). A best-fit estimate of k in the formulae by Breusers et al. equals 1.25 based on the Scroby Sands data and with a standard deviation of $\sigma_{S/D} = 0.2$. This is based on a statistically small number of 30 data. The members in present study propose to use Breusers's equation with the parameters $k=1.25$ and $\sigma_{S/D} = 0.2$ for the estimation of the maximum scour depth developed around circular monopiles in a strong tidal current (live-bed).

2. Introduction

There seem to be no dedicated formulae available for the prediction of the depth of local scour developed around a monopile situated in a strong tidal current and a relative shallow water depth with a high probability of breaking waves. Such a scenario is often the case in present and future offshore wind farm projects.

One objective with the present study was to establish the influence between local scour and breaking waves. Wave breaking will often be present when the water depth is relative shallow. It is later shown in Ref /5/ that wave breaking do not induce any significant scour. A strong current without the presence of waves will develop the largest scour around monopile structures.

Many formulae have been predicted for the estimation of local scour developed in a uniform current. In a tidal environment the change in current direction seem to influence the development of the scour hole depending on various parameters. It is still believed that the existing research based on a uniform current can be useful in the estimation of the scour depth with conditions as wide monopiles in a changing strong current. Therefore, a review has been performed in Ref /3/. The objective with the review was to identify candidate scour formulae for prediction of scour depth. The selection criterion has been formulations taking into consideration a small water depth compared with the pile diameter but also some of the most referred formulae in the literature have been chosen. It is anticipated that these formulae can also be used when a tidal current is present.

In order to evaluate the candidate formulae the equations are tested against full-scale measurements of scour. Especially important are the recent scour measurements obtained from 30 monopiles located in the Scroby Sands Wind Farm. Also, small-scale tests are included in the evaluation of the candidate scour formulae.

Candidate local scour formulae are presented in Section 3. Experimental scour data have been obtained in the hydraulic laboratory and are presented in Section 4. Existing full-scale measurements have recently been announced. These measurements are presented in Section 5. The evaluation in Section 6. of the candidate scour formulae is based on existing experimental data and full-scale data. Finally, a formula is recommended for the prediction of local scour depth in Section 7. References are given in Section 8.

3. Candidate local scour formulae

In Ref /3/ a number of candidate local scour formulae are presented. The formulae have been chosen as a combination of "often referred formulae" and "recent and comprehensive formulae". In Table 3-1 a summary of these formulae is given.

Author	Formulae for prediction of local scour depth
Breusers et al. (1977)	$\frac{S}{D} = 1.5 \tanh\left(\frac{h}{D}\right),$ (for design 1.5 shall be replaced with 2.0)
Sumer et al. (1992)	$\frac{S}{D} = 1.3, (for design \sigma_{S/D} = 0.7)$
Richardson & Davis "CSU/HEC-18/CEM" (2001)	$\frac{S}{D} = 2.2 \left(\frac{D}{h}\right)^{-0.35} Fr^{0.43}, (prepared for design)$
Sheppard (2003)	$\frac{S}{D} = K_s f_1(h, D) \left[2.2 \left(\frac{U - U_c}{U_{lp} - U_c} \right) + 2.5 f_3(D, d_{50}) \left(\frac{U_{lp} - U}{U_{lp} - U_c} \right) \right]$ (prepared for design)

Table 3-1: Candidate local scour formulae.

Originally, None of the equations are intended to be used in relation to scour in a tidal environment.

All equations are written with the assumption that the pile is circular. For a detailed description of all formulae see Ref /3/.

Only the CSU/HEC-18/CEM equation can be used for both clear-water scour and live-bed scour. The equation by Breusers et al. introduces a factor when clear-water scour is present. The equation by Sheppard is somewhat different for clear-water scour.

The CSU/HEC-18/CEM equation is written assumed that only smaller dunes are present (< 3m) and that the sediment size is smaller than 2 mm.

The formulae by Sheppard are not directly comparable with the other formulae because conservative factors are chosen giving somewhat conservative scour depths. The other formulae are all calibrated to give the most likely equilibrium scour depth. That said, a factor of 1.5 is assumed used in the case of the Breusers et al. formulae and likewise no standard deviation is included the Sumer et al. formula.

4. Experimental tests in the hydraulic laboratory

Experimental tests have been carried out at the hydraulic laboratories of Aalborg University. For a full description of the tests see Ref /4/. The main objective of the tests is to produce data regarding development of scour around monopiles. The data are to be tested by the candidate formulae described in Section 3. The environmental parameters used reflect a range of typical conditions at existing and planned offshore wind farms.

4.1. Description of the tests

Offshore wind farms are placed in areas with a relative shallow water depth. The mean water level is typically in the range 5-20 m. A strong tidal current is often encountered and a wind farm placed at shallow waters in combination with an aggressive tidal current is likely to experience breaking waves. After reviewing a number of existing and planned offshore wind farms the following prototype characteristics is simulated in the experimental tests:

Diameter of pile:	4-6 m
Water depth:	5-30 m
Environment:	A tidal system with and without waves
Tidal peak current:	1-2 m/sec (all in the live-bed regime).

The scale in the laboratory is 1:30 and the layout is shown in Figure 4-1. The scour is measured as the scour develops with a laser profiler.

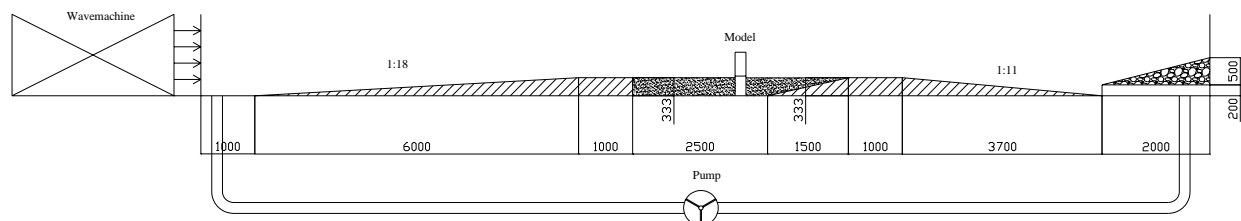


Figure 4-1: Experimental layout in the laboratory.

4.2. Summary of test results

The results obtained in tests with breaking waves are in details given in Ref /5/. It is shown that breaking waves has a small influence on the scour development.

In Figure 4-2 are the developments of scour for all tests depicted. Both a uniform current and a tidal current are represented in the tests. Tests including wave action are omitted. Two tests have been simulated for a longer time, ie test 2.11 (with tidal effects) and test 4.11 (uniform current). It is seen that test 2.11, which include tidal effects, seem to develop slightly more scour compared to test 4.11. It is observed that the development of scour seems to have not stabilized. This is because there is very slight global erosion present in the test area even though such effects has been minimised by placing sediment upstream the pile. The global scour is not simple to eliminate from the raw data and therefore it has not been attempted. It is furthermore acknowledged that there are scale effects

present in the study, especially the time scale and the characteristics of the simulation of the tidal effects has not been analysed in depth. It is still believed to be an important result that there seem to be no distinctive difference in the results between the tidal tests and the uniform tests. This is not comparable with the tests performed by Escarameia. Escarameia predicts that the depth of the scour holes is larger for a uniform flow than for a scenario with a tidal current regime.

It shall be noted that the results from the lowest velocity (0.3 m/s in the scale model) are not used in a later analysis of data because the scour holes for these test are most likely not fully developed.

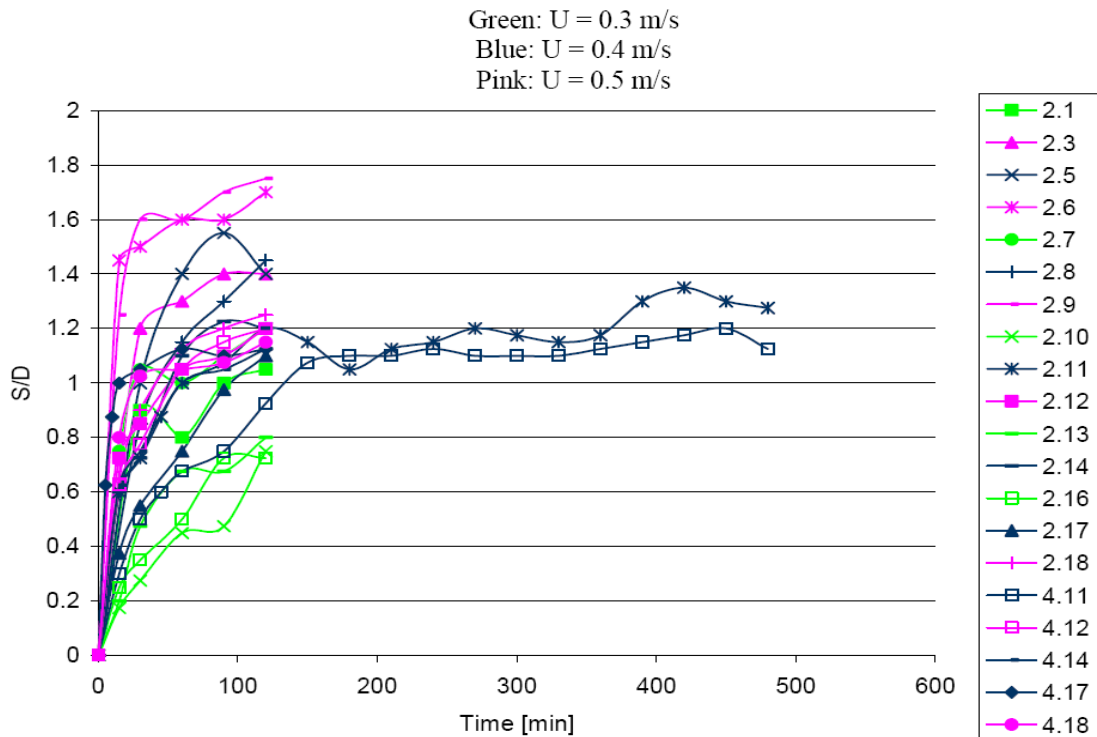


Figure 4-2: Development of scour in experimental tests at Aalborg University.

The results of the tests can be summarized as:

- Development of a useful set of data with varying parameters as the diameter of the pile, flow velocities and water depths.
- It is observed in the tests that breaking waves with or without a combination of a strong current could not produce scour holes even close to the scour developed when only a current is present.
- A comparison between developments of scour during a tidal current and a uniform current, respectively, indicates that the tidal current system produce marginally larger scour holes compared to a uniform current.

5. Existing local scour data

An overview of existing data available is given in Table 5-1. A more detailed description of the data is given in Ref /3/.

Origin of data	Year	Scale	Pile Diameter [m]	Environment
Scroby Sands Norfolk, UK	2004	Prototype	4.2	Tidal currents and waves (live-bed)
Ozumer Balje Tidal inlet	2003	Prototype	1.5	Tidal currents and waves (live-bed)
OCD (Denmark)	2005	Flume	0.1-0.2	Tidal and unidirectional currents (live-bed)
Escameia (UK)	1998	Flume	0.075	Tidal and unidirectional currents (clear-water scour)
Sheppard (New Zealand)	2002	Flume	0.15	Unidirectional currents (live-bed)

Table 5-1: Overview of existing local scour measurements.

It is important to assure that the data are comparable. The scour measured at Scroby Sand is assumed to be equilibrium scour depths. Also the scour reported at Ozumer Balje is expected to be equilibrium scour. All the flume test results are also given as equilibrium scour depths. It is noted that data given by Sheppard is based on unidirectional tests and the data given by Escameia is given in the case of clear-water scour, but close to the live-bed regime (the candidate formulae are only chosen for live-bed scour). It should also be mentioned that the test program performed by Sheppard included many tests with a very high current velocity, in some cases more than 2 m/s, which yield a Froude number higher than 1.0.

6. Evaluation of candidate scour formulae

In Figure 6-1 the candidate formulae from Table 3-1 is tested against the prototype data from Scroby Sands.

The parameters used in the various equations are given in Table 6-1.

Parameters	Size
Water depth after Mean Still Water Level	Varying (x-axis)
Pile diameter	4.2 m
Current velocity (depth averaged)	1.5 m/s
Mean grain size, d_{50}	0.2625 mm

Table 6-1: Scroby Sand parameters.

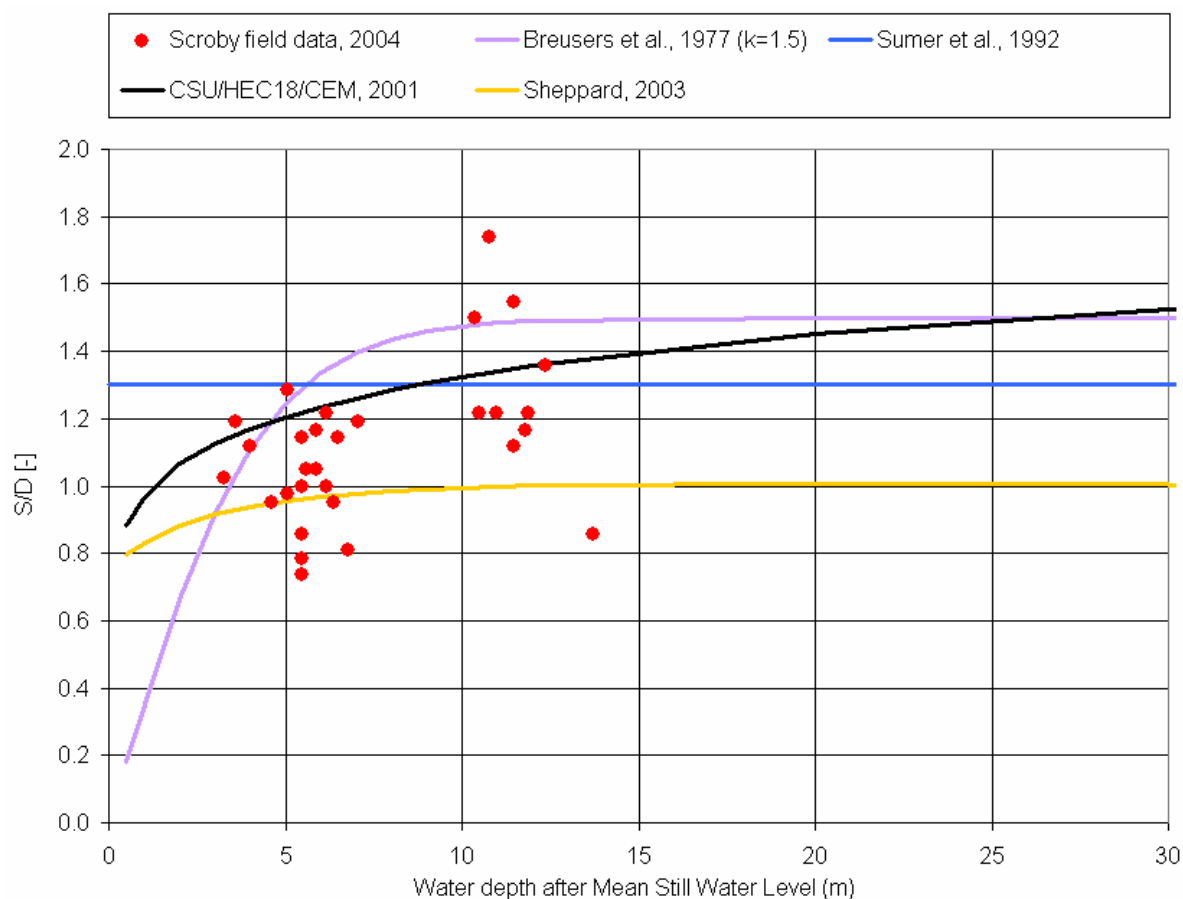


Figure 6-1: Predictive equations compared to prototype data from Scroby.

The monopiles at Scroby Sands are all located at water depths that are relative shallow. The ratio of water depth over pile diameter is between 1-3. It is clear from Figure 6-1 that the monopiles with a water depth over pile diameter ratio of 3 experiences deeper scour than the monopiles with a water depth over pile diameter ratio of 1 to 2.

The CSU/HEC-18/CEM formulae correlate well with the Scroby data. The concern with the CSU/HEC-18/CEM formulae is that the scour depth continues to develop for increasing water depths (this is why a water depth of 30 m is included in the graph). Care shall be taken when using the CSU/HEC-18/CEM formulae for very large water depths.

The formulae by Sumer et al. seems quite reasonable. The prediction of maximum scour at a ratio of 2.0 might in this case be too high, especially when the water depth over pile diameter ratio is below 2.

The formulae by Breusers et al. also correlates well with the Scroby data. Using $k=1.5$ an upper envelope seem to be reached. The equation does not have the same problem as the CSU/HEC-18/CEM regarding increasing water depths.

The equation given by **Sheppard** seems to under-predicts the scour depths. The reason is given in Figure 6-2. The graph illustrates, in this case for a specific condition, how the scour depth decreases significantly when the ratio of D/d_{50} increases above 46. The ratio of D/d_{50} in the case of Scroby Sands is 16,000. Apparently, the assumption regarding the dependency of D/d_{50} is not the case at Scroby Sands. The trend of the curve is similar to that of Breusers et al. because the hyperbolic tangent function is also present in the formulae proposed by Sheppard.

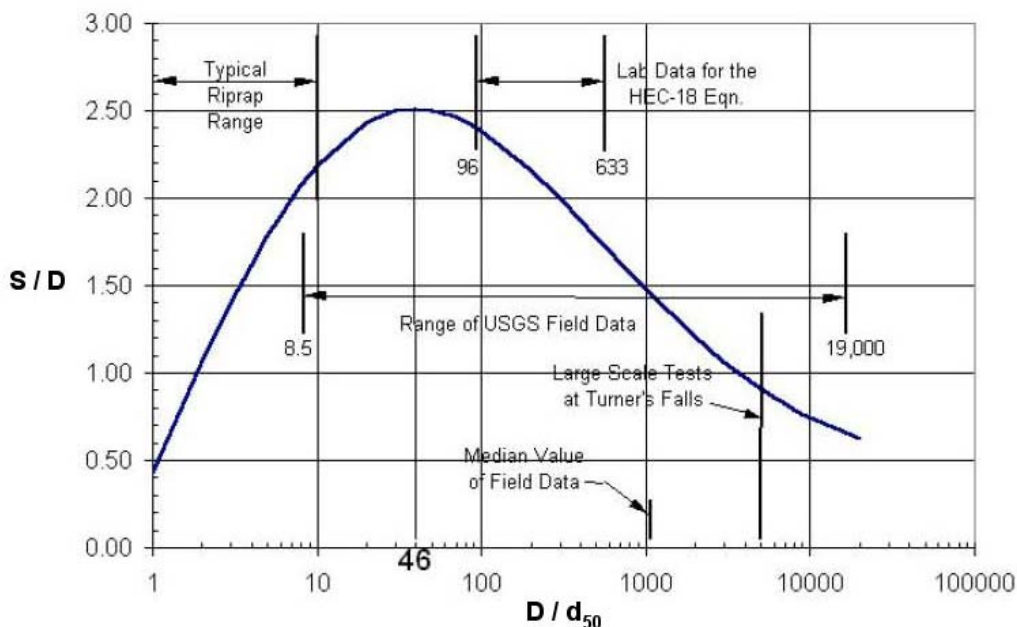


Figure 6-2: Dependence of normalised scour depth on D/d_{50} for a circular pile. For the curve shown $U/U_c=1$, and $h/D > 2$ (Ref /1).

In the following all existing data available as shown in Table 5-1 are used to further test the candidate formulae.

In Figure 6-3 the formulae by Breusers et al. is compared to all existing data. As seen before the formulae provide an upper envelope of the prototype data from Scroby Sand. The measurements at Otzumer and the data obtained under the present study (OCD data) are predicted well. The data provided by Sheppard is under-estimated.

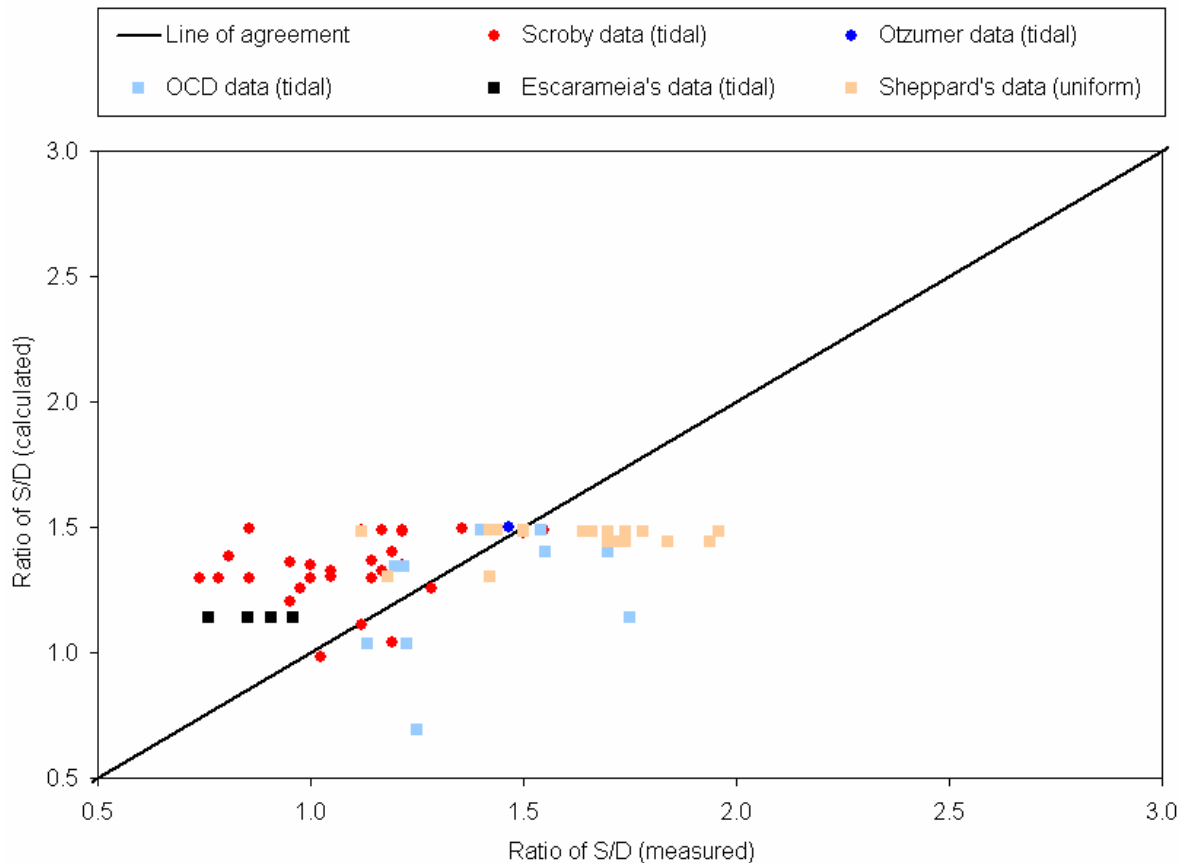


Figure 6-3: Existing data tested with Breusers et al. formulae ($k=1.5$).

In Figure 6-4 is the CSU/HEC-18/CEM formulae compared to existing data. As seen before the equation correlates well with the prototype data. Also the OCD data seem to correlate well. The data provided by Sheppard is overestimated by the equation and this can be said regarding the Escarameia data as well. The CSU/HEC-18/CEM formulae gives increasing scour depth as the velocity increases. The tests performed by Sheppard were performed under extreme velocities (up to 2 m/s in the laboratory) and this is why the CSU/HEC-18/CEM formulae over-estimate the Sheppard data. The results indicate that care should be taken using the CSU/HEC-18/CEM formulae when the flow velocities are very high, as it is believed that the scour depth should stabilize even for increasing velocities.

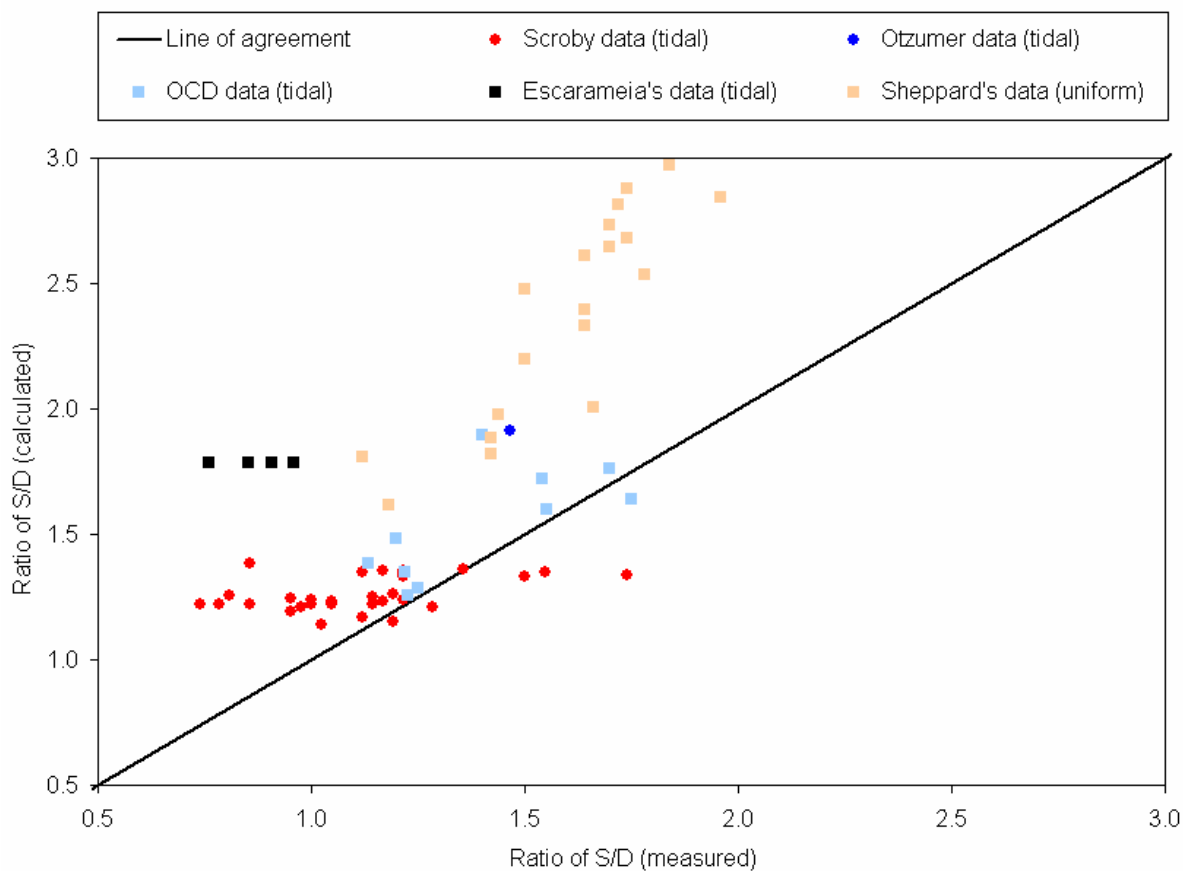


Figure 6-4: Existing data tested with the CSU/HEC-18/CEM formulae.

In Figure 6-5 is the formulae provided by Sheppard compared to existing data. As seen in Figure 6-1 the equation correlates not well with the prototype data from Scroby Sands because the formulae under-predicts the local scour depths. The OCD tests seem to correlate well. The data given by Escameia are not shown, as the chosen formulae by Sheppard are dedicated live-bed scour. As the formula is fitted to the data from Sheppard a reasonably correlation is expected. Sheppard's formulae give design values and are calibrated conservatively. This is why Sheppard's formulae over-predict the test results.

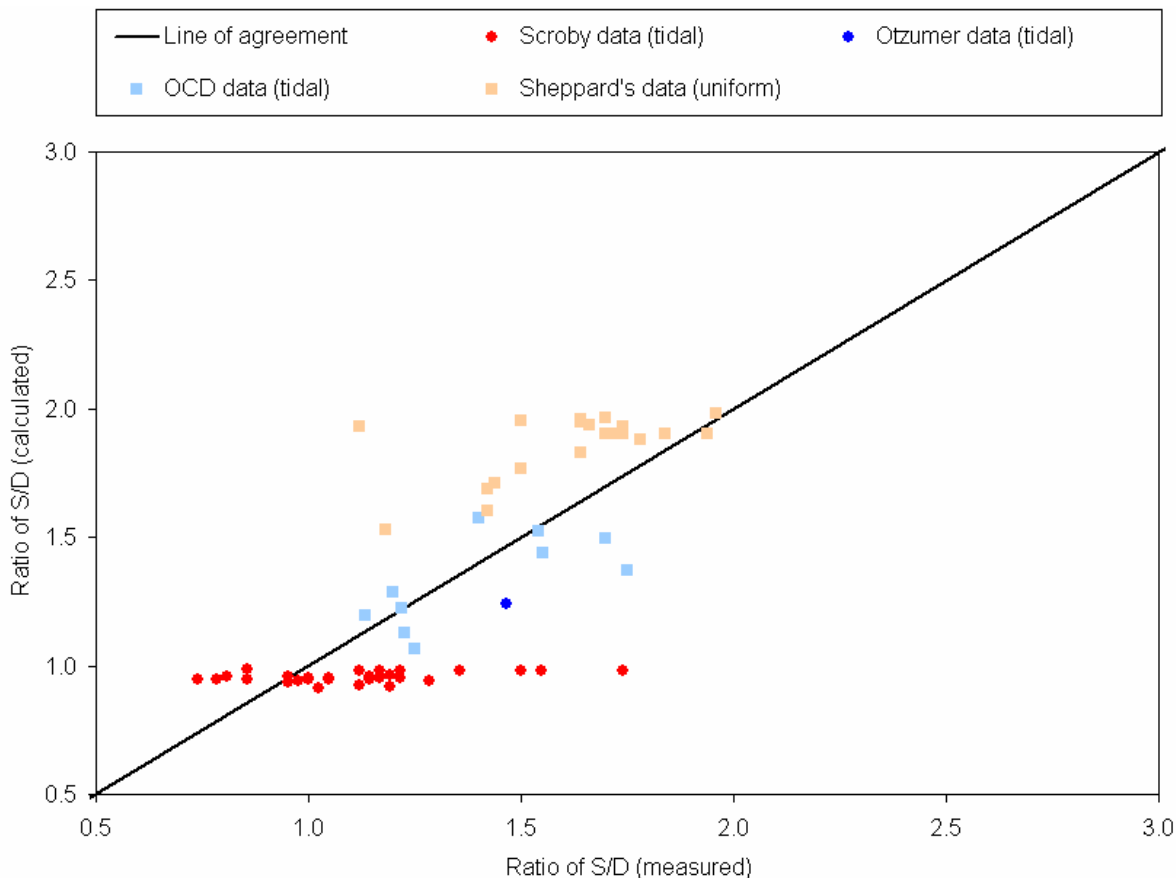


Figure 6-5: Existing data tested with Sheppard's formulae.

7. Recommendations for prediction of scour

The formulae by Breusers et al. are recommended for prediction of local scour for piles located in a tidal environment. The equation is simple and the hyperbolic tangent function seems to reflect the pile width relationship well. For slender piles, $h/D > 1$, the hyperbolic tangent of h/D approaches 1, and the scour depth can be found as $S \approx k \cdot D$. For wide piles, $h/D < 1$, the hyperbolic tangent of h/D approaches h/D and the scour depth can be found as $S \approx k \cdot h$.

A best-fit estimate of k in the equation by Breusers et al. equals 1.25 based on the Scroby Sands data. The standard deviation is 0.2. It is recognized that statistically a number of 30 data is small. The members in present study finally propose this formula. The formula is illustrated in Figure 7-1 and given as:

$$\text{OCD, 2006} \quad \frac{S}{D} = 1.25 \tanh\left(\frac{h}{D}\right), \quad (\sigma_{S/D} = 0.2)$$

As sparse data are available for a small ratios of water depth and pile diameter the proposed equation should not be used when h/D is below 1. This implies that the maximum equilibrium scour depth shall never be taken less than 0.95 D.

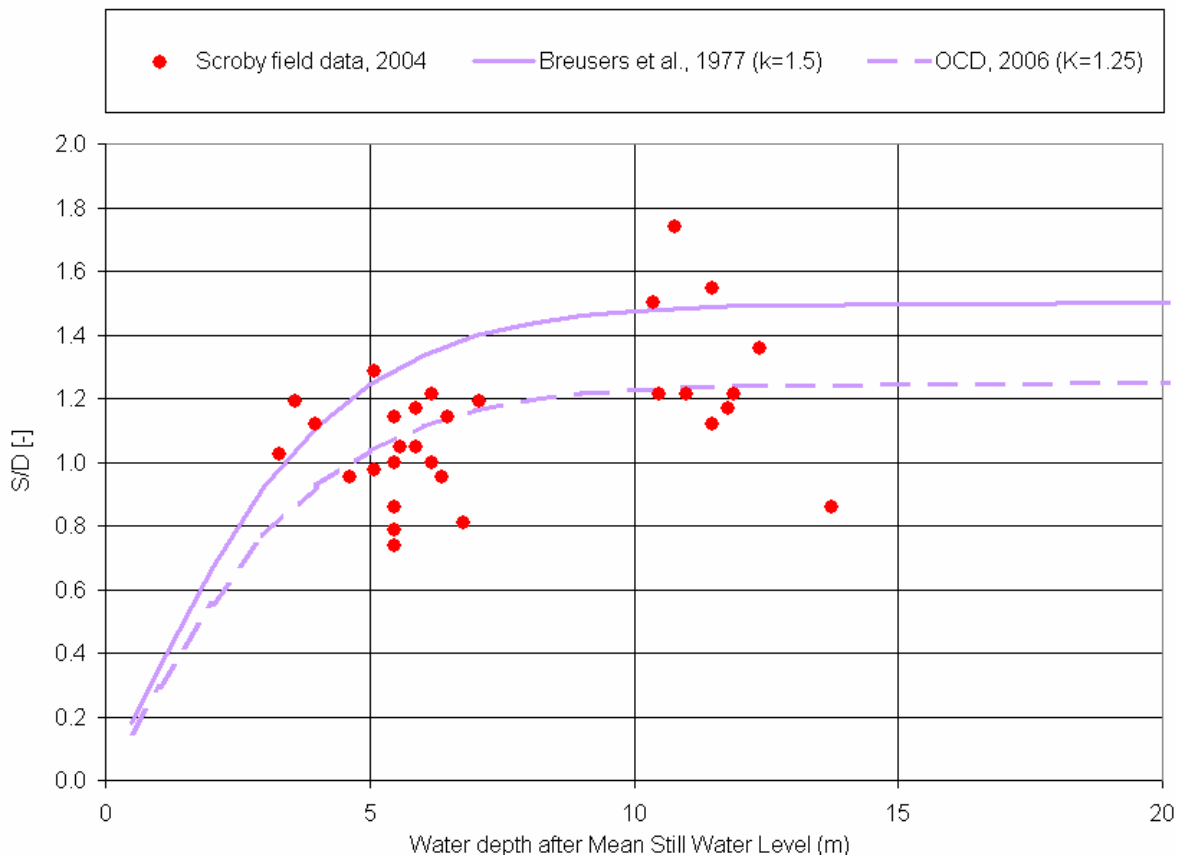


Figure 7-1: Proposed local scour formulae.

8. References

- Ref /1/ Breusers, H., Nicollett, G. & Shen, H. (1977). Local scour at cylindrical piers. *Journal of Hydraulic Research*, 15, 211-252.
- Ref /2/ Jones, J.S. & Sheppard, D.M. (2000). Scour at wide bridge piers. ASCE, US Department of Transportation, Federal Highway Administration, Turner-Fairbank Highway Research Center, 10 pp.
- Ref /3/ Offshore Center Danmark. Review of monopile scour, (2006). Report 2. "Offshore Wind Turbines Situated in Areas with Strong Currents". Offshore Center Danmark (OCD).
- Ref /4/ Offshore Center Danmark. Experimental study of scour around offshore wind turbines in areas with strong currents, (2006). Report 3. "Offshore Wind Turbines Situated in Areas with Strong Currents". Offshore Center Danmark (OCD).
- Ref /5/ Offshore Center Danmark. Influence of breaking waves on scour processes around circular offshore wind turbine foundations, (2006). Report 4. "Offshore Wind Turbines Situated in Areas with Strong Currents". Offshore Center Danmark (OCD).
- Ref /6/ Richardson, E.V and S.R. Davis (2001). HEC-18. Evaluating scour at Bridges. *Hydraulic Engineering Circular No. 18*. Fourth edition. National Highway Institute, Federal Highway Administration, U.S. Dept. of Transportation.
- Ref /7/ Sheppard, D.M. (2003) Large scale and live bed local pier scour experiments, phase 2, live bed experiments, final report, University of Florida.
- Ref /8/ Sumer, B., Fredsoe, J., Christiansen, N (1992). Scour around vertical piles in waves. *Journal of waterway, Port, Coastal and Ocean engineering*, 118(1), 15-31.

OFFSHORE WIND TURBINES SITUATED IN AREAS WITH STRONG CURRENTS

REPORT 2

Review of monopile scour

Author

Morten Sand Jensen, Rambøll

Work Group

Morten Sand Jensen, Rambøll

Erik Asp Hansen, DHI - Water & Environment (Local scour in Waves)

Table of contents

1.	Summary	25
2.	Introduction	26
3.	Concept of scour	27
3.1.	Clear-water scour and live-bed scour	27
3.2.	Local Scour	28
4.	Local scour equations	31
5.	Candidate local scour equations	34
5.1.	Background	34
5.1.1.	CSU/HEC-18 pile scour equation	35
5.1.2.	Johnson's adjustment (1999)	38
5.1.3.	Richard May (1998)	38
5.1.4.	Breusers et al. (1977)	39
5.1.5.	Sumer et al.	40
5.1.6.	Predictive equations developed by Sheppard (2000)	40
5.1.7.	Predictive equations developed by Sheppard after live-bed tests (2003)	44
6.	Tidal flows influence on local scour	48
7.	Experimental tidal scour studies	54
7.1.	Escameia's study	55
7.2.	Test results from Escameia's study	56
8.	Field studies of monopile scour in a tidal flow	61
8.1.	Otzumer Balje tidal inlet	61
8.2.	Scroby Sands Offshore Wind Farm	62
9.	Local scour in waves	64
9.1.	Equilibrium scour in waves	64
9.2.	Equilibrium scour in combined waves and currents	65
9.3.	Equilibrium scour in breaking waves	67
10.	Specifications of experimental tests	69
11.	Glossary	70
12.	References	74
	Attachment A – A case study	78

1. Summary

The literature review has found numerous studies concentrated on local scour applicable for wide piles subjected to strong currents. Some of these are described in more details.

Well-established and convincing empirical equations seem to be available to predict scour for a wide pile subject to a strong unidirectional current. This seems not to be the case regarding a pile subject to a tidal flow environment. Few documented studies are reported. The most recent and comprehensive study is reported by Escarameia and supported by experimental tests. Escarameia predicts, based on few tests, which do not cover a broad range of parameters (as water depth to pile diameter), that the reversal of the flow during the tidal cycle will produce equilibrium scour depths that are smaller than those achieved in purely unidirectional flows.

Several well-documented studies are described in this review. In the Oetzumer Balje tidal inlet a 1.5 m wide pile is located. Most important data are 30 installed monopiles at Scroby Sands with a diameter of 4.2 m. These foundations are situated in a tidal environment with strong currents.

Bijker et al. reports that breaking waves causes even bigger scour holes around a pile compared with a strong current alone. A discussion is given, as Bijker's results are believed to appear due to other processes than local scour.

Finally, a recommended agenda is proposed regarding the forthcoming tests to be performed in the hydraulic laboratory at Aalborg University.

2. Introduction

Present report is a literature review regarding estimating local scour depths at wide monopiles located in shallow waters subject to significant current velocities. The latest development on the subject is given in detail. It is the objective with this review to identify candidate predictive equations and prepare forthcoming tests in a best possible way by including the most recent research.

It is decided under the research project "Offshore Wind Turbines situated in Areas with Strong Currents" to perform laboratory tests with the focus on evaluating the scour development induced by a monopile (in the following referred to as a pile). The purpose and objective of these tests are given earlier in a memo describing the experimental tests and their objective, see Ref /37/.

The tests will be performed in the range of parameters valid for piles used in present and planned offshore wind farm parks. Existing piles are placed near-shore and therefore characterised by shallow water conditions, often influenced with strong tidal currents and breaking waves. The diameter of the pile is often large compared with the water depth.

The focus of the review will be on large, circular piles dominated by a tidal current system. Of interest are the most referred formulae, laboratory tests and information of prototype observations.

In Section 3 is given a brief introduction to the concept of scour and parameters, which affect the magnitude of local scour depth at piles. Section 4 deals with a general overview of scour research and the most referred formulae for prediction local scour are given. Important and recent research on local scour in unidirectional current is given in detail in Section 5 with special focus on wide piles in shallow water. Tidal flows influence on local scour are in general described in Section 6. Section 7 includes research taking into account a changing current environment (tidal environment). Available field studies are described in Section 8. Scour caused by waves is briefly mentioned in Section 9. Section 10 deals with the objectives and specifications regarding future laboratory tests to be performed at the University of Aalborg.

A glossary list is given in Section 11 and references are listed in Section 12.

3. Concept of scour

In the following, a short introduction to the concept of scour is given. Attention is given to local scour associated with circular piles. Important conditions as clear-water scour and live-bed scour are described. Influence of various parameters are briefly discusses.

3.1. Clear-water scour and live-bed scour

Clear-water scour occurs when there is no movement of the bed material in the flow upstream of the pile or the bed material is transported in suspension through the scour hole at the pile at less than the capacity of the flow. At the pile the acceleration of the flow and vortices created by the obstruction of the pile causes the bed material to move. Live-bed scour occurs when there is transport of bed material upstream the pile. Live-bed local scour is cyclic in nature.

During a flood event, bridges over streams with coarse-bed material are often subjected to clear-water scour at low discharges, live-bed scour at the higher discharges and then clear-water scour at the lower discharges on the falling stages. Clear-water scour reaches its maximum over a longer period of time than that of live-bed scour, see Figure 3-1. Maximum local clear-water pile scour is about 10 % greater than the equilibrium local live-bed pile scour.

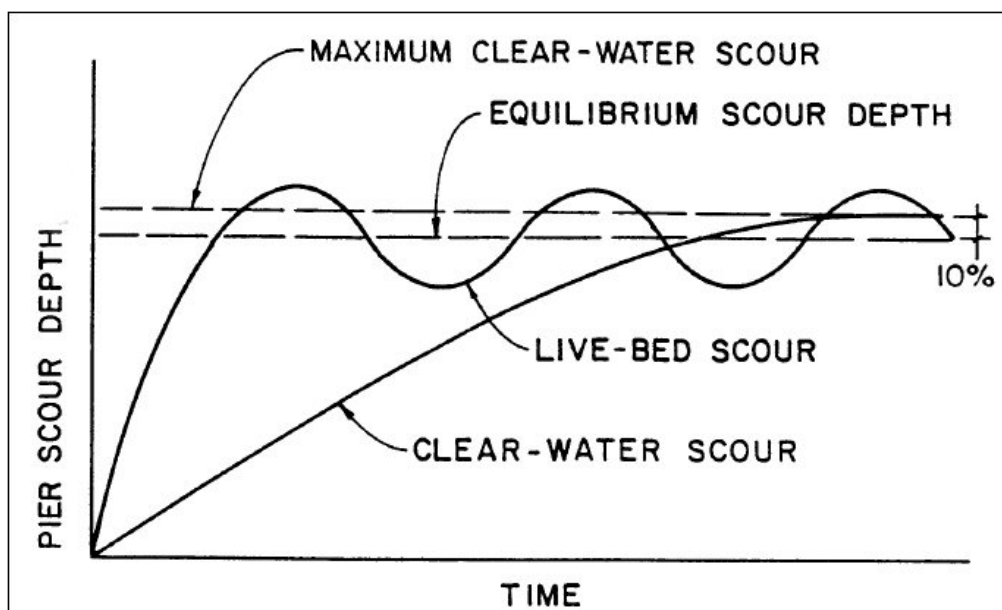


Figure 3-1: Pile scour depth in a sand-bed stream as a function of time.

Critical velocity equations with the reference particle size d_{50} are used to determine the velocity associated with the initiation of motion. They are used as an indicator for clear-water or live-bed scour conditions. If the mean velocity U upstream the pile is equal to or less than the critical velocity U_c of the median diameter d_{50} of the bed material, then local scour will be clear-water scour. Also, if the ratio of the shear velocity of the flow to the fall velocity of the d_{50} of the bed material is greater than 2, local scour may be clear-water. If the mean velocity is greater than the

critical velocity of the median bed material size, live-bed scour will occur. Several equations are derived to determine the critical velocity for a given flow depth and size of bed material. One of these is given in Section 5.1.1.

Live-bed pile scour in sand-bed streams with a dune bed configuration fluctuates around the equilibrium scour depth, see also see Figure 3-1. This is due to the variability of the bed material sediment transported in the approach flow when the bed configuration of the stream is dunes. In this case (dune bed configuration in the channel upstream), maximum depth of pile scour is about 30 % larger than the equilibrium depth of scour. For general practice, the maximum depth of pile scour is approximately 10 % greater than the equilibrium scour.

3.2. Local Scour

The basic mechanism causing local scour at piles is the formation of vortices (known as horseshoe vortex) at their base.

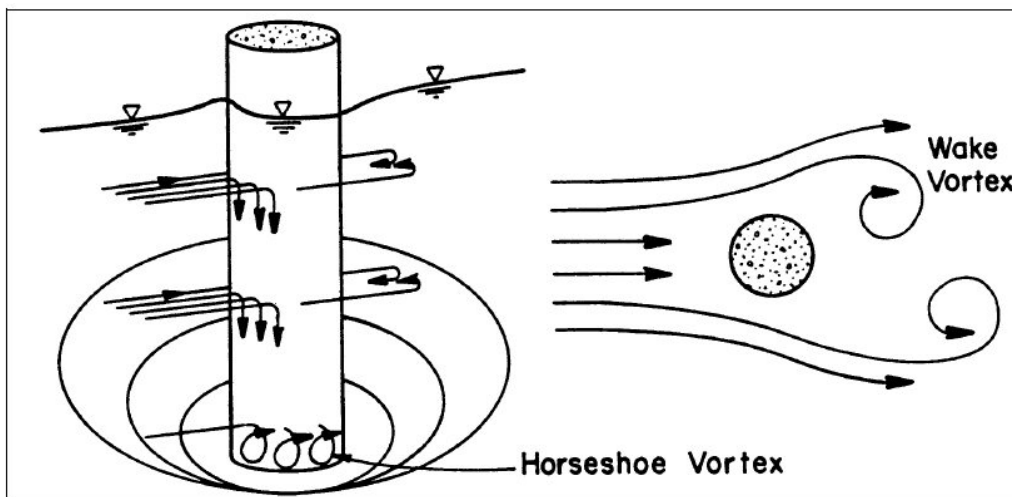


Figure 3-2: Schematic representation of scour at a cylindrical pile.

The horseshoe vortex results from the pile up of water on the upstream surface of the obstruction and subsequent acceleration of the flow around the nose of the pile. The action of the vortex removes bed material from around the base of the obstruction. The transport rate of sediment away from the base region is greater than the transport rate into the region, and, consequently, a scour hole develops. As the depth of scour increases, the strength of the horseshoe vortex is reduced, thereby reducing the transport rate from the base region. Eventually, for live-bed local scour, equilibrium is re-established between bed material inflow and outflow and scouring ceases. For clear-water scour, scouring ceases when the shear stress caused by the horseshoe vortex equals the critical shear stress of the sediment particles at the bottom of the scour hole. In addition to the horseshoe vortex around the base of a pile, there are vertical vortices downstream of the pile called wake vortex. Both the horseshoe and wake vortices remove material from the pile base region. However, the intensity of wake vortices diminishes rapidly as the distance downstream of the pile increases. Therefore, immediately downstream of a long pile there is often deposit of material. Factors that affect the magnitude of local scour depth at piles are:

- (1) Flow velocity.
- (2) Water depth.
- (3) Width of the pile.
- (4) Length of the pile if skewed to flow.
- (5) Size and gradation of bed material.
- (6) Shape of the pile (here circular).
- (7) Bed configuration.
- (8) Marine growth, ice formation or jams and debris.

Ad 1) Flow velocity affects local scour depth. The greater the velocity, the deeper the scour. There is a high probability that scour is affected by whether the flow is subcritical or supercritical. However, most research and data are for subcritical flow (ie flow with a Froude Number less than 1.0, $Fr < 1$).

Ad 2) Flow depth or water depth also has an influence on the depth of local scour. An increase in water depth can increase scour depth by a factor of 2 or greater for piles.

Ad 3) Pile width has a direct influence on depth of local scour. As pile width increases, there is an increase in scour depth. There is a limit to the increase in scour depth as width increases. Very wide piles do not have scour depths as deep as predicted by existing equations.

Ad 4) Pile length has no appreciable effect on local scour depth as long as the pile is aligned with the flow. When the pile is skewed to the flow, the pile length has a significant influence on scour depth. For example, doubling the length of the pile increases scour depth from 30 to 60 % (depending on the angle of attack), Ref /42/.

Ad 5) Bed material characteristics such as size, gradation and cohesion can affect local scour. Bed material in the sand-size range has little effect on local scour depth. Likewise, larger size bed material that can be moved by the flow or by the vortices and turbulence created by the pile or abutment will not affect the maximum scour, but only the time it takes to attain it. Very large particles in the bed material, such as coarse gravel, cobbles or boulders, may armour the scour hole.

It is later described that the sediment size actually matters when scaling experimental test data to prototype data, especially when the pile is wide (compared to the water depth).

Flume experiments have shown that for Froude Numbers less than 1.0 ($Fr < 1.0$), and a range of bed material sizes, that when the upstream velocity of the flow is less than the critical velocity of the d_{90} size of the bed material, the d_{90} size will decrease the scour depth, Ref /20/. The size of the bed material also determines whether the scour at a pile is clear-water or live-bed scour.

Fine bed material (silt and clay) will have scour depths as deep as sand-bed streams, Ref /42/. This is true even if bonded together by cohesion. The effect of cohesion is to influence the time it takes to reach maximum scour. With sand-bed material the time to reach maximum depth of scour is measured in hours and can result from a single event. With cohesive bed materials, it may take much longer to reach the maximum scour depth.

Ad 6) The shape of a pile can have up to a 20 % influence on scour depth. Streamlining the front end of a pile reduces the strength of the horseshoe vortex, thereby reducing scour depth. Streamlining the downstream end of piles also reduces the strength of the wake vortices. A square pile will have maximum scour depths about 20 % greater than a sharp-edged pile and 10 % greater than a cylindrical pile, Ref /42/.

Ad 7) Bed configuration of sand-bed channels affects the magnitude of local scour. In streams with sand-bed material, the shape of the bed (bed configuration) may be ripples, dunes, plane bed or antidunes. The bed configuration depends on the size distribution of the sand-bed material, hydraulic characteristics and fluid viscosity. The bed configuration may change from dunes to plane bed or antidunes during an increase in flow for a single flood event. It may change back with a decrease in flow. The bed configuration may also change with a change in water temperature or suspended sediment concentration of silt and clay. The type of bed configuration and change in bed configuration will affect flow velocity, sediment transport and scour. Hydraulic Series No. 6 discusses bed configuration in detail, Ref /41/.

Ad 8) Potentially, ice, marine growth and debris can increase the width and shape of the pile. This will increase the scour. The magnitude of the increase is still largely undetermined. Marine growth can be taken into account by increasing the pile diameter because marine growth is normally uniform. Debris can also be taken into account in the scour equations by estimating how much the debris will increase the width of a pile.

4. Local scour equations

Local scour has been studied extensively in both unidirectional (river or flume) and oscillatory (wave or wave tank) water movement. Studies have mainly been focused towards bridge piers. Detailed studies on the mechanism of scour bridge piers were made amongst others by Laursen and Toch 1956 (Ref /25/), Shen et al. 1969 (Ref /43/), Nakagawa and Suzuki 1975 (Ref /32/), Hjorth 1975 (Ref /14/), Melville 1975 (Ref /27/), Ettema 1980 (Ref /11/), Qadar 1981 (Ref /35/), Baker 1981 (Ref /2/), Raudkivi and Ettema 1983 (Ref /38/), Chiew and Melville 1987, (Ref /8/), Raudkivi 1988 (Ref /39/), Kothyari et al. 1992a (Ref /22/), Hoffmans & Verheij 1997 (Ref /15/), Ahmad and Rajaratnam 1998 (Ref /1/), Graf and Yulistiyanto 1998 (Ref /12/), Whitehouse 1998 (Ref /52/), Melville & Coleman 2000 (Ref /29/); Sumer et al. 2001(Ref /49/) and Sumer et al. 2002 (Ref /50/).

A list of referred equations for estimation of scour depth is listed in Table 4-1.

Author	Year	Formula	Ref.	Eq.
Laursen & Toch	1956	$\frac{S}{D} = 1.5 \left(\frac{h}{D} \right)^{0.3}$	Ref /25/	(1)
Laursen	1963	$\frac{S}{D} = 1.34 \left(\frac{h}{D} \right)^{0.5}$	Ref /26/	(2)
Shen et al.	1969	$\frac{S}{D} = 3.4 \left(\frac{U_c}{\sqrt{gD}} \right)^{0.66}$	Ref /43/	(3)
Coleman	1971	$\frac{S}{D} = 0.54 \left(\frac{h}{D} \right)^{0.19} \left(\frac{U_c}{\sqrt{gh}} \right)^{1.19} h^{0.41}$	Ref /29/	(4)
Hancu	1971	$\frac{S}{D} = 3.3 \left(\frac{d}{D} \right)^{0.2} \left(\frac{h}{D} \right)^{0.13}$	Ref /13/	(5)
Breusers et al.	1977	$\frac{S}{D} = f_1 \left[k \tanh \left(\frac{h}{D} \right) \right] f_2 f_3$	Ref /4/	(6)
Qadar	1981	$\frac{S}{D} = 1.33 D^{-0.36}$	Ref /35/	(7)
Jain	1981	$\frac{S}{D} = 1.84 \left(\frac{h}{D} \right)^{0.3} \left(\frac{U_c}{\sqrt{gh}} \right)^{0.25}$	Ref /17/	(8)
Sumer et al.	1992	$\frac{S}{D} = 1.3$	Ref /50/	(9)
Ansari & Qadar	1994	$\frac{S}{D} = 3.6 D^{-0.6} (D > 2.2m)$	Ref /36/	(10)
Melville & Coleman	2000	$\frac{S}{D} = \frac{K_{hd} K_l K_d K_s K_\theta}{D}$	Ref /29/	(11)

Author	Year	Formula	Ref.	Eq.
Jones & Sheppard	2000	$\frac{S}{D} = c_2 \left(\frac{U_{lp} - U}{U_c} \right) + c_3$ (Clear water scour)	Ref /21/	(12)
Richardson & Davis (HEC-18, fourth edition)	2001	$\frac{S}{D} = 2.0 K_1 K_2 K_3 K_4 \left(\frac{D}{h} \right)^{-0.35} Fr^{0.43}$	Ref /42/	(13)
Sheppard	2003	$\frac{S}{D} = K_s f_1(h, D) \left[2.2 \left(\frac{U - U_c}{U_{lp} - U_c} \right) + 2.5 f_3(D, d_{50}) \left(\frac{U_{lp} - U}{U_{lp} - U_c} \right) \right]$ (live-bed scour)	Ref /45/	(14)

Table 4-1: Predictive equations for estimation of local scour depth.

The most common symbols used throughout the report are defined in Table 4-2.

Symbol	Definition	Unit
S	Depth of scour	m
D	Pile diameter	m
g	Acceleration of gravity	m/s ²
h	Depth of water	m
ρ_s	Sediment density	kg/m ³
d_{50}	Average grain diameter	m
ρ_w	Water density	kg/m ³
ν	Viscosity	m ² /s
U	Flow velocity, current	m/s
U_c	Critical flow velocity	m/s
K	Correction factors for shape, sediment size, angle of attack etc.	-
f	Correction factors for shape, sediment size, angle of attack etc.	-
Fr	Froude Number	-

Table 4-2: Definition of parameters referenced in Table 4-1.

The formulae in Table 4-1 cover cases of both clear-water and live-bed scour. All above-mentioned studies pertain to scour around piers founded in cohesionless sediment. A study on the problem of local scour around piers/piles in cohesive sediments is still in its initial phase.

Most of the methods available for determination of scour depth are applicable to steady flow conditions. However, the flow can be unsteady and change direction, eg in a tidal environment. The temporal variation of scour depth is studied in detail by Chabert & Engeldinger 1956 (Ref /7/), Ettema 1980 (Ref /11/), Yanmaz and Altinbilek 1991 (Ref /53/), Kothyari et al. 1992a, 1992b (Ref /22/ and Ref /23/) and Melville and Chiew 1999, (Ref /28/). The complexity of scour analysis in tidal waterways is most recently outlined by Richardson & Davis 2001 (Ref /42/), the reference is also known as the Hydraulic Engineering Circular No. 18 (HEC-18).

Only one known tide-simulated flume study is available. Escameia performed this study in 1998 (Ref /10/).

Field data on local scour in tidal environments are extremely scarce. A case study from the Otzumer Balje tidal inlet, Southern North Sea, Noormets et al. 2003 (Ref /34/) is known. Most important are the very recent prototype scour measurements from the Scroby Sands Offshore Wind Farm. A detailed description is given in Ref /16/. The Scroby Sands Offshore Wind Farm comprises of 30 wind turbines and is located on a large sand bank 3 km east of the Great Yarmouth Borough coastline in Norfolk, UK. These field measurements are further described in Section 8.

5. Candidate local scour equations

In the following, the most recent and the most referred local scour equations are described in greater detail in order to identify candidate scour equations for prediction of local scour at wide monopiles located in a strong tidal environment.

It is the experience of the author that there is no equation available in the literature for the prediction of local scour in a tidal regime. All equations are based on data for a uniform current flow.

When selecting candidate scour equations there will be special focus on equations, which deals with the so-called *wide pile problem*. This is because monopiles used as foundation for offshore wind turbines in general are wide compared to the water depth.

5.1. Background

Engineers have long been of the opinion that empirical scour prediction equations based on laboratory data over-predict scour depths for large structures. The local scour equations typically predict the scour depth as a multiple of the diameter and scour depths of 1.7 to 2.4 times the diameter width for a pile being 5-8 m leads to very costly foundation designs.

There are a number of methods and equations in the literature for estimating local scour at piles located in cohesionless soils as listed in Table 4-1. All of these equations are empirical and were derived using laboratory data from steady flow experiments. Due to the complexity of the flow and the complexity of the sediment transport associated with local scour processes, there are a number of dimensionless groups needed to fully characterise the scour. Many of these groups, such as the ratio of water depth to structure diameter, can be maintained constant between the laboratory model and the prototype structure. However, since there is a lower limit on the sediment particle size before cohesive forces become important, those groups involving sediment size cannot be maintained constant between the model and the prototype. In fact, most laboratory experiments are performed with near prototype scale sediment. If the sediment to structure length scales is not properly accounted for in the predictive equations, then problems arise when the equations are applied to situations different from the laboratory conditions on which they are based. The problems associated with not being able to maintain the proper scale between model and prototype sediment increases with the size of the prototype structure.

Engineers have long recognised the problem of predicting local scour depths at large structures (using equations based on laboratory data). The known equations tend to over-predict scour depths under these conditions. An important part of this discussion is a consideration of the often referenced guideline for calculation of scour associated with bridge piles; Hydraulic Engineering Circular No. 18 (HEC-18) by Federal Highway Administration, U.S. Dept. of Transportation (FHWA) and the data set from which it was derived to determine what conditions that equation reasonably represents. The data set that was used to derive the original HEC-18 pile scour equation was reviewed by Jones & Sheppard, 2000 (Ref /21/). Their paper outlines several methods that are available for dealing with the so-called wide pile problem.

Research in the US reported by Johnson et al. 1994 (Ref /18/) resulted in a "wide pile" correction to the equation given in HEC-18. Researchers in the Netherlands and the UK use a hyperbolic tangent function that essentially shifts the characteristic length dimension from the pile width to the flow depth as the pile width enlarges relative to the flow depth.

Sheppard 1999 (Ref /44/) concluded that the pile width impacts the equilibrium scour depth in two ways. First, the pile size to flow depth ratio is important and can best be represented by a hyperbolic tangent function, which makes the scour depth primarily a function of the pile size for relatively slender piles but a function of the flow depth for relatively wide piles. Second, the pile size to sediment size ratio can have an even greater impact on the scour prediction. Laboratory tests being performed by Jones & Sheppard in 2000 (Ref /21/) were designed to test Sheppard's hypothesis and to provide clear-water scour data for larger structures. Live-bed scour tests were later performed by Sheppard in 2003 (Ref /45/).

In the following chosen contributions to the wide pile problem are described in detail.

5.1.1. CSU/HEC-18 pile scour equation

HEC-18 was revised (fourth edition) by Richardson & Davis 2001 (Ref /42/). As mentioned earlier, the work was performed under U.S. Department of Transportation, Federal Highway Administration (FHWA). Guidance has been issued as Hydraulic Engineering Circular (HEC-18), *Evaluating Scour at Bridges*.

The HEC-18 is the standard used by most US highway agencies for evaluating scour at bridge pile. The scour equation was derived from laboratory data by researchers at Colorado State University (CSU) and was presented as the CSU equation in an earlier FHWA publication (Ref /40/).

The equation is recommended for both live-bed and clear-water pile scour. It is noted that the prediction equation is primarily based on bridge piers in rivers and not a tidal environment.

The equation predicts maximum scour depths as:

$$\frac{S}{D} = 2.0 K_1 K_2 K_3 K_4 \left(\frac{h}{D} \right)^{0.35} Fr^{0.43} \quad \text{Eq.(15)}$$

Most often the equation is written as the ratio between scour depth and water depth:

$$\frac{S}{h} = 2.0 K_1 K_2 K_3 K_4 \left(\frac{h}{D} \right)^{0.65} Fr^{0.43} \quad \text{Eq.(16)}$$

where K_1 to K_4 are correction factors for pile shape (K_1), angle of flow attack (K_2), bed condition (K_3) and bed sediment size (K_4), respectively, and Fr is the Froude Number given by:

$$Fr = \frac{U}{(gh)^{0.5}} \quad \text{Eq.(17)}$$

where g is acceleration due to gravity.

For a circular pile aligned with flow $K_1=1.0$ and $K_2=1.0$. The correction factor K_3 results from the fact that for plane-bed conditions, which are typical of most bridge sites, the maximum scour may be 10 % greater than computed with Eq.(15). In the unusual situation where a dune bed configuration with large dunes exists at a site during flood flow, the maximum scour may be 30 % greater than the predicted equation value. This may occur in very large rivers. For smaller streams that have a dune bed configuration at flood flow, the dunes will be smaller and the maximum scour may be only 10 to 20 % larger than equilibrium scour. For antidune bed configuration, the maximum scour depth may be 10 % greater than the computed equilibrium pile scour depth. See Table 5-1 for estimation of K_3 .

Bed condition	Dune height (m)	K_3
Clear-water scour	N/A	1.1
Plane bed and antidune flow	N/A	1.1
Small dunes	$3 > \text{height} \geq 0.6$	1.1
Medium dunes	$9 > \text{height} \geq 3$	1.2 to 1.1
Large dunes	$\text{height} \geq 9$	1.3

Table 5-1: Estimation of correction parameter K_3 .

The correction factor K_4 decreases scour depths for armouring of the scour hole for bed materials that have a d_{50} equal to or larger than 2.0 mm and d_{95} equal to or larger than 20 mm. The correction factor results originate from recent research by Molinas, 1990 (Ref /30/). Mueller and Jones, 1999 (Ref /31/) developed a K_4 correction coefficient from a study of 384 field measurements of scour at 56 bridges. Estimation of K_4 is as given in the following:

- If $d_{50} < 2$ mm or $d_{95} < 20$ mm, then $K_4 = 1.0$
- If $d_{50} \geq 2$ mm and $d_{95} \geq 20$ mm then $K_4 = 0.4 U_*^{0.15}$ where

$$U_* = \frac{U - U_{ic,d_{50}}}{U_{c,d_{50}} - U_{ic,d_{95}}} > 0 \quad \text{Eq.(18)}$$

where $U_{ic,d_{50}}$ is the approach current velocity required to initiate scour for the grain size d_{50} calculated as:

$$U_{ic,d_{50}} = 0.645 \left(\frac{d_{50}}{D} \right)^{0.053} U_{c,d_{50}} \quad \text{Eq.(19)}$$

and $U_{c,d_{50}}$ is the critical current velocity for incipient motion for the grain size d_{50} calculated as:

$$U_{c,d_{50}} = K_u h^{1/6} d_{50}^{1/3} \quad \text{Eq.(20)}$$

K_u is a constant being 6.19. The minimum value of K_4 is 0.4.

If no larger sand dunes are present and the seabed sediment characteristics fall in the “range” $d_{50} < 2$ mm or $d_{95} < 20$ mm then Eq.(16) can be written ($K_3 = 1.1$ is the only factor different from unity):

$$\frac{S}{h} = 2.2 \left(\frac{h}{D} \right)^{0.65} Fr^{0.43} \quad \text{Eq.(21)}$$

This formula is also the one proposed in the Coastal Engineering Manual (CEM), 2002 (Ref /9/).

Jones & Sheppard 2000 (Ref /21/) looked into the data used to derive the CSU/HEC-18 scour equation in order to determine its range of applicability. The CSU/HEC-18 equation was derived from laboratory data published by Chabert & Engeldinger 1956 (Ref /7/) and CSU data published by Shen et al. 1969 (Ref /43/). Although the sources of the data used in the derivation are well documented, the actual data had not been tabulated prior to Jones & Sheppard 2000 (Ref /21/). A regression analysis of this data produced an equation very close to the original equation as shown in Figure 5-1.

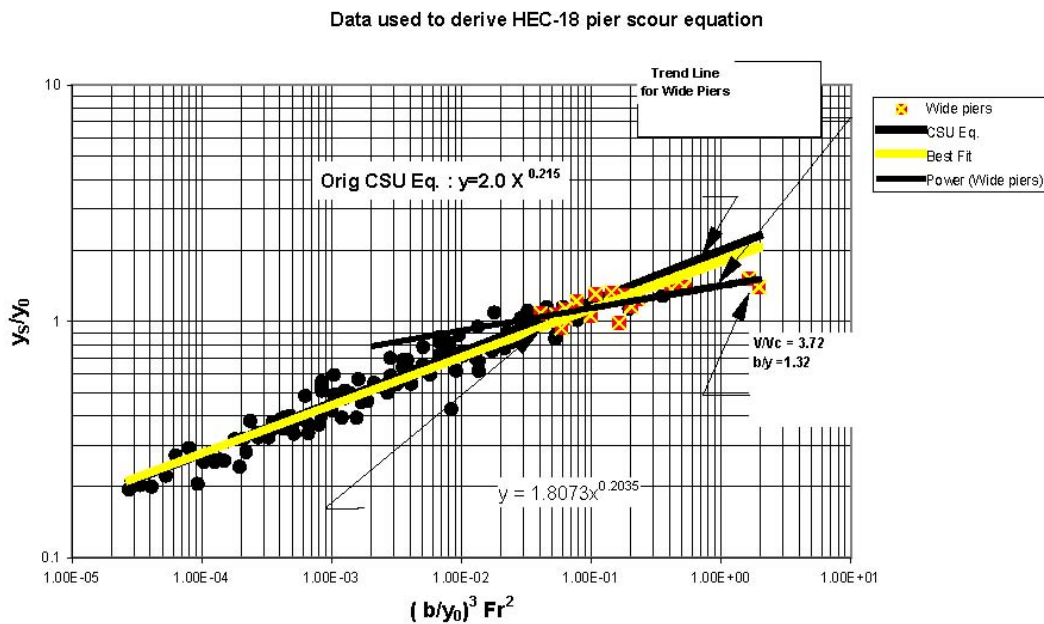


Figure 5-1: Data used to derive the CSU Equation in HEC-18 (Ref /21/).

Note that the used denomination of parameters in Figure 5-1 is different than the one chosen in this report and given in Table 4-2. In Figure 5-1 the notations are given as: y_s is the equilibrium scour depth, y_0 is the flow depth, b is the pile width and Fr is the Froude number.

All of the data used for the original equation was for circular piles in relatively uniform fine grain sand. Correction factors were added later to account for various pile shapes, angle of attack, bed forms and coarse bed material fractions as described above.

The study performed by Jones & Sheppard 2000 (Ref /21/) reveals that there were several data points with the ratio between water depth and the pile diameter, h/D , less than 1.0. From that point one could argue that the equation could apply to wide piles. The second part of the question, though, is whether the data for small relative depths were consistently below the regression line. The data points for h/D less than 1.0 are plotted with different symbols in Figure 5-1 and almost all of them do fall below the regression line, which suggests that the equation could at least be adjusted for wide piles or low relative depths.

5.1.2. Johnson's adjustment (1999)

Johnson 1999 (Ref /19/) defined a wide pile as one situated in shallow, low velocity flows so that $h/D < 0.8$ and $Fr < 0.8$. Johnson isolated the data that met these conditions in the original data set used in the CSU equation and added data from other sources to derive a new equation for wide piles using the same parameters. That equation can be written:

$$\frac{S}{h} = 2.08 K_1 K_2 K_3 K_4 \left(\frac{D}{h} \right)^{0.504} Fr^{0.639} \quad \text{Eq.(22)}$$

Then Johnson divided Eq.(22) by the CSU/HEC-18 equation to express the difference as another correction factor, K_w , for the CSU/HEC-18 equation.

$$K_w = 1.04 \left(\frac{D}{h} \right)^{-0.15} Fr^{0.21} \quad \text{Eq.(23)}$$

Eq.(23) can be applied to the CSU/HEC-18 equation when $h/D < 0.8$ and $Fr < 0.8$. If both of these conditions are just met, K_w is approximately 0.95 which means there would be a 5% reduction in the estimated scour depth. But if $h/D = 0.5$ and $Fr = 0.5$, which could occur, then $K_w = 0.81$ which is a 19% reduction.

5.1.3. Richard May (1998)

Richard May of H.R. Wallingford presented during the Oct. 1998 US Bridge Scour Scanning meeting (mentioned in Ref /21/) a preferred wide pile equation as:

$$\frac{S}{h} = k \left[0.55 \left(\frac{D}{h} \right) \right]_{Max=1.0}^{0.40} \left[0.6 \left(\frac{2.07 \cdot U}{U_c} - 1 \right) \right]_{Max=1.0} \quad \text{Eq.(24)}$$

where $k = 3.2$ for rectangular piles, $k = 2.4$ for round piles and the maximum value in either of the bracket terms is 1.0. That means they assume no additional scour for increases in D/h above 4.45 ($h/D = 0.22$) and that peak scour occurs at $U/U_c = 0.80$.

5.1.4. Breusers et al. (1977)

Breusers pile scour equation, see Eq.(6), is widely preferred, especially in the Netherlands:

$$\frac{S}{D} = f_1 \left[k \tanh\left(\frac{h}{D}\right) \right] f_2 f_3 \quad \text{Eq.(25)}$$

where k is 1.5 but shall be taken as 2.0 in design, Ref /4/.

The factor f_1 depends on the ratio between the average current velocity and the critical velocity as:

$$\begin{aligned} f_1 \left\langle \frac{U}{U_c} \right\rangle &= 0 \quad \text{for} \quad \left(\frac{U}{U_c} \right) \leq 0.5 \\ f_1 \left\langle \frac{U}{U_c} \right\rangle &= \left(2 \frac{U}{U_c} - 1 \right) \quad \text{for} \quad 0.5 \leq \left(\frac{U}{U_c} \right) \leq 1.0 \\ f_1 \left\langle \frac{U}{U_c} \right\rangle &= 1 \quad \text{for} \quad \left(\frac{U}{U_c} \right) \geq 1.0. \end{aligned}$$

The factor f_2 is a shape factor and given as:

$$\begin{aligned} f_2 \langle \text{shape} \rangle &= 1.0 \quad \text{circular and rounded piers} \\ f_2 \langle \text{shape} \rangle &= 0.75 \quad \text{streamlined shapes} \\ f_2 \langle \text{shape} \rangle &= 1.3 \quad \text{rectangular piers} \end{aligned}$$

The factor f_3 depends on the angle of attack and is 1.0 for a circular pile.

For a circular pile the expected (not design) live-bed local scour can be found as:

$$\frac{S}{D} = 1.5 \tanh\left(\frac{h}{D}\right)$$

The hyperbolic tangent function seems to reflect the pile width relationship well. For slender piles, $h/D > 1$, the hyperbolic tangent of h/D approaches 1, and the scour depth can be found as $S \approx k \cdot D$. For wide piles, $h/D < 1$, the hyperbolic tangent of h/D approaches h/D and the scour depth can be found as $S \approx k \cdot h$

Breusers et al Ref /4/ states that for $h/D \rightarrow 0$ the relation over-estimates the scour depth if compared to the regime theory, but experiments also point to higher S/D values for $h/D = 0.4$ to 1.

5.1.5. Sumer et al.

Based on a large number of experimental data from Breusers et al., Ref /4/, Sumer et al., Ref /48/, proposed a mean value and a standard deviation for the equilibrium scour depth for a vertical circular cylinder in a steady current.

$$\frac{S}{D} = 1.3 \quad \text{and} \quad \sigma_{S/D} = 0.7 \quad \text{Eq.(26)}$$

where $\sigma_{S/D}$ is the standard deviation of S/D . That is, for design purpose Sumer et al. propose to use a ratio of S/D of 2.0. Many have adopted the equation, as it is simple and well documented. It is noted that Breusers, Ref /5/, proposed in 1965 a somewhat similar equation where $S/D = 1.4$.

5.1.6. Predictive equations developed by Sheppard (2000)

J. Sterling Jones (first author of Ref /21/) has conducted a number of site-specific model studies for very large piles located in fine sand and has studied the literature to determine why there are inconsistencies in the scour prediction equations. He concluded that the wide pile problem is not so much with the relative water depth, h/D , as it is with the lack of sediment scaling in the laboratory tests. The laboratory data on which most, if not all, empirical local scour depth equations are based, scale the relative water depth properly. The quantity that is not scaled in the model tests is the sediment size. Since cohesive forces between the particles become significant when the sediment particle size is less than 0.074 mm (by sieve diameter), model sediment is seldom smaller than 0.1 mm in laboratory experiments. Many laboratory experiments have been conducted with much larger sediments, as large as 5 mm while the widths of the structures have been relatively small due to the widths of the laboratory flumes. For local scour it is reasonable to normalise the sediment size with the structure length scale, ie the structure width. Thus d_{50}/D or more conveniently D/d_{50} has been used by a number of researchers. Note that if prototype sediment is used in the model tests, this parameter is vastly different for model and prototype. The range of the D/d_{50} ratio included in the data used to derive the CSU/HEC-18 pile scour equation was from 96 to 633 and two thirds of the data had values less than 200. For 384 field measurements tabulated by Landers and Mueller (Ref /24/) D/d_{50} ratios ranged from 8.5 to 19763 with an average value of 2145 with a median value of 1024. Sheppard (Ref /44/) has shown that the maximum relative clear-water scour occurs when the D/d_{50} ratio is about 46, and that scour tends to diminish on both sides of this value for constant values of U/U_c and h/D , as illustrated in Figure 5-3. Since D/d_{50} cannot be properly scaled in the laboratory, the equilibrium scour depths' dependence on this quantity must be established if prototype scour depths are to be predicted from equations developed from laboratory data. The range of this ratio obtainable in the laboratory is limited due to size limitations of existing flumes. Experiments by Jones & Sheppard (2000) have extended the range of experimental data by conducting clear-water local scour experiments using 0.91 m diameter piles in sand with a d_{50} of 0.22 mm ($D/d_{50} = 4136$). Even though there is a significant quantity of local scour data for circular piles reported in the literature, much of this data is not usable. For example, the duration of many experiments were not sufficient for the scour depth to reach (or even be extrapolated to) an equilibrium value. In other situations, vital information about the flow, sediment and/or structure is missing. A thorough review by Jones & Sheppard of the literature resulted in 215 usable data points from nine different sources for clear-water scour conditions and 244 data points for live-bed scour conditions. Included in this data set are data from tests conducted by the Jones & Sheppard at The

United States Geological Survey (USGS) Conte Research Centre using 0.11 m, 0.305 m and 0.914 m diameter piles in 0.22 mm, 0.8 mm and 2.9 mm diameter sand. See Figure 5-2.



Figure 5-2: Large scale tests in USGS flume ($D = 0.914$ m and $h = 2.44$ m).

These data have been used in the development of Sheppard's local scour equations, which are outlined later. Sheppard's equations include the structure width to sediment size ratio and thus should be directly applicable to large structures as wide piles.

The equation works well for the range of structure to sediment size ratios obtainable in the laboratory, which now extends to values as high as 4168. These equations have also been applied to prototype structures from the USGS measurement programme, which range in width from 1 m to 10 m with good agreement. Of the numerous dimensionless groups that affect local equilibrium scour depths, Sheppard found three of the groups h/D , U/U_c , and D/d_{50} to be the most important for circular piles.

The critical velocity, U_c , is the velocity required to initiate movement of the median diameter sediment on the flat bed upstream of the structure, see also Eq.(20). In the live-bed scour range there is one additional dimensionless group, U_{lp} / U_c , where U_{lp} is the velocity at which the bed upstream of the structure flattens and becomes a plain bed. This is assumed to be the velocity at which the live-bed peak scour occurs. Note that the magnitude of the scour depth at transition from clear-water to live-bed conditions (clear-water peak) is highly dependent on the ratio D/d_{50} as opposed to the scour peak in the live-bed range, which appears to be independent of this ratio. However, the value of U/U_c , where the live-bed peak occurs, does depend on the sediment and flow parameters. There are several papers on bedforms in the literature that give the conditions under which dunes disappear and the bed becomes plane, see eg Simons and Richardson 1966, (Ref /46/), Snamenskaya 1969 (Ref /47/), van Rijn 1993 (Ref /51/). The values for the bed planing velocities predicted by these various methods differ in magnitude. The results given by Snamenskaya have been used in Sheppard's equations and have resulted in good agreement with field measurements as stated above.

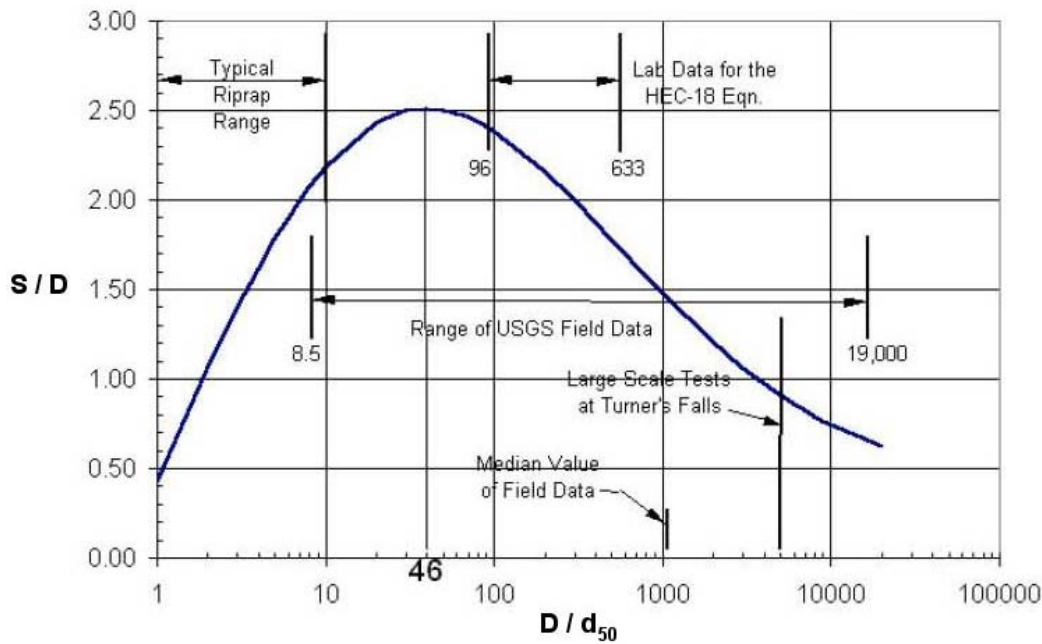


Figure 5-3: Dependence of normalised scour depth on D/d_{50} for a circular pile. For the curve shown $U/U_c = 1$, and $h/D > 2$ (Ref /21/).

For design purposes the local scour depth can be reduced to the simple relationship given in the equations below.

For clear-water scour $\left(0.4 \leq \frac{U}{U_c} \leq 1.0\right)$

$$\frac{S}{D} = c_1 \left[\frac{5}{2} \left(\frac{U}{U_c} \right) - 1.0 \right] \quad \text{Eq.(27)}$$

where $c_1 = \frac{2}{3}k$ and

$$k = \tanh \left[2.18 \left(\frac{h}{D} \right)^{2/3} \right] \left[-0.279 + 0.049 \exp \left(\log \frac{D}{d_{50}} \right) + 0.78 \left(\log \frac{D}{d_{50}} \right)^{-1} \right]^{-1}$$

If the design velocity is in the live-bed regime then the velocity at the live-bed scour peak U_{lp} must be determined. Determination of the live-bed scour peak velocity requires knowledge of the sediment properties and the water depth. The equilibrium (live-bed) local scour depth can then be computed using the following equations.

Live-bed scour $\left(1.0 < \frac{U}{U_c} \leq \frac{U_{lp}}{U_c}\right)$

$$\frac{S}{D} = c_2 \left(\frac{U_{lp} - U}{U_c} \right) + c_3 \quad \text{Eq.(28)}$$

where

$$c_2 = (k - c_3) \left(\frac{U_{usp}}{U_{cr}} - 1 \right)^{-1}$$

and

$$c_3 = 2.4 \tanh \left[2.18 \left(\frac{h}{D} \right)^{2/3} \right]$$

if $\frac{U}{U_c} > \frac{U_{lp}}{U_c}$ then

$$\frac{S}{D} = 2.4 \tanh \left[2.18 \left(\frac{h}{D} \right)^{2/3} \right] \quad \text{Eq.(29)}$$

Johnson & Sheppard state that the scour depth for a non-circular single pile can be computed by multiplying the scour depths computed by the above equations by the appropriate shape coefficient in CSU/HEC-18 (K_s).

5.1.7. Predictive equations developed by Sheppard after live-bed tests (2003)

High velocity live-bed scour tests have been performed at the University of Auckland in Auckland, NZ under supervision of D.M. Sheppard. The objective of the tests was to obtain data in the live-bed scour range data and to determine if live-bed peak exists.

The flume was 1.5 m wide, 1.2 m deep and 45 m long. The flow capacity was as high as 1200 l/s (≈ 1.6 m/s). The pile diameter was 0.152 m, two sediment sizes being 0.27 mm and 0.84 mm. A sediment re-circulation system was provided. A flume cross section with instrumentation is shown in Figure 5-4 and a live-bed test is shown in Figure 5-5 and Figure 5-6.

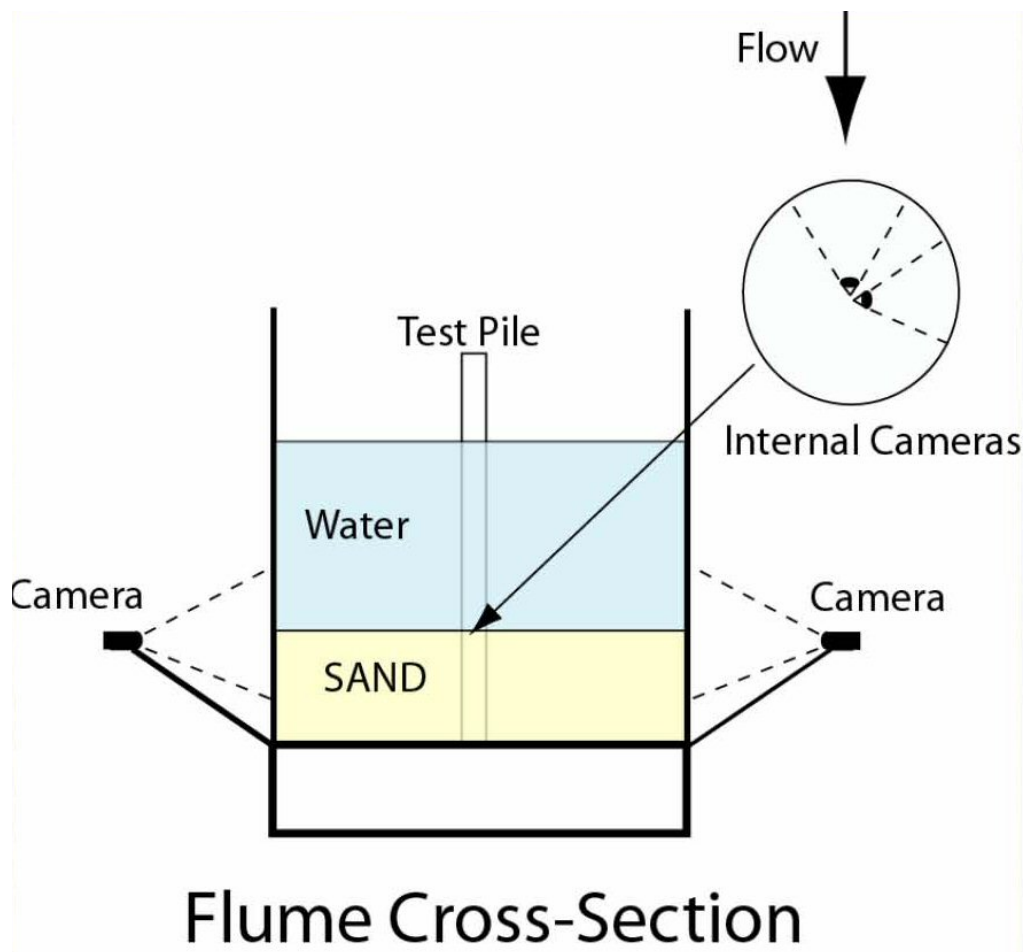


Figure 5-4: Instrumentation - a flume cross-section is shown.



Figure 5-5: Live-bed scour tests at University of Auckland.



Figure 5-6: A live-bed scour hole.

Live-bed scour data are seen in Figure 5-7.

Exp 207, video, fit eqn 8146

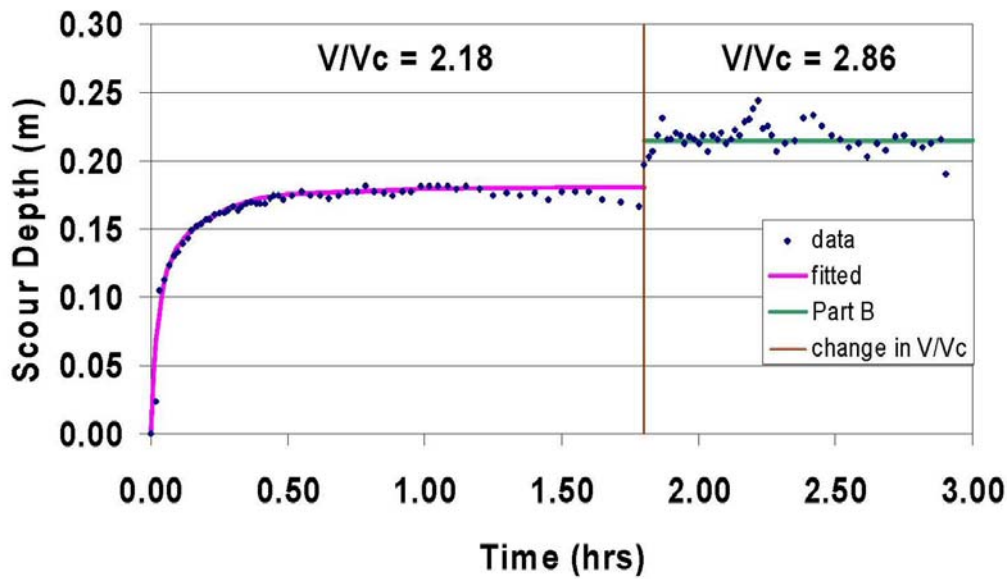


Figure 5-7: Live-bed scour data.

Sheppard proposed the following equilibrium equations based on the tests and prior tests (Ref /21/).

For clear-water Scour $\left(0.47 \leq \frac{U}{U_c} \leq 1.0\right)$

$$\frac{S}{D} = K_s 2.5 f_1\left(\frac{h}{D}\right) f_2\left(\frac{U}{U_c}\right) f_3\left(\frac{D}{d_{50}}\right) \quad \text{Eq.(30)}$$

where

$$f_1\left(\frac{h}{D}\right) = \tanh\left[\left(\frac{h}{D}\right)^{0.4}\right]$$

and

$$f_2\left(\frac{U}{U_c}\right) = 1 - 1.75 \left[\ln\left(\frac{U}{U_c}\right) \right]^2$$

and

$$f_3\left(\frac{D}{d_{50}}\right) = \frac{D/d_{50}}{0.4(D/d_{50})^{1.2} + 10.6(D/d_{50})^{-0.13}}$$

The equilibrium (live-bed) local scour depth can then be computed using the following equations.

Live-bed Scour $\left(1.0 < \frac{U}{U_c} \leq \frac{U_{lp}}{U_c}\right)$

$$\frac{S}{D} = K_s f_1 \left[2.2 \left(\frac{U - U_c}{U_{lp} - U_c} \right) + 2.5 f_3 \left(\frac{U_{lp} - U}{U_{lp} - U_c} \right) \right] \quad \text{Eq.(31)}$$

if $\frac{U}{U_c} > \frac{U_{lp}}{U_c}$ then

$$\frac{S}{D} = K_s 2.2 \tanh \left[\left(\frac{h}{D} \right)^{0.4} \right] \quad \text{Eq.(32)}$$

K_s is the structure shape coefficient ($K_s = K_l = 1$) and U_{lp} is the velocity where the live bed peak scour occurs, ie flow and sediment conditions where the bed planes out. See Ref /45/ for calculation of U_c (Shields curve) and U_{lp} (Van Rijn's method).

Sheppard state that the equations are intended for design and thus are, by design, conservative, especially at lower velocities in the live bed scour range.

6. Tidal flows influence on local scour

The main difference in relation to bridge piles compared to most wind turbine monopiles is that the latter is subjected to a tidal environment. In the following the scour development around a monopile located in a tidal system is described.

The development of scour around a monopile is very dependent on the specific coastal processes at the actual location. Wave action diminished the scour holes and the strong currents develop the holes. The relation between these coastal processes and the characteristic of the tidal system is important and a detailed analysis is required before design of any offshore structure.

In the coastal region, scour at coastal structures can be subjected to the effects of astronomical tides or a storm surge. The scour mechanisms are the same compared to non-tidal streams. Although many of the flow conditions are different in a tidal system, the empirical equations commonly used to determine scour might be applicable if the hydraulic conditions (depth, discharge, velocity, etc.) are carefully evaluated. This chapter presents some description and characteristics of tidal inlets or tidal estuaries in the context of tidal scour analyses. See the glossary list in Chapter 11 for a description of the most common terms used in this chapter.

Analysis of tidal regions or waterways is complicated. The hydraulic analysis must consider the magnitude of the extreme storm surge, the characteristics and geometry of the tidal inlet, estuary, bay or tidal stream. See Figure 6-1 for different tidal waterway crossings. In addition, the analysis must consider the long-term effects of the normal tidal cycles on long-term aggradations or degradation, contraction scour, local scour, and stream instability. Often the aim of the engineer is to evaluate the maximum scour holes, but the inclusion of the development in time might be a more correct way to design the foundations. This is in fact the case regarding fatigue of the pile, which in several recent wind farm projects in fact has been the limiting factor in the design of the monopile foundation.

A storm tide or storm surge in coastal waters results from astronomical tides, wind action, and rapid barometric pressure changes. The astronomical tidal cycle means there is a reversal in flow direction. Local scour at piles can occur at both flow direction and the scour hole will alternate with the reversal in flow direction.

Figure 6-2 illustrates the elevation and time variable nature of astronomical tides. For astronomical tides, maximum flood and ebb (or the time of maximum current and discharge) can be assumed to occur at the inflection point of (or halfway between) high tide and low tide, but actually can occur before or after the midtide level depending on the location. The addition of a storm surge to a high astronomical tide can lead to additional water surface elevations (High water, large tide plus storm surge in Figure 6-2), additional current and associated flooding. In the most conservative scenario, the greatest potential flood elevation would occur at the time where the high astronomical tide and maximum storm surge height coincide in time. In this circumstance, the maximum discharge would occur when the astronomical tidal period and the period associated with the storm surge event are the same value. The presence of any inland flood discharge would influence this discharge, particularly during the period when the flood levels recede (ebb). Hydraulically, the above discussion presents two limiting cases for evaluation of the flow velocities. With negligible flow from the upland areas, the flow through the bay or estuary is based solely on the ebb and flood resulting from tidal fluctuations or storm surges. Alternatively, when the flow from the streams and

ivers draining into the bay or estuary (inland flood) is large in relationship to the tidal flows (ebb and flood tide), the effects of tidal fluctuations are negligible.

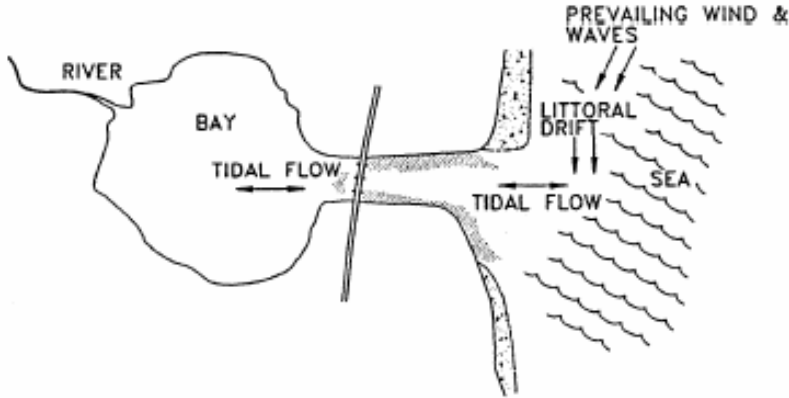
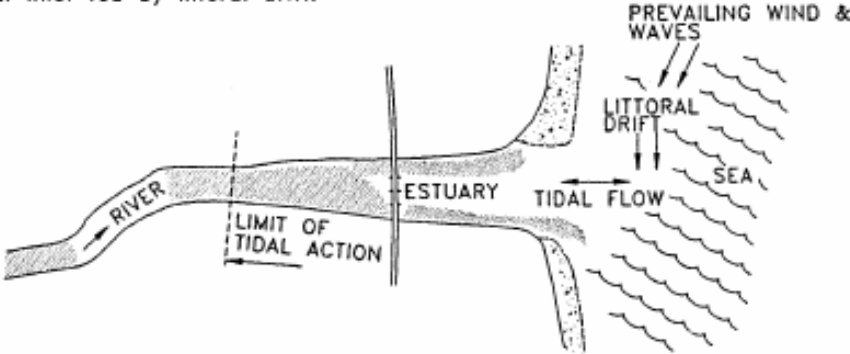
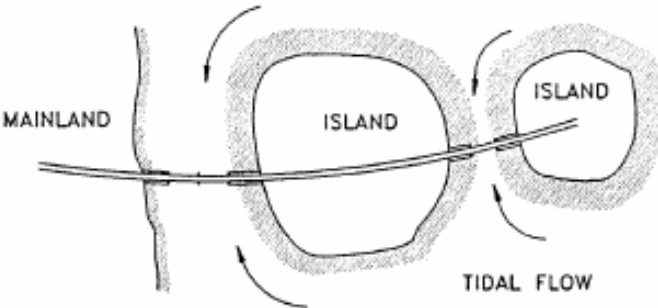
- 
1. Inlets between the open sea and an enclosed lagoon or bay, where most of the discharge results from tidal flows. Tidal inlet fed by littoral drift.
- 
2. River estuaries where the net discharge comprises river flow as well as tidal flow components
- 
3. Passages between islands, or between an island and the mainland, where a route to the open sea exists in both directions.

Figure 6-1: Types of tidal waterway crossings, Ref /33/.

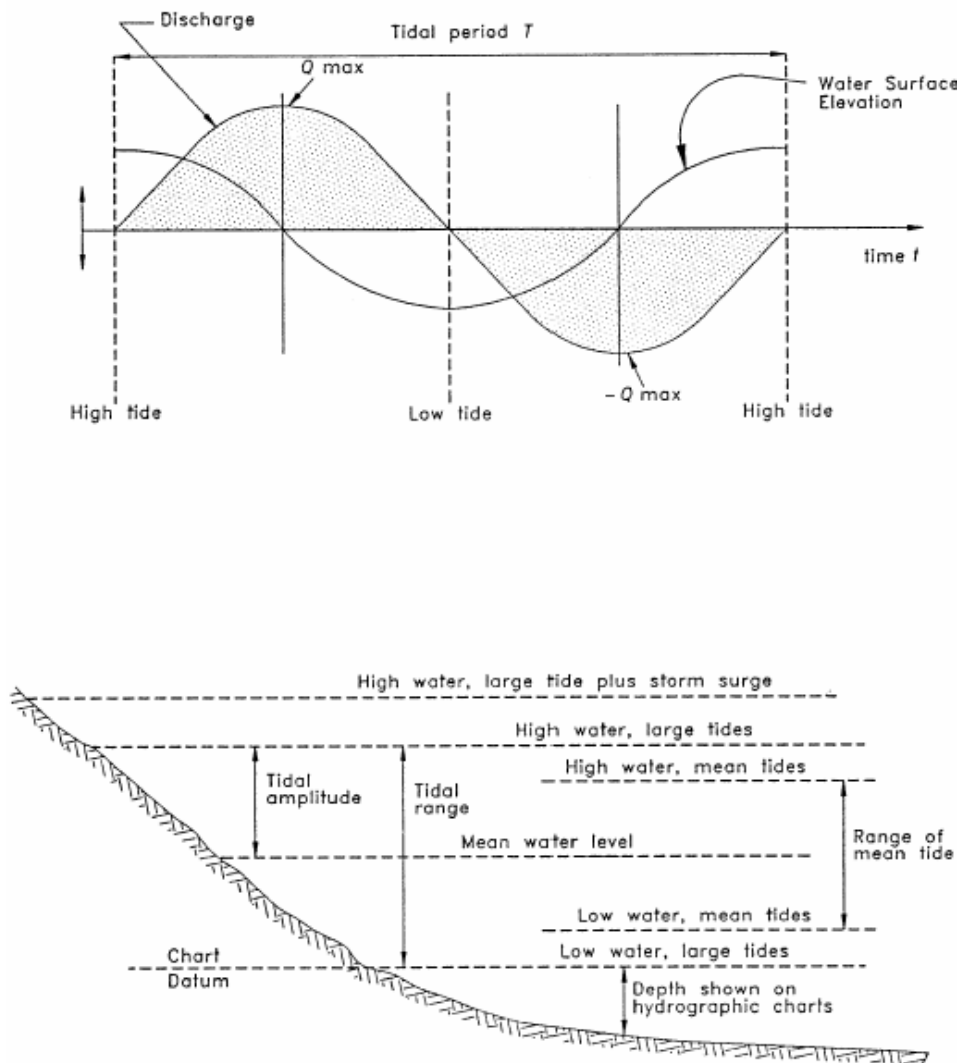


Figure 6-2: Principal tidal terms, Ref /33/.

Scour around a monopile in the coastal region results from the unsteady diurnal and semi-diurnal flows resulting from astronomical tides, large flows that can result from storm surges and the combination of river and tidal flows. The forces, which drive tidal fluctuations, are primarily the result of the gravitational attraction of the sun and moon on the rotating earth (astronomical tides), wind and storm set-up. These different forces, which drive tides, produce varying tidal periods and amplitudes. In general semi-diurnal astronomical tides having tidal periods of approximately 12 hours occur in the lower latitudes while diurnal tides having tidal periods of approximately 24 hours occur in the higher latitudes. Typically, the storm surge period correlates with the associated storm type. In general, storm surge periods may be assumed to be longer than astronomical tidal periods.

The continuous rise and fall of astronomical tides will usually influence long-term trends of local scour. Worst-case hydraulic conditions for local scour are usually the result of infrequent tidal events such as storm surges. Storm surges are a single event phenomenon, which, due to their magnitude, can develop a significant velocity.

The hydraulic variables (discharge, velocity, and depths) in the coastal region can be determined with relative good precision. The magnitude of the combined flows shall be evaluated. Mass density stratification of the water typically has a minor influence on local scour. Peak flows from storm surges may not have durations long enough to reach the ultimate scour depths determined from existing scour equations. The time dependent characteristics of local scour require further research. It is noted that existing scour equations can predict the magnitude of this scour, but not the time history.

Mass density stratification (saltwater wedges), which can result when the denser more saline ocean water enters an estuary or tidal inlet with significant freshwater inflow, can result in larger velocities near the bottom than the average velocity in the vertical velocity profile. With careful evaluation, the correct velocity can be determined for use in the scour equations. With storm surges, mass density stratification will not normally occur. The density difference between salt and freshwater, except as it causes saltwater wedges, is not significant enough to affect scour equations. Density and viscosity differences between fresh and sediment-laden water can be much larger in river flows than the density and viscosity differences between salt and freshwater.

In general the scour process under a typical tide condition can be illustrated as seen in Figure 6-3.

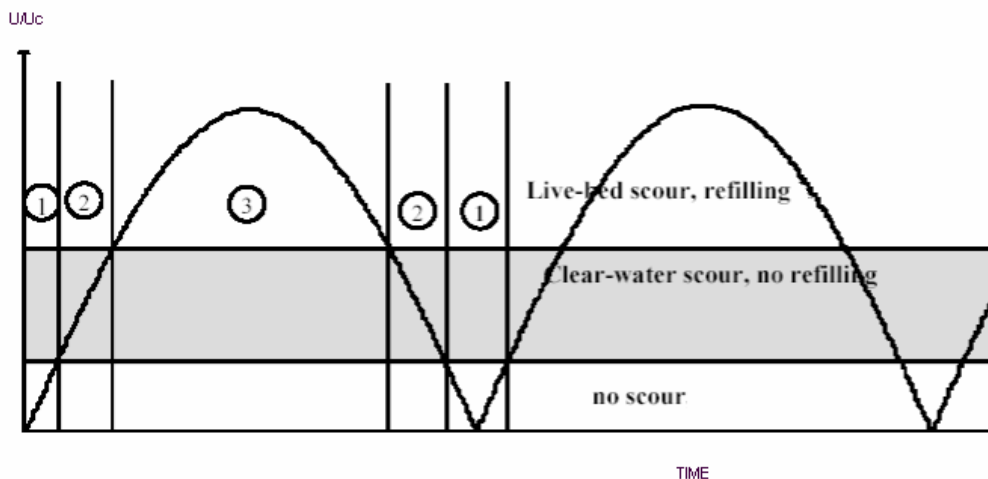


Figure 6-3: The scour process during a normal tidal cycle.

The numbered phases in Figure 6-3 are described in the following:

Phase 1

No scour development because the velocity is too low.

Phase 2

Clearwater scouring. Scouring will occur until the hole is at the maximum scour for $U/U_c = 1$ and the maximum S/D . Refilling will not occur because the upstream velocity is not strong enough to initiate transport of the sediment.

Phase 3

Livedbed scouring. Scouring will continue, but at a faster pace than Phase 2. If the scour hole depth is greater than (from previous tidal cycle) the equilibrium scour depth for a particular time, refilling of the hole will occur.

The following important points to be noted are:

- The relation between U/U_c and S/D are changing continuously and therefore the scour depth will change accordingly.
- The scour process depends on the magnitude of the velocity and occurs on both ebb and flood.
- Conditions are oscillating from no scour ($U/U_c < 0.5$) to clear-water scour ($0.5 < U/U_c < 1$) to live-bed scour ($U/U_c > 1$) and back down the ladder.
- Refilling of the scour hole will only occur under live-bed conditions.

It is often the task of the engineer to predict the scour depth developed after numerous tidal cycles, ie 1-2 months after installation of a monopile. In the following an example of such a prediction is given.

It is assumed that only tidal flows are present. Based on the fundamentals illustrated in Figure 6-3 the following predictions can be made of the development of the scour.

If the water depth is not varying much (eg. 5m to 10 m) the critical velocity of the sand sediment does not change significantly and the critical velocity of the sediment can be assumed constant.

If U/U_c did not exceed 1 and clear-water scour conditions were true over the entire cycle, then the flow would increase the scour hole depth a little over each cycle and no refilling would occur since no sand would be transported from upstream. The result would be a gradual approach to the maximum equilibrium scour depth. Once this depth was reached, scouring would stop.

However, if U/U_c exceeds 1 over most of the cycle (eg. $U/U_c < 1$ for less than 4 hours in any 12 hour period) live-bed scour conditions exist over most of the cycle. This means that the scour hole depth will increase initially. At some point when the velocity goes down, the scour hole depth will exceed the equilibrium depth for the velocity at that time and the hole will be partially refilled

because sediment is still being transported into the scour hole due to live-bed conditions. Long-term, the scour hole will establish a quasi-equilibrium state where scouring at a high velocity magnitude will be countered by refilling when the velocity magnitude is reduced. Thus, the scour hole depths will likely "stabilize" at some value just below the maximum equilibrium scour depth.

7. Experimental tidal scour studies

In the past, considerable effort has been directed towards the study of scour in unidirectional flows, but the important effects produced by tidal conditions have not previously been quantified, especially not concerning wide piles in tidal waters. This is of interest because piles used in the offshore wind farm industry are often situated in such a tidal environment influenced by strong shifting currents.

An article published by Escameia 1998 (Ref /10/) will be described and referred to because it is a well-documented study and it considers tidal flows. Furthermore, the study is supported with extensive laboratory testing at HR Wallingford to investigate scour development around large obstructions.

In Figure 7-1 is shown a picture during unidirectional flow. The test is performed at HR Wallingford.

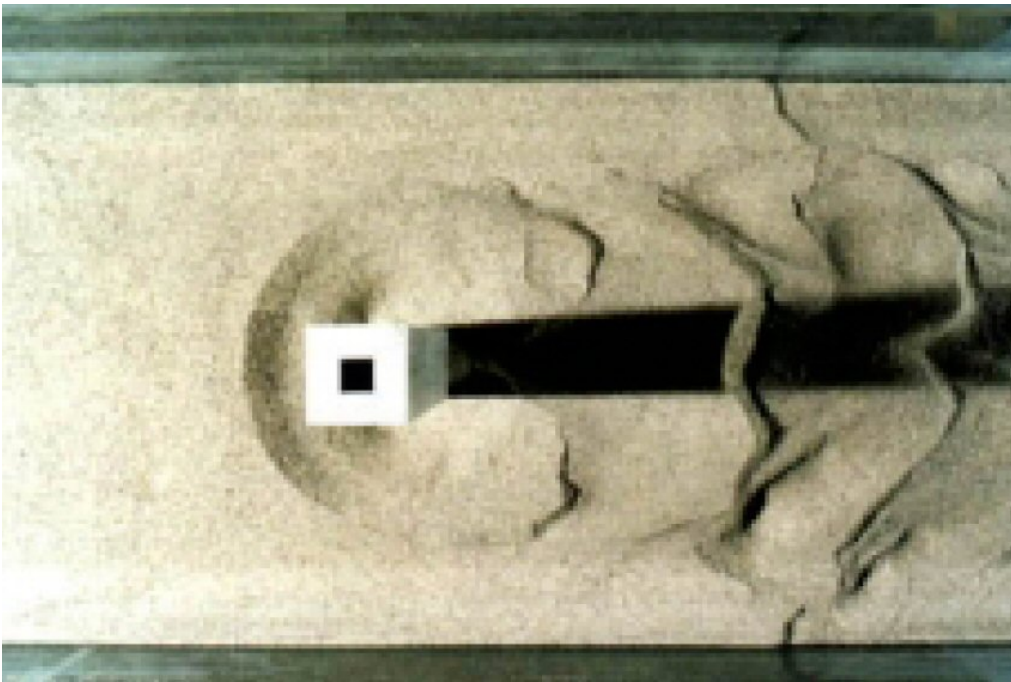


Figure 7-1: Unidirectional flow in laboratory (HR Wallingford 1999).

Escameia found that once the scour hole is developed, it is found to play an important role in determining the flow pattern around the structure. The hole significantly increases the magnitude of the down-flow (when compared with flat bed) and by allowing a part of the flow through the hole, it reduces the flow acceleration at the sides of the pile. This fact is particularly important for tidal flows, where scour holes will develop on both sides of the structure.

In tidal flows, both the velocity and flow depth vary with depth throughout the tidal cycle. Escameia concludes that the reversal of the flow during the tidal cycle will produce equilibrium scour depths that are smaller than those achieved in purely unidirectional flows. Arguments are that

the scour hole formed around a structure during the first tidal half cycle will be partly filled up again by sediment transported by the flow when it reverses direction. As the flow changes direction, it will also encounter changes in the state of the bed, which will be disturbed both upstream and downstream of the structure. A sequence of tidal cycles will tend to increase the scour depth until equilibrium is reached between the input and output of sediment.

7.1. Escarameia's study

Escarameia study of local scour in tidal flows is supported with extensive laboratory testing at HR Wallingford to investigate scour development around large obstructions under the influence of the following parameters:

- Reversal of the flow direction.
- Tidal cycle duration.
- Water depth.
- Shape of the obstruction.
- Sediment size.

The experimental facility used in the study was a 24 m long flume fitted with an axial pump that allowed reversal of the flow direction. A 4 m long granular mobile bed formed the test section where the model structures were placed. Preliminary tests were performed to measure scour development in unidirectional flows in order to allow later comparisons with tidal flow conditions. During the test programme, the above flow parameters were varied to provide a wide range of conditions, and several typical shapes of structures were investigated (circular, rectangular and square shapes). Tests were carried under clear-water scour conditions, ie with no transport of sediment into the scour hole where it was expected that the conditions would cause the biggest scour depths. These correspond to flow velocities at the threshold of sediment transport, i.e. at critical velocity U_c .

Escarameia calculated the critical velocity using the following formula ascribed to Hancu 1971 (Ref /13/), which had proved accurate in previous experimental studies carried out at HR Wallingford.

$$U_c = a [g(s-1)d_{50}]^{0.5} (h/d_{50})^{0.2} \quad \text{Eq.(33)}$$

where s is the relative density of the sediment and a is a coefficient such that $a = 1.0$ for $d_{90} > 0.7\text{mm}$ and $a = 1.2$ to 1.4 for $d_{90} < 0.7\text{mm}$. Another approach is previously given as Eq.(20).

A criterion for selecting the bed material was the need to avoid rippling of the bed at critical flow velocities, since rippling has been found to reduce the scour depth by about 70%. It has been observed that ripples tend to start forming before the critical velocity is reached for uniform sediments with d_{50} smaller than about 0.5 to 0.7 mm. Most of the tests that were designed to determine the influence on scour of the various flow and structure-related parameters were carried out with sediment having $d_{50} = 0.75$ mm, but some tests were carried out with sand size 0.44 mm in order to check the influence of sediment sizes on scour depths.

Based on tests Escarameia developed design equations for predicting scour around large obstructions both in tidal and unidirectional flow conditions.

7.2. Test results from Escarameia's study

The results from Escarameia's tests are described in the following.

The scour depth is defined as the biggest scour depth recorded during a test. In a unidirectional test, since the scour hole tends to increase with time until an equilibrium platform is reached, the scour depth is also the equilibrium one. In a tidal test, the maximum scour depth may or may not coincide with the equilibrium depth, as it can occur as a result of one of the earlier half tidal cycles. It was observed in the tests that the time and conditions for occurrence of the maximum scour depth in tidal flows were quite unpredictable. Figure 7-2 illustrates the scour patterns observed during tidal tests.

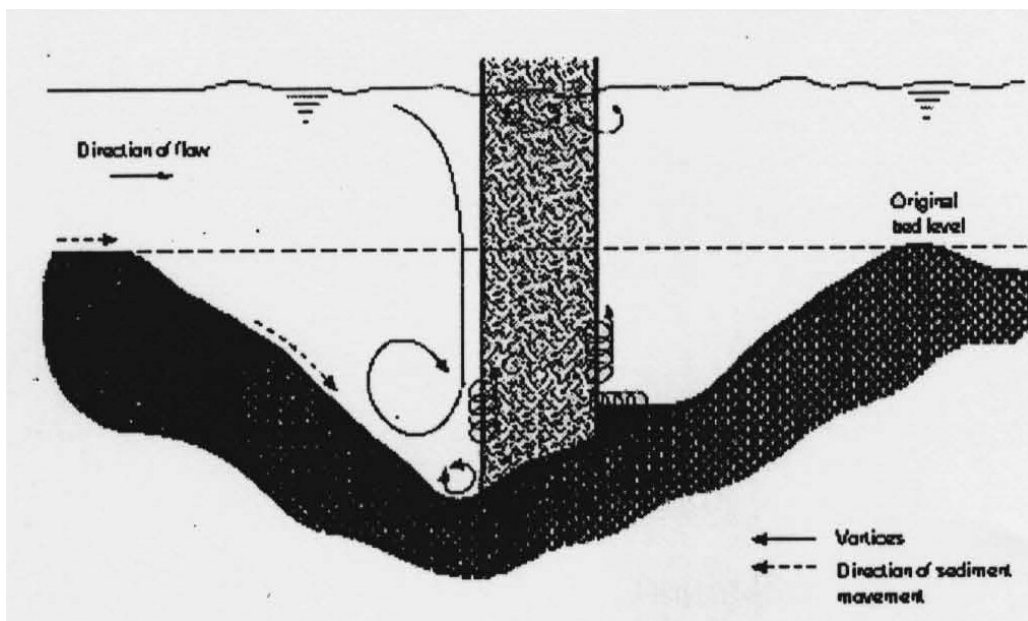


Figure 7-2: Scour pattern during a tidal test, taken from Ref /10/.

Effect of flow direction

A comparison between tidal and unidirectional flow conditions showed that in general the equilibrium scour depths measured in the tidal tests are always well below the equilibrium depth for equivalent unidirectional conditions, see Figure 7-3. The velocity used in these tests was similar to the critical velocity, ie $U_{max} = U_c$.

It is noted that in Figure 7-3 there seem to be an error when the “tidal cycle tests” results were plotted, as these results are misplaced 2 hrs along the x-axis (C3 had a constant velocity of 4 hrs and not 2 hrs). In summary, the statement that the “equilibrium scour depths measured in the tidal tests are always well below the equilibrium depth for equivalent unidirectional conditions” is understood in such way that the C3 test yields an equilibrium scour depth significant less than the equilibrium scour during unidirectional current. The unidirectional test reached equilibrium after approximately

35 hrs and created an equilibrium scour depth of 0.116 m compared. Test C3 yielded an equilibrium scour depth of 0.079 m with a constant velocity for each 4 hrs tidal cycle.

Escaraméia makes the following comment regarding Figure 7-3 “*Closer observation of the results revealed that the equilibrium scour depths for the tidal tests could be slightly higher than the scour depths at corresponding times for unidirectional conditions, which is thought to be due to experimental scatter*”. As the data in Escaraméia’s study does not comply with the graph he plotted it is certainly not clear whether the equilibrium scour depths for the tidal tests could be slightly higher than the scour depths at corresponding times for unidirectional condition. Still, his results seem to show that the scour development during tidal conditions gives smaller holes compared to an unidirectional condition where the current are given enough time to develop an equilibrium scour.

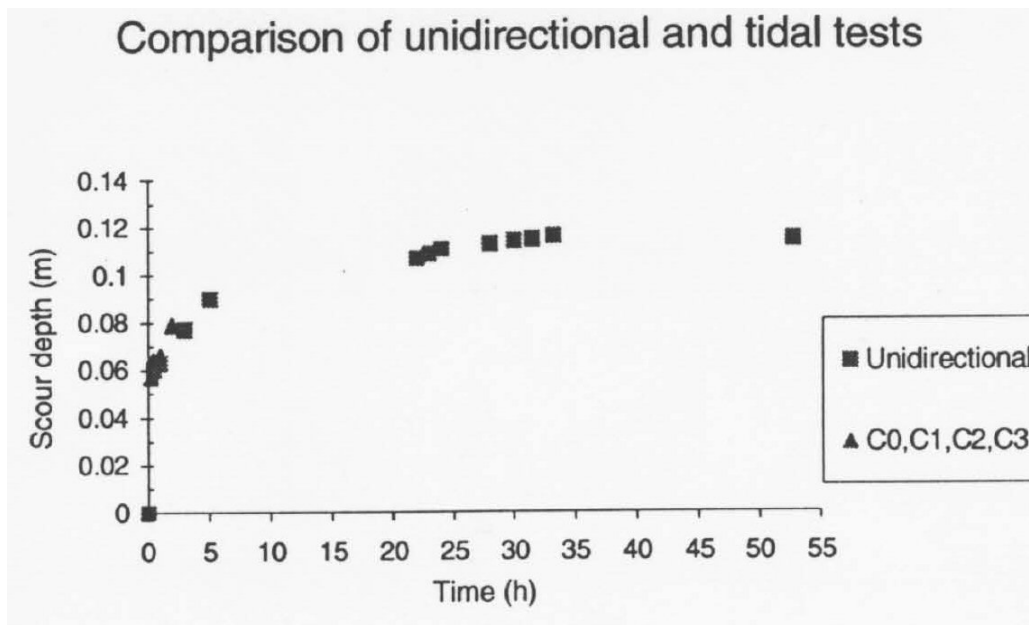


Figure 7-3: Scour depth in unidirectional and tidal tests (C0, C1 etc refer to tests tidal cycles of different time length), taken from Ref /10/.

Effect of tidal cycle

One of the aspects that required considerable thought was the way (or ways) in which the tidal cycles could be simulated in the laboratory tests. During a tide, the water levels vary with time according to approximately sinusoidal curves and there is a corresponding variation in the flow velocities. In the test facility it was impractical to vary the water level and the flow velocities simultaneously, but separately they could easily be adjusted to simulate the changes that occur during a tidal cycle.

The effect of the tidal cycle was further investigated by Escaraméia performing another series of tests with constant velocity above the critical value for sediment movement (live-bed scour). A comparison between the different test series is illustrated by the graph of Figure 7-4, where it can be seen that tidal flows with $U_{max} = U_c$ (series denoted C0, C1, C2, C3 and V0B, V1B, V2B, V3B) produced scour depths that were considerably smaller than those of unidirectional flow (Equilibrium scour of 0.116 m), which can be taken as an upper limit. However, contrary to what

has been observed in unidirectional flow conditions, there is some indication that in tidal conditions larger scour depths can be reached for flow velocities above the critical value than at critical velocity. The tests carried out with $U_{max} > U_c$ (Series C0M, C1M and V0A, V1A, V2A) produced scour depths, which were very close to the unidirectional equilibrium value. In view of the limited data, it is difficult to draw general conclusions or give full explanation for this finding. It seems plausible, however, that the alternation of flow direction and the subsequent generation of bed forms created conditions which were significantly different from those in unidirectional flow: after the first tidal cycle, the bed forms will affect the velocity distribution both in the vertical and the horizontal plane as well as the capacity of the flow to transport sediment into and out of the scour hole.

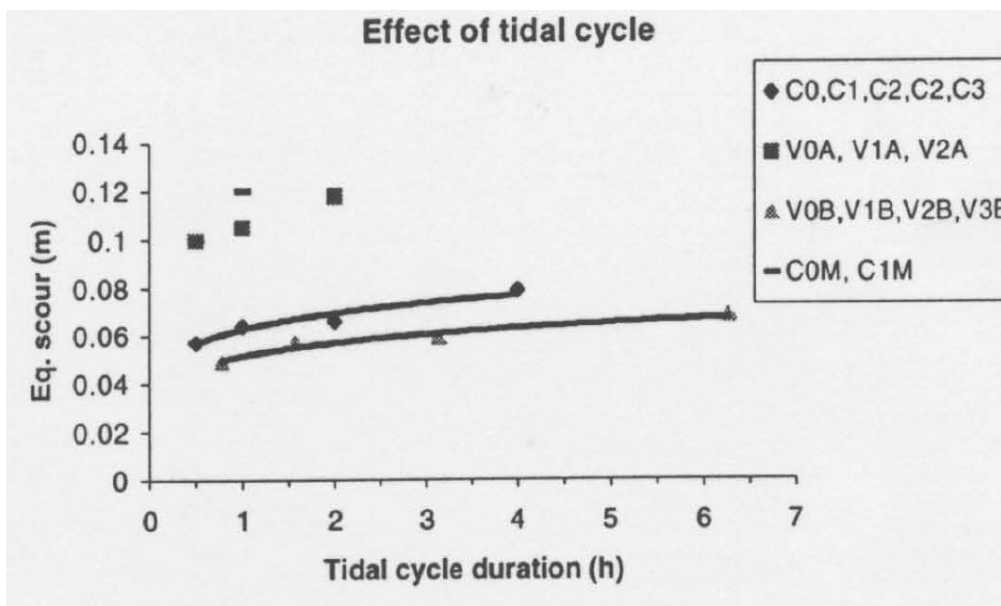


Figure 7-4: Effect of tidal cycle duration, taken from Ref /10/.

Effect of flow depth

Equilibrium scour depths were plotted against the tidal cycle duration in Figure 7-5, where it is apparent that the flow depth has a marked effect on the equilibrium scour depths. For the same tidal cycle duration, the scour depth decreases with the flow depth (or the relative flow depth). The scour depth for a very wide pile $h/D=0.5$ is approximately only 50% compared to a narrower pile (though still wide) $h/D=1.0$.

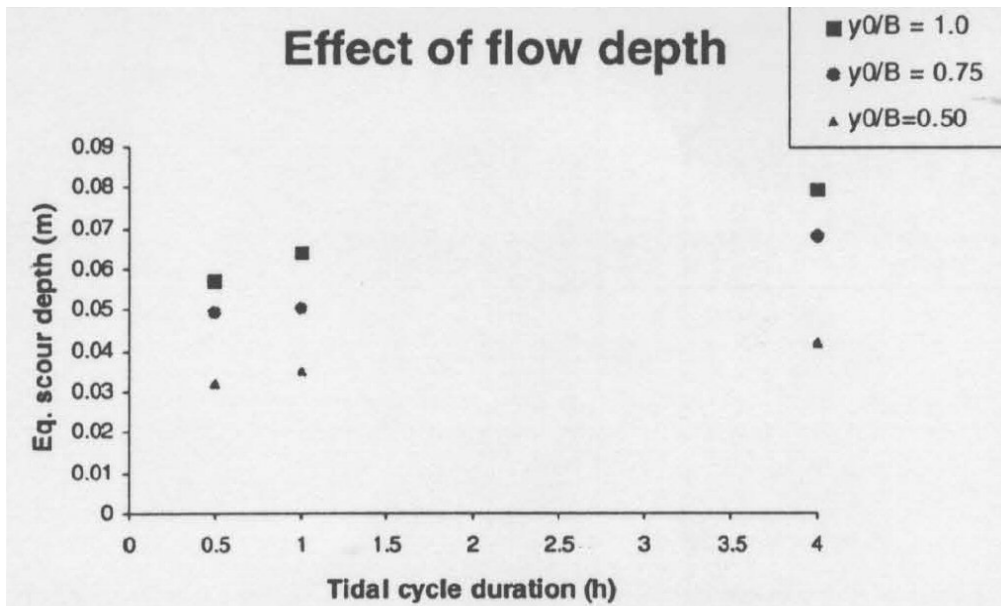


Figure 7-5: Effect of flow depth ($y_0/B (=h/D)$ is water depth / pile diameter, taken from Ref /10/.

Effect of structure shape

All the structures tested (square, circular, rectangular and square pier with transverse sill) had the same width, $D = 0.075$ m, so that they presented similar obstruction relative to the flow. The values of equilibrium scour depth for the four shapes are plotted in Figure 7-6 against the duration of the tidal cycle in the tests. The following conclusions were made:

1. As the tidal cycle duration increased (ie the length of time of exposure to unidirectional flow), so did the differences in the equilibrium scour depths for the various shapes;
2. The square shape was generally associated with the largest equilibrium scour depths;
3. The square pier with transverse sill and the rectangular structure produced the lowest equilibrium scour depths;
4. For tidal cycle durations of less than about two hours (in the model), the square and circular shapes produced similar values of equilibrium scour depths but the circular shape became more "efficient" than the square shape for longer cycle durations (ie it produced less scour).

The ratio between equilibrium scour depth for square and circular piers (for a four-hour tidal cycle duration in the tests) was found to be 1.10 and 1.20 for the maximum scour depths. Visual observations during the test with a transverse sill showed that the shape of the scour hole was significantly affected by the presence of the sill. Particularly at the upstream face of the structure (ie the face last subjected to the flow), the hole extended much further width-wise than in the isolated square structure case. This was a result of the obstruction caused by the sill, which did not allow the free progression of scour around the sides of the pile. The equilibrium scour depths measured for rectangular structures were found to be between 10 and 14% smaller than those measured for square structures in similar flow conditions. This behaviour appears to be logical for structures with a length greater than the width because the localised scour holes that tend to form around the corners at the front of the structure will have to extend further to reach the scour holes formed in the

previous tidal cycle at the opposite face. The longer the cycle duration the more likely it will be in principle to approach the scour levels corresponding to the square structure.

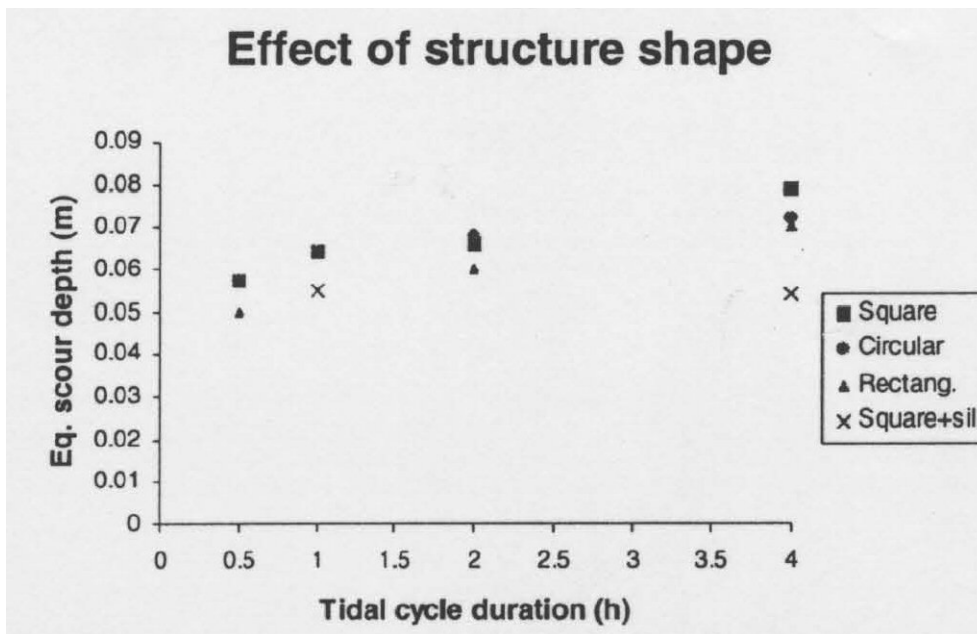


Figure 7-6: Effect of structure shape, taken from Ref /10/.

Effect of sediment size

The above depicted results were carried out with sand of $d_{50} = 0.44$ mm and the results were compared to those obtained with sediment size $d_{50} = 0.75$ mm. This comparison indicated that for the type and sizes of sediment tested the bed sediment size has a negligible effect on the development of the scour hole and on the equilibrium scour depths reached.

Conclusion by Escameia

An extensive laboratory study showed the influence of the various flow and geometric parameters on equilibrium scour depths around large obstructions in the tidal conditions. The study confirmed the importance of parameters such as the flow velocity, water depth and structure shape and highlighted the need for inclusion of the tidal cycle duration in future design equations. Escameia finds it likely that the scour depth in tidal flows is smaller compared to those developed for a uniform flow.

8. Field studies of monopile scour in a tidal flow

Field data on local scour around monopiles and similar in tidal environments seem to be scarce. Complete field data on local scour for piles in tidal environments are scarce. Complete data include information on currents, seabed sediment and development of the scour. In the following two studies are described.

8.1. Otzumer Balje tidal inlet

One well-documented field measurement from the Otzumer Balje tidal inlet, Southern North Sea, Noormets et al. 2003 (Ref /34/) is known, see also details in Attachment A – A case study. In Figure 8-1 to the right is seen a steel cylinder rammed into the bed in the tidal channel. A bathymetry survey has been performed and is shown on the left of the picture.

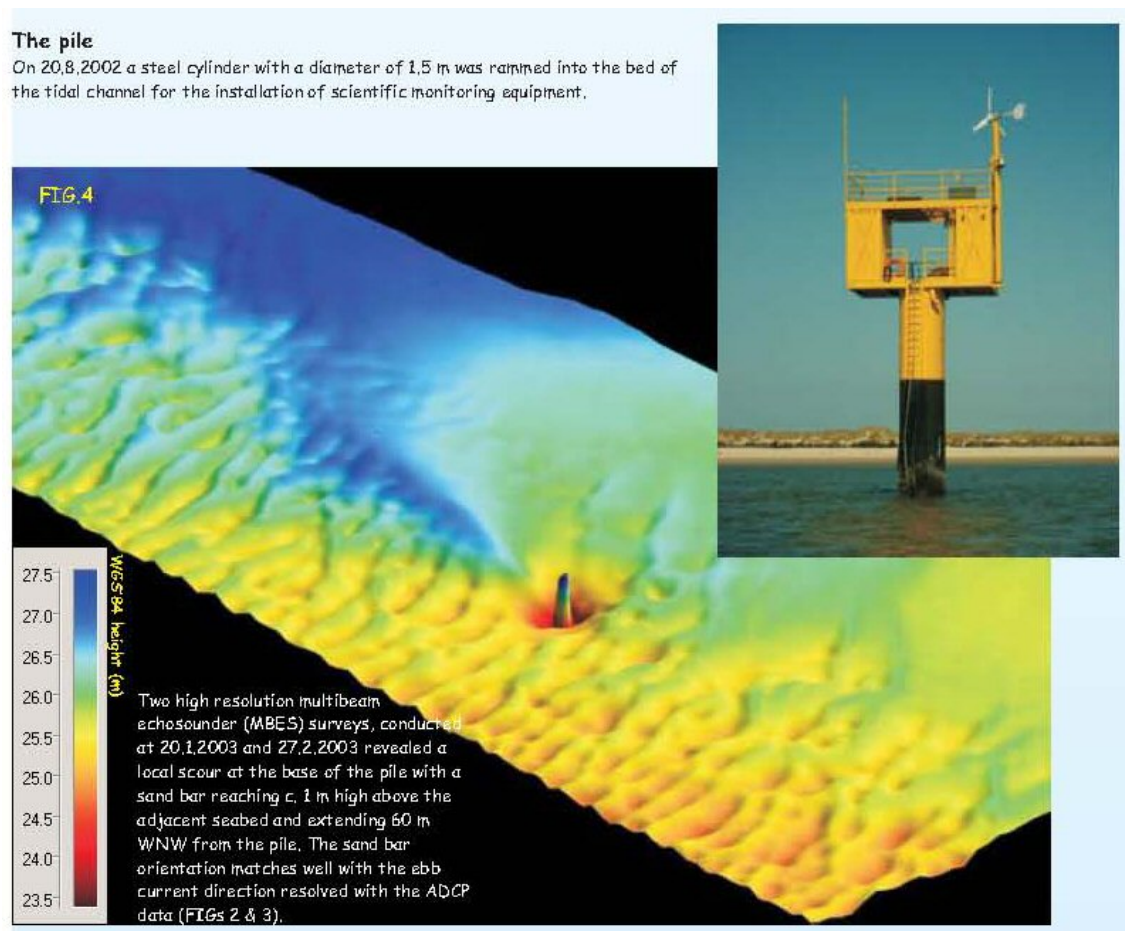


Figure 8-1: A case study from Otzumer Balje tidal inlet (see Attachment A).

Data from Otzumer Balje tidal inlet are given Table 8-1. It is noted that the pile is not considered wide because $D/h \approx 9$.

Symbol	Definition
$S = 2.2$ m	Depth of scour
$D = 1.5$ m	Pile diameter
$h = 13.3$ m	Mean flow depth
$d_{50} = 0.3$ mm	Average grain diameter
$U = 1.4$ m/s	Maximum depth averaged flow velocity
$U_c = 0.64$ m/s	Critical flow velocity (after Eq.(20))
$U_{lp} = 1.98$ m/s	Flow velocity at the transition to upper stage plane bed (van Rijn, 1984, 1993)

Table 8-1: Data reported from Otzumer Balje tidal inlet.

8.2. Scroby Sands Offshore Wind Farm

Most important are the very recent prototype scour measurements from the Scroby Sands Offshore Wind Farm, see Figure 8-2. A detailed description is given in Ref /16/. The Scroby Sands Offshore Wind Farm comprises of 30 wind turbines and is located on a large sand bank 3 km east of the Great Yarmouth Borough coastline in Norfolk, UK. The seabed mainly consists of sand, however, with some layers of clay or silt. The water depth at the turbines varies between 1 m and 11 m below Lowest Astronomical Tide (LAT), with a maximum depth being 4 m below LAT across the bank. Consequently even moderate waves at the wind farm are depth limited. The tidal range is limited to app. 1.9 m (spring) but a strong tidal current runs across the bank. There are also sea states where a strong wave induced current runs across the bank.

Data from Scroby Sands are given in Table 8-2. A majority of the piles can be considered wide because the range of D/h is 1 to 3.

Symbol	Definition
$D = 4.2$ m	Pile diameter
$h = 3-14$ m	Water depth after MSL
$d_{50} = 0.2625$ mm	Average grain diameter
$U = 1.5$ m/s	Maximum depth averaged flow velocity

Table 8-2: Data reported from Scroby Sands.

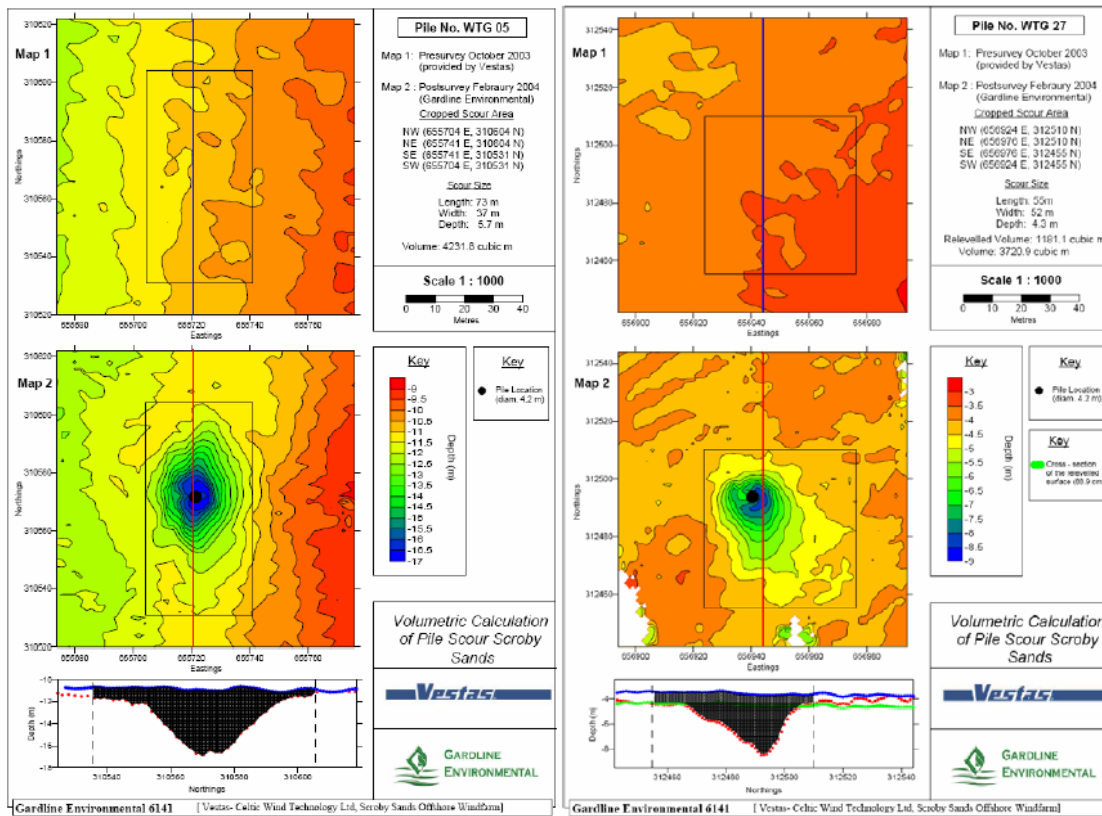


Figure 8-2: Seabed surveys at Scroby Sands prior to pile driving and prior to installation of scour protection, Ref /16/.

9. Local scour in waves

Numerous research projects have been addressed scour around piles caused by waves alone and by waves and currents in combination, respectively. Not much attention has been given scour around piles caused by breaking waves. In the following a brief review of before mentioned processes are given.

9.1. Equilibrium scour in waves

Sumer and Fredsøe 2002, Ref /50/, presented experimental data of equilibrium scour depth around slender piles exposed to waves. They found that the equilibrium scour depth, S , is well described by Eq.(34):

$$\frac{S}{D} = 1.3(1 - e^{-0.03(KC-6)}) \quad \text{for } KC > 6 \quad \text{Eq.(34)}$$

where KC is the Keulegan-Carpenter number and D is the pile diameter.

In regular waves the KC number is given as:

$$KC = \frac{U_w * T}{D} \quad \text{Eq.(35)}$$

where T is the wave period and U_w is the near bed orbital velocity.

In case of irregular waves the formula is still valid if the peak period T_p is used as the period and the nearbed orbital velocity is taken as $U_m = \sqrt{2}\sigma_u$, where σ_u is the root mean square root of the orbital velocity. The formula in case of irregular waves can then be written as:

$$KC = \frac{U_m * T_p}{D} \quad \text{Eq.(36)}$$

For typical offshore wind farm locations, the Keulegan-Carpenter number is less than 10-15. Hence the scour depth is expected to be smaller for pure waves than for pure current according to Figure 9-1.

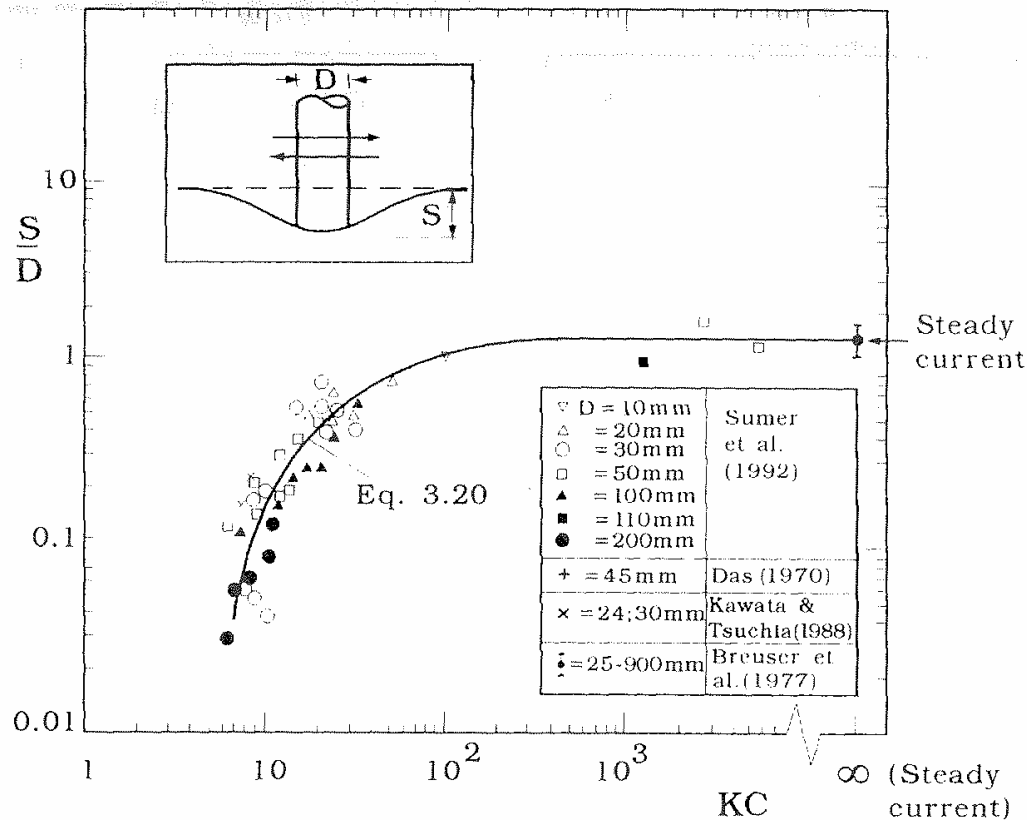


Figure 9-1. Equilibrium scour regarding a circular pile and live bed condition (taken from Sumer et al. 1992).

9.2. Equilibrium scour in combined waves and currents

Sumer and Fredsøe 2002, Ref /50/ has presented results for equilibrium scour depth determined from experiments. Their main findings are presented in Figure 9-2 and Figure 9-3. They found that the ratio between the current velocity and the wave induced velocity and the KC number mainly determines the scour depth. For typical offshore wind farms (locations where KC numbers are less than 10-15) the equilibrium scour depths are smaller in combined wave and current conditions than for current alone.

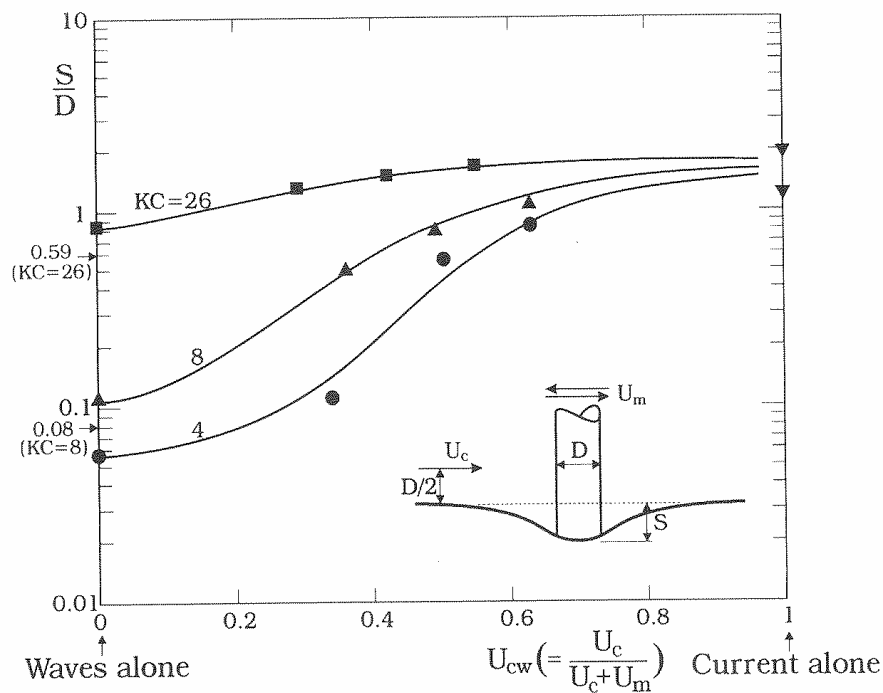


Figure 9-2: Equilibrium scour depth in co-directional combined waves and current. Circular pile and a live bed condition (taken from Sumer at Fredsøe, 2002).

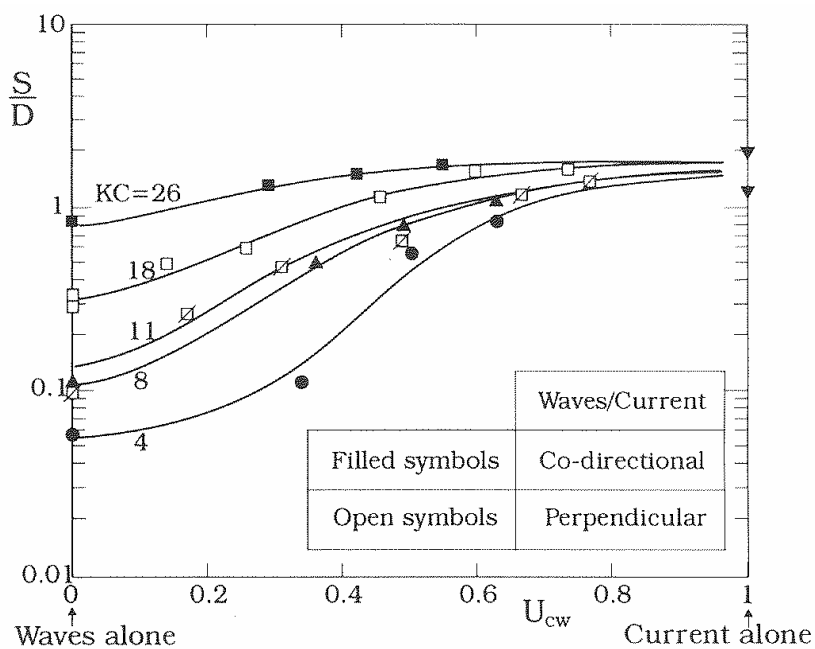


Figure 9-3: Equilibrium scour depth in co-directional and perpendicular combined waves and current. Circular pile and a live bed condition (taken from Sumer at Fredsøe, 2002).

9.3. Equilibrium scour in breaking waves

There is a lack of knowledge of development of scour around a pile when the pile is located where waves are breaking. A few papers regarding this topic have been found, eg Carreiras et al. 2000, Ref /6/ and Bijker and Bruyn 1988, Ref /3/.

A scour hole might be caused by the presence of the pile itself or by general bed level changes. Figure 9-4 taken from Bijker and Bruyn and Figure 9-5 taken from Carreiras illustrates this problem.

In the conclusion by Bijker and Bruyn is written, “Normally waves will not increase, but even decrease the scour around a structure as compared with that of current only. The depth of this scour is in the order of 1.5 times the pile diameter. In case of breaking waves this value can be, however, considerably higher”. This conclusion is based on Figure 9-4.

The authors of the present review believe that the scour development may rather be caused by a general bed development rather than by the presence of the pile.

In order to gain more knowledge of the phenomena, a number of physical tests have been defined as described in Section 10.

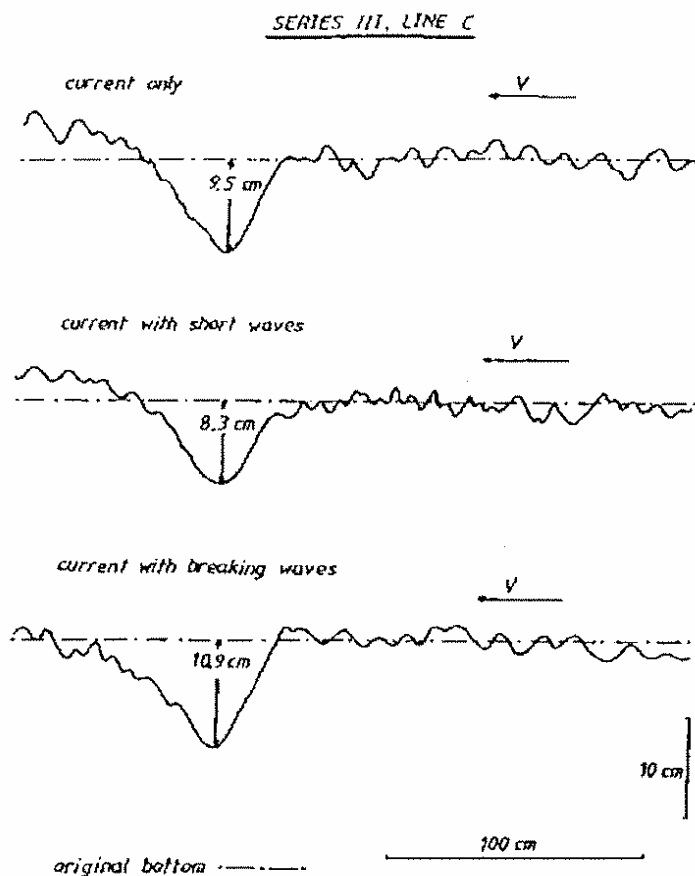


Figure 9-4: Typical scour profiles taken Bijker and Bruyn, Ref /3/.

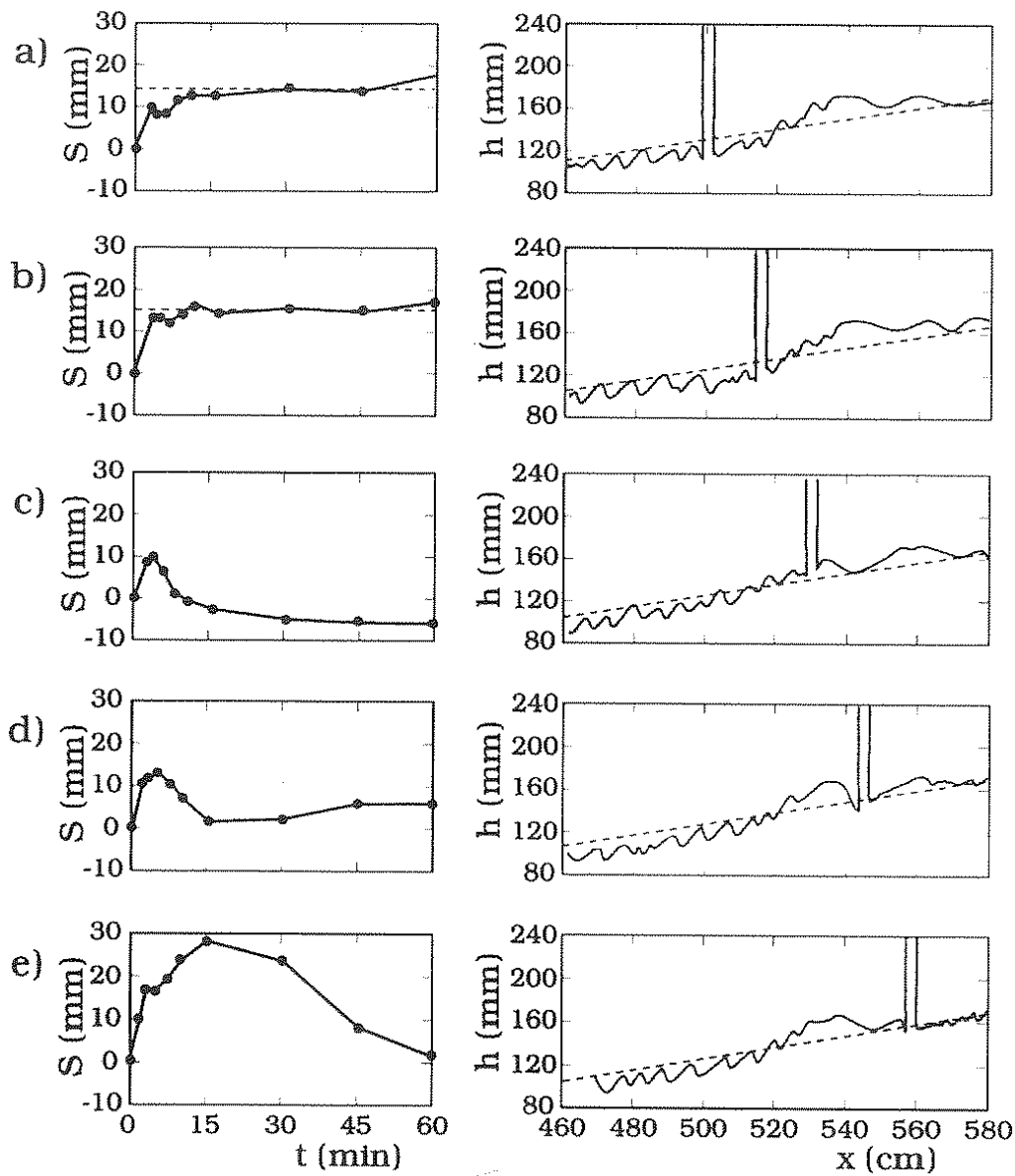


Figure 9-5: Scour depth time developments and equilibrium bed profile taken from Carreiras et al, 2000, Ref /6/.

10. Specifications of experimental tests

Experimental tests are to be performed at the hydraulic laboratories of Aalborg University. The main objective is to produce data regarding development of scour around monopiles. The environmental parameters used shall reflect a range of typical conditions at existing and planned offshore wind farms.

Offshore wind farms are placed in areas with a relative shallow water depth. The mean water level is typically in the range 5-20 m, but also piles placed at 30 m are being planned. A strong tidal current is often encountered. A wind farm placed at shallow water in combination with an aggressive tidal current is likely to experience breaking waves. The following characteristics shall be reflected in the experimental tests after reviewing a number of existing and planned offshore wind farms:

Diameter of pile:	4-6 m
Water depth:	5-30 m
Environment:	A tidal system with and without breaking waves
Tidal peak current:	1-2 m/sec.

As mentioned earlier, the diameter of the pile is a main factor governing the size of the scour. Also the current velocity and the water depth influence the development of the scour. The characteristic of the non-cohesive sediment seems to have less influence in the development of the scour. A strong tidal current is expected to create largest scour holes where a combination of current and waves reduces the scour development. Some researcher claims that breaking waves can cause even larger scour holes compared to a strong current.

In summary, the experimental tests shall be developed to produce data to study the following:

- A comparison between breaking waves and a strong current regarding development of scour.
- A comparison between a tidal current and a uniform current regarding development of scour.
- Influence of the current speed and influence of water depth / pile diameter ratio.

11. Glossary

Abutment	End support of eg a bridge; walls flanking the water channel through a hydraulic structure.
Accretion	Process by which particles carried by the flow of water are deposited and accumulated (the opposite of erosion).
Bay	A body of water connected to the ocean with an inlet.
Bed form	A recognisable flow-related relief feature on the bed of a channel.
Caisson	A hollow structure with substantial impermeable walls sunk through ground or water to form a permanent shell of a deep foundation.
Clear-water scour	Scour (normally local scour) where the bed material in the flow upstream of the scour hole is at rest.
Critical flow	Water flow at which the specific energy is a minimum for a given discharge (and Froude number is unity).
Diurnal tide	Tides with an approximate tidal period of 24 hours.
Discharge	Flow rate expressed in volume per unit time.
Ebb (or ebb tide)	Tidal flow associated with falling tide; flow from estuary to sea.
Eddy	Single vertical vortex.
Erosion	Process by which particles are removed by the action of wind, flowing water or waves (the opposite of accretion).
Estuary	Tidal reach at the mouth of a river
Flood/flood tide	Flow of water from the ocean to the bay or estuary.
Froude number	Dimensionless parameter representing the ratio between the inertia and gravity forces in a fluid, taking the value of unity for critical flow.

Local scour	Scour that results directly from the impact of individual structural elements (eg piles and abutments) on the flow and occurs only in the immediate vicinity of those elements.
Littoral transport	Transport of beach material along a shoreline by wave action also longshore sediment transport.
Live-bed scour	Scour (normally local scour) where there is a general movement of bed material, ultimately with a balance between the sediment entering and leaving the scour hole.
Pile	Slender (compared to height) structural member substantially underground intended to transmit forces into loadbearing strata below the surface of the land.
Scour	Erosion resulting from the shear forces associated with flowing water and wave action. In this report normally used to represent erosion associated with currents.
Sediment	Fine material transported in a liquid that settles or tends to settle.
Semi-diurnal tide	Tides with an approximate tidal period of 12 hours.
Shear stress	Force per unit area exerted by fluid on seabed (due to fluid flow) and acting tangential to its surface in the direction of flow.
Shear velocity	A measure of the shear stress, having the dimensions of velocity.
Shields criterion	Threshold of movement of particles, expressed in terms of two dimensionless numbers, the entrainment function and the particle Reynolds number, based on experimental work by Shields (and others) on granular sediment.
Spring tides	Tides on the two occasions per lunar month when the predicted range between successive high water and low water is greatest.

Still-water elevation:	Flood height to which water rises as a result of barometric pressure changes occurring during a storm event.
Storm surge	Coastal flooding phenomenon resulting from wind and barometric changes. The storm surge is measured by subtracting the astronomical tide elevation from the total flood elevation (Hurricane surge).
Storm tide	Coastal flooding resulting from combination of storm surge and astronomical tide (often referred to as storm surge).
Sub critical flow	Flow in a channel at greater than critical velocity, at which the Froude number is greater than unity.
Tidal amplitude	Generally, half of tidal range.
Tidal cycle	One complete rise and fall of the tide.
Tidal day	Time of rotation of the earth with respect to the moon. Assumed to equal approximately 24.84 solar hours in length.
Tidal inlet	A channel connecting a bay or estuary to the ocean.
Tidal period	Duration of one complete tidal cycle. When the tidal period equals the tidal day (24.84 hours), the tide exhibits diurnal behaviour. Should two complete tidal periods occur during the tidal day, the tide exhibits semi-diurnal behaviour.
Tidal prism	Volume of water contained in a tidal bay, inlet or estuary between low and high tide levels.
Tidal range	Vertical distance between specified low and high tide levels.

Tidal waterways	A generic term that includes tidal inlets, estuaries, bridge crossings to islands or between islands, inlets to bays, crossings between bays, tidally affected streams, etc.
Tides	Periodic rising and falling of water resulting from the gravitational attraction of the moon, sun and other astronomical bodies, together with the effects of coastal aspect and bathymetry.
Uniform flow	Flow of water in which the depth and velocity remain constant.
Waterway opening	Width or area of bridge opening at a specific elevation, measured normal to principal direction of flow.
Wave period	Time interval between arrivals of successive wave crests at a point.

12. References

- Ref /1/ Ahmed, F. and Rajaratnam, N. (1998) Flow around bridge piers J. Hyd. Engg., A.S.C.E., Vol. 124, No. 3, March pp. 288-299.
- Ref /2/ Baker, C.J. (1981). New design equation for scour around bridge piers. J. of Hydraulic Division, A.S.C.E., Vol. 107, HY-4.
- Ref /3/ Bijker, E. W. and de Bruyn, C. A. (1988). Erosion around a pile due to current and breaking waves, Proc. 21th International Conf. Coastal Eng., Vol. 2.
- Ref /4/ Breusers, H., Nicollett, G. & Shen, H. (1977). Local scour at cylindrical piers. Journal of Hydraulic Research, 15, 211-252.
- Ref /5/ Breusers, H. (1965). Scouring around drilling platforms; Hydr. Res. 1964/1965, IAHR Bulletin, 19, p.276.
- Ref /6/ Carreiras J., Seabra Santos F.J. Scour around vertical piles under the effect of breaking waves (2000). 5^o Congresso da Agua, Lisbon, Portugal.
- Ref /7/ Chabert, J. and Engeldinger, P. (1956). Etude des affouillements autour des piles des points. Laboratoire National d'Hydraulique, Chatou, France.
- Ref /8/ Chiew, Y.M. and Melville, B.M. (1987). Local scour around bridge piers. J. of Hydraulic Reserach, I.A.H.R., Vol. 25, No.1.
- Ref /9/ Coastal Engineering Manual, (CEM) (2002). CEM chapters VI-5-3-f and VI-5-6 (Author Steven Hughes). (Chapters I-IV were released as USACE guidance on 16 May 2002).
- Ref /10/ Escameia, M. (1998). Laboratory investigation of scour around large structures in tidal waters. Basics of Sediment Transport and Scouring. HR Wallingford.
- Ref /11/ Ettema, R. (1980). Scour at bridge piers. Report No. 216, Dept. of Civil Engg., Univ. of Auckland, Auckland, New Zealand.
- Ref /12/ Graf, W.H. and Yulistiyan (1998). Experiments on flow around a cylinder the velocity and vorticity fields. J. Hydraulic Research, I.A.H.R., Vol. 36, No. 4, pp. 637-653.
- Ref /13/ Hancu, S. (1971) Sur le Calcul Des affouillements Locaux Dans la Zone Des Piles de Ponts, Proceedings 14th IAHR Congress", 3: 299-313, (in French).
- Ref /14/ Hjorth, P. (1975). Studies on the nature of local scour. Dept. of Water Resources Engg., University of Lund, Bulletin No. 46.

- Ref /15/ Hoffmans, G.J.C.M. & Verheij, H.C. (1997): Scour manual. Balkema, Rotterdam, The Netherlands.
- Ref /16/ Høgedal, M. & Hald, T. (2005) Scour Assessment and Design for Scour for Monopile Foundations for Offshore Wind Turbines. Presented at Copenhagen Offshore Wind 2005.
- Ref /17/ Jain, S.C. (1981). Maximum clear-water scour around cylindrical piers. J. of Hydraulic Div., A.S.C.E., Vol. 107, HY-5, pp. 611- 626.
- Ref /18/ Johnson, P.A. and E.F. Torrico (1994). Scour Around Wide Piers in Shallow Water, Transportation Research Board Record 1471, Transportation Research Board, Washington, D.C.
- Ref /19/ Johnson, Peggy A. (1999). Scour at Wide Piers Relative to Flow Depth, Stream Stability and Scour at Highway Bridges, Compendium of ASCE conference papers edited by E. V. Richardson and P. F. Lagasse, pp280-287.
- Ref /20/ Jones, J.S., 1995, Personal communication (FHWA) (mentioned in HEC-18, Ref /42/).
- Ref /21/ Jones, J.S. & Sheppard, D.M. (2000). Scour at wide bridge piers. ASCE, US Department of Transportation, Federal Highway Administration, Turner-Fairbank Highway Research Center, 10 pp.
- Ref /22/ Kothyari, U.C.,Garde, R.J. and RangaRaju, K.G. (1992 a). Temporal variation of scour around circular bridge piers. J. of Hydraulic Engg., A.S.C.E., Vol. 118, No. 8, Aug., pp. 1091-1105.
- Ref /23/ Kothyari, U.C.,Garde, R.J. and RangaRaju, K.G. (1992 b). Live-bed scour around cylindrical bridge piers. J. of Hydraulic Research, I.A.H.R., Vol. 30, No. 5, pp. 701-715.
- Ref /24/ Landers, Mark N., and Mueller, David S. (1986). Channel Scour at Bridges in the United States, Report No. FHWA-RD-95-184.
- Ref /25/ Laursen, E.M. and Toch, A. (1956). Scour around bridge piers and abutments. Bull. No. 4, Iowa Highway Research Board, U.S.A.
- Ref /26/ Laursen E.M. (1963). An Analysis of Relief Bridge Scour, ASCE Journal of Hydraulic Division, Vol. 89, n. HY3, 93-118.
- Ref /27/ Melville, B.W. (1975). Local scour at bridge sites. Report No.117, Univ. of Auckland, School of Eng., Auckland, New Zealand.
- Ref /28/ Melville, B.W. and Chiew, Y.M. (1999). Time Scale for Local Scour at Bridge Piers, J. of Hydraulic Engineering, ASCE, 125(1), 59-65.
- Ref /29/ Melville, B.W. & Coleman, S.E. (2000). Bridge scour. Water Resources Publications, CO, USA.

- Ref /30/ Molinas, A. (1990). Bridge Stream Tube Model for Alluvial River Simulation (BRISTARS). User's Manual, National Cooperative Highway Research Program, Project No. HR15-11, Transportation Research Board, Washington, D.C.
- Ref /31/ Mueller, D.S. and J.S. Jones (1999). Evaluation of Recent Field and Laboratory Research on Scour at Bridge Piers in Coarse Bed Materials, ASCE Compendium, Stream Stability and Scour at Highway Bridges, Richardson and Lagasse (eds.), Reston, VA.
- Ref /32/ Nakagawa, H. and Suzuki, K. (1975). An application of stochastic model of sediment motion of local scour around a bridge pier. Proc. 16th Congress, I.A.H.R., Sao Paulo, Brazil, Vol, 2, pp. 228-235.
- Ref /33/ Neill, C.R. (1973). "Guide to Bridge Hydraulics," (Editor) Roads and Transportation. Association of Canada, University of Toronto Press, Toronto, Canada.
- Ref /34/ Noormets, R., Ernstsens, V.B., Bartholoma A., Flemming B.W., Hebbeln D. Local scour in a tidal environment (2003). (Poster - see Attachment A).
- Ref /35/ Qadar, A. (1981). The vortex scour mechanism at bridge piers. Proceedings of Institution of Civil Engineers, Vol. 71, Pt. 2.
- Ref /36/ Qadar, A., Ansari, S.A. (1994). Bridge Pier Scour Equations - An Assessment, Hydraulic Engineering, 1, 61-67. (Proceedings of the 1994 Conference).
- Ref /37/ Rambøll/DHI document. Beskrivelse af eksperimentelle forsøg og deres formål. Note 1 (010001 2004-07-02).
- Ref /38/ Raudkivi, A.J. and Ettema, R. (1983). Clear-water scour at cylindrical piers. J. of Hydraulic Div., A.S.C.E., Vol. 109, No.10, pp. 338-350.
- Ref /39/ Raudkivi, A.J., (1986). Functional Trends of Scour at Bridge Piers. American Soc. of Civil Engineers, Journal Hydraulic Division, Vol. 112, No.1. (or Raudkivi, A.J. (1988). Functional trends of scour at bridge piers. J. of Hydraulic Engg., A.S.C.E., Vol 112, No.1, pp.1-13.)
- Ref /40/ Richardson, E.V., Simons, D.B., Karaki, S., Mahmood, K. and Stevens, M.A., (1975). Highways in the River Environment Design Considerations. Training and Design Manual Prepared for the Federal Highway Administration, May 1975.
- Ref /41/ Richardson, E.V., D.B. Simons, and P.F. Lagasse (2001). River Engineering for Highway Encroachments - Highways in the River Environment. FHWA NHI 01-004, Federal Highway Administration, Hydraulic Series No. 6, Washington, D.C.

- Ref /42/ Richardson, E.V and S.R. Davis (2001). HEC-18. Evaluating scour at Bridges. Hydraulic Engineering Circular No. 18. Fourth edition. National Highway Institute, Federal Highway Administration, U.S. Dept. of Transportation
- Ref /43/ Shen, H.W., Schneider, V.R. and Karaki, S. (1969). Local scour around bridge piers. J. of Hydraulic Div., A.S.C.E., Vol. 95, No. 6, pp. 1919-1940.
- Ref /44/ Sheppard, D. M. Budianto Ontowirjo and Gang Zhao (1999). Local Scour Near Single Piles in Steady Currents, Stream Stability and Scour At Highway Bridges, Compendium of Papers, ASCE Water. Resources Engineering Conferences 1991 to 1998, Edited by E.V. Richardson and P.F. Lagasse.
- Ref /45/ Sheppard, D.M. (2003) Large scale and live bed local pier scour experiments, phase 2, live bed experiments, final report, University of Florida.
- Ref /46/ Simons, D.B. and Richardson, E.V. (1966). Resistance to Flow in Alluvial Channels. Geological Survey Prof. Paper 422-I, Washington, USA.
- Ref /47/ Snamenskaya, N.S. (1969). Morphological Principles of Modeling of River Process International Association of Hydraulic Research, pp195-200.
- Ref /48/ Sumer, B., Fredsoe, J., Christiansen, N (1992). Scour around vertical piles in waves. Journal of waterway, Port, Coastal and Ocean engineering, 118(1), 15-31.
- Ref /49/ Sumer, B.M., Whitehouse, R.J.S. & Toerum, A. (2001): Scour around coastal structures: a summary of recent research. Coastal Engineering, 44, p.153-190.
- Ref /50/ Sumer B.M, J. Fredsøe (2002). The mechanics of scour in the marine environment. Advanced Series on Ocean Engineering. Vol. 17. 2002.
- Ref /51/ Van Rijn, L.C. (1993). Principles of sediment transport in rivers, estuaries and coastal seas. Aqua Publications, The Netherlands.
- Ref /52/ Whitehouse, R.J.S. (1998). Scour at marine structures. Thomas Telford, London, 216 pp.
- Ref /53/ Yanmaz, M.A. and Altinbilek, H.D. (1991). Study of time dependent local scour around bridge piers. J. of Hydraulic Engg., A.S.C.E. Vol. 117, No. 10, Oct., pp. 1247-1263.

OFFSHORE WIND TURBINES SITUATED IN AREAS WITH STRONG CURRENTS

REPORT 3

Experimental study of scour around offshore wind
turbines in areas with strong currents

Author

Brian Juul Larsen, Aalborg University

Work Group

Peter Frigaard, Aalborg University
Erik Asp Hansen, DHI - Water & Environment
Morten Sand Jensen, Rambøll

Table of contents

1.	Introduction	81
2.	Tests	82
2.1.	Scaling	82
2.2.	Description of Model	82
2.3.	Description of Set-up	82
2.4.	Test programme	82
2.5.	Measurements	85
3.	Results	86
3.1.	Pictures	96
Appendix 1 – Irregular Waves		102

1. Introduction

In connection to the project “Offshore Wind Turbines situated in Areas with Strong Currents” a series of model tests have been made at Aalborg University. The project is lead by Offshore Center Denmark and the companies involved are: DHI, Rambøll, Vestas, A2SEA and Aalborg University in Aalborg and Esbjerg.

The overall purpose of the project is to establish a better understanding of the development of scour at circular monopiles of offshore windturbines.

The purpose of the model tests is to illuminate various aspects of scour developed under typical conditions but also to shed light on the influence on scour from various parameters thought to have a significant impact on scour. Furthermore it is the ambition to use the test results in a design situation.

For further information on the conducted test programme contact Brian Juul Larsen (phone: 96 35 72 31, email: i5bjl@civil.aau.dk) or Peter Frigaard (phone: 96 35 84 79, email: peter.frigaard@civil.aau.dk).

2. Tests

2.1. Scaling

The tests are performed with a length scale of 1:30. All values are scaled according to Froudes modellaw:

$$\begin{aligned}\text{Length:} & \quad \lambda_L = 30 \\ \text{Time:} & \quad \lambda_T = \lambda_L^{1/2} = 5.48\end{aligned}$$

All measures in the following report will be in model scale values.

2.2. Description of Model

The two types of foundation that are being tested are monopiles of 0.1 and 0.2 meters in diameter.

2.3. Description of Set-up

The tests are conducted in a wave flume that is 18.7 meters long and 1.2 meters wide, see figure 1.

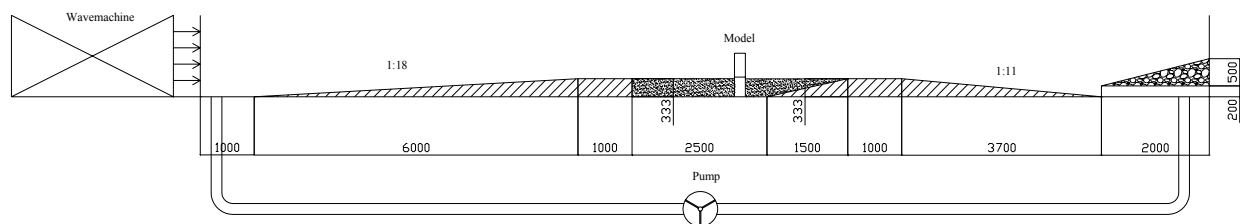


Figure 1. The wave flume. All measures in millimeters.

The top half of the piles can be removed. This feature is used during the profiling of the bed. Sand is spread out in a thin layer across the concrete slopes to reduce the global scour in the sandbox.

2.4. Test programme

The test programme has been designed by Morten Sand Jensen from the consultancy company Rambøll. In relation to the present report on offshore windturbines in areas with strong currents Morten Sand Jensen has also published a review on scour under such conditions.

Test No	Comments	Diameter of monopile D [m]	Significant wave height H_s [m]	Spectral peak period T_p [s]	Water depth seaward d_0 [m]	Water depth at pile h_t [-]	Current induced velocity U_c [m/s]
1.1	<i>breaking waves, with and without unidirectional current</i>	0.10	0.12	1.28	0.62	0.29	0.00
1.2		0.10	0.12	2.01	0.62	0.29	0.00
1.3		0.10	0.08	1.28	0.50	0.17	0.00
1.4		0.10	0.08	2.01	0.50	0.17	0.00
1.5		0.10	0.12	1.28	0.62	0.29	0.30
1.6		0.10	0.12	2.01	0.62	0.29	0.30
2.1	<i>Only current - tidal current</i>	0.10			0.62	0.29	0.30
2.2		0.10			0.62	0.29	0.40
2.3		0.10			0.62	0.29	0.50
2.4		0.10			0.50	0.17	0.30
2.5		0.10			0.50	0.17	0.40
2.6		0.10			0.50	0.17	0.50
2.7		0.10			0.43	0.10	0.30
2.8		0.10			0.43	0.10	0.40
2.9		0.10			0.43	0.10	0.50
2.10		0.20			0.62	0.29	0.30
2.11		0.20			0.62	0.29	0.40
2.12		0.20			0.62	0.29	0.50
2.13		0.20			0.50	0.17	0.30
2.14		0.20			0.50	0.17	0.40
2.15		0.20			0.50	0.17	0.50
2.16		0.20			0.43	0.10	0.30
2.17		0.20			0.43	0.10	0.40
2.18		0.20			0.43	0.10	0.50
3.1	<i>Regular waves</i>	0.20	0.10	1.28	0.50	0.17	0.00
3.2		0.20	0.10	2.01	0.50	0.17	0.00
3.3		0.20	0.10	2.50	0.50	0.17	0.00

Test No	Comments	Diameter of monopile D [m]	Wave height H [m]	Period T [s]	Water depth seaward d_0 [m]	Water depth at pile h_t [-]	Current induced velocity U_c [m/s]
4.1	<i>Unidir. current</i>	0.10			0.62	0.29	0.30
4.2		0.10			0.62	0.29	0.40
4.3		0.10			0.62	0.29	0.50
4.4		0.10			0.50	0.17	0.30
4.5		0.10			0.50	0.17	0.40
4.6		0.10			0.50	0.17	0.50
4.7		0.10			0.43	0.10	0.30
4.8		0.10			0.43	0.10	0.40
4.9		0.10			0.43	0.10	0.50
4.10		0.20			0.62	0.29	0.30
4.11		0.20			0.62	0.29	0.40
4.12		0.20			0.62	0.29	0.50
4.13		0.20			0.50	0.17	0.30
4.14		0.20			0.50	0.17	0.40
4.15		0.20			0.50	0.17	0.50
4.16		0.20			0.43	0.10	0.30
4.17		0.20			0.43	0.10	0.40
4.18		0.20			0.43	0.10	0.50

Table 1. Test programme for the scour tests.

2.5. Measurements

The wave elevation signal is measured beside the model by means of three wave gauges. The wave spectres and the elevation signals are shown in appendix 1. The current velocities are measured with an ultrasonic flowmeter. The scour is measured in a 1.5 cm by 1.5 cm grid with a laser (profiler). The measured grid is 1.5 meter long and 0.93 meters wide. In addition to that the scour holes are measured manually. Figure 2 shows the definitions of stretch and depth (S) of the scour hole.

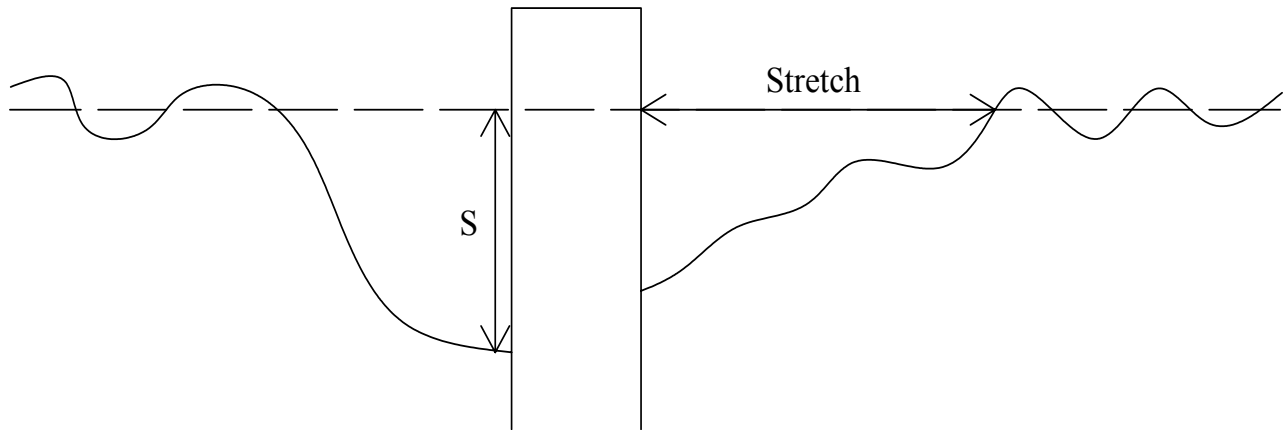


Figure 2. Definitions of stretch and depth (S) of the scour hole.

3. Results

Table 2 shows the maximum reached scour depths over the course of the tests. These maxima are the largest depths found from the profiling and / or the manual measurements.

Test No	Diameter of monopile D [m]	Significant wave height H_s [m]	Spectral peak period T_p [s]	Water depth at pile h_t [-]	Current induced velocity U_c [m/s]	Scour depth S [m]	Relative scour depth S/D [-]
1.1	0.10	0.11	1.31	0.29	0.00	0.012	0.120
1.2	0.10	0.12	1.97	0.29	0.00	0.020	0.200
1.3	0.10	0.07	1.28	0.17	0.00	0.011	0.110
1.4	0.10	0.08	1.97	0.17	0.00	0.014	0.140
1.5	0.10	0.11	1.31	0.29	0.30	0.078	0.780
1.6	0.10	0.12	1.97	0.29	0.30	0.078	0.780
2.1	0.10			0.29	0.30	0.118	1.180
2.2	0.10			0.29	0.40	0.154	1.540
2.3	0.10			0.29	0.50	0.140	1.400
2.4	0.10			0.17	0.30	0.129	1.290
2.5	0.10			0.17	0.40	0.155	1.550
2.6	0.10			0.17	0.50	0.170	1.700
2.7	0.10			0.10	0.30	0.120	1.200
2.8	0.10			0.10	0.40	0.145	1.450
2.9	0.10			0.10	0.50	0.175	1.750
2.10	0.20			0.29	0.30	0.150	0.750
2.11	0.20			0.29	0.40	0.270	1.350
2.12	0.20			0.29	0.50	0.240	1.200
2.13	0.20			0.17	0.30	0.160	0.800
2.14	0.20			0.17	0.40	0.245	1.225
2.15	0.20			0.17	0.50	0.227	1.135
2.16	0.20			0.10	0.30	0.150	0.750
2.17	0.20			0.10	0.40	0.220	1.100
2.18	0.20			0.10	0.50	0.250	1.250

Test No	Diameter of monopile D [m]	Wave height H [m]	Period T [s]	Water depth at pile h_t [-]	Current induced velocity U_c [m/s]	Scour depth S [m]	Relative scour depth S/D [-]
3.1	0.20	0.10	1.28	0.17	0.00	0.019	0.095
3.2	0.20	0.11	2.01	0.17	0.00	0.032	0.160
3.3	0.20	0.09	2.50	0.17	0.00	0.026	0.260
4.1	0.10			0.29	0.30	0.085	0.850
4.2	0.10			0.29	0.40	0.118	1.180
4.3	0.10			0.29	0.50	0.118	1.180
4.4	0.10			0.17	0.30	0.138	1.380
4.5	0.10			0.17	0.40	0.131	1.310
4.6	0.10			0.17	0.50	0.165	1.650
4.7	0.10			0.10	0.30	0.105	1.050
4.8	0.10			0.10	0.40	0.085	0.850
4.9	0.10			0.10	0.50	0.160	1.600
4.10	0.20			0.29	0.30	0.055	0.275
4.11	0.20			0.29	0.40	0.240	1.200
4.12	0.20			0.29	0.50	0.240	1.200
4.13	0.20			0.17	0.30	0.095	0.475
4.14	0.20			0.17	0.40	0.225	1.125
4.15	0.20			0.17	0.50	0.150	0.750
4.16	0.20			0.10	0.30	0.070	0.350
4.17	0.20			0.10	0.40	0.225	1.125
4.18	0.20			0.10	0.50	0.230	1.150

Table 2. Maximum reached scour depths over the course of the tests.

Due to global scour in the sand box the scour depths in table 2 can be slightly uncertain if they are regarded purely as local scour. The global scour has been estimated and subtracted but it can be difficult to quantify and separate from the local scour.

For tests 2.* and 4.* the average S/D values are:

Tidal current	1.26
Unidirectional current	1.04
$\varnothing = 0.1$ m	1.34
$\varnothing = 0.2$ m	0.96
$U = 0.3$ m/s	0.86
$U = 0.4$ m/s	1.25
$U = 0.5$ m/s	1.33

Table 3. Average S/D values.

Column 7 and 8 of table 2 are presented graphically in figure 3 and 4.

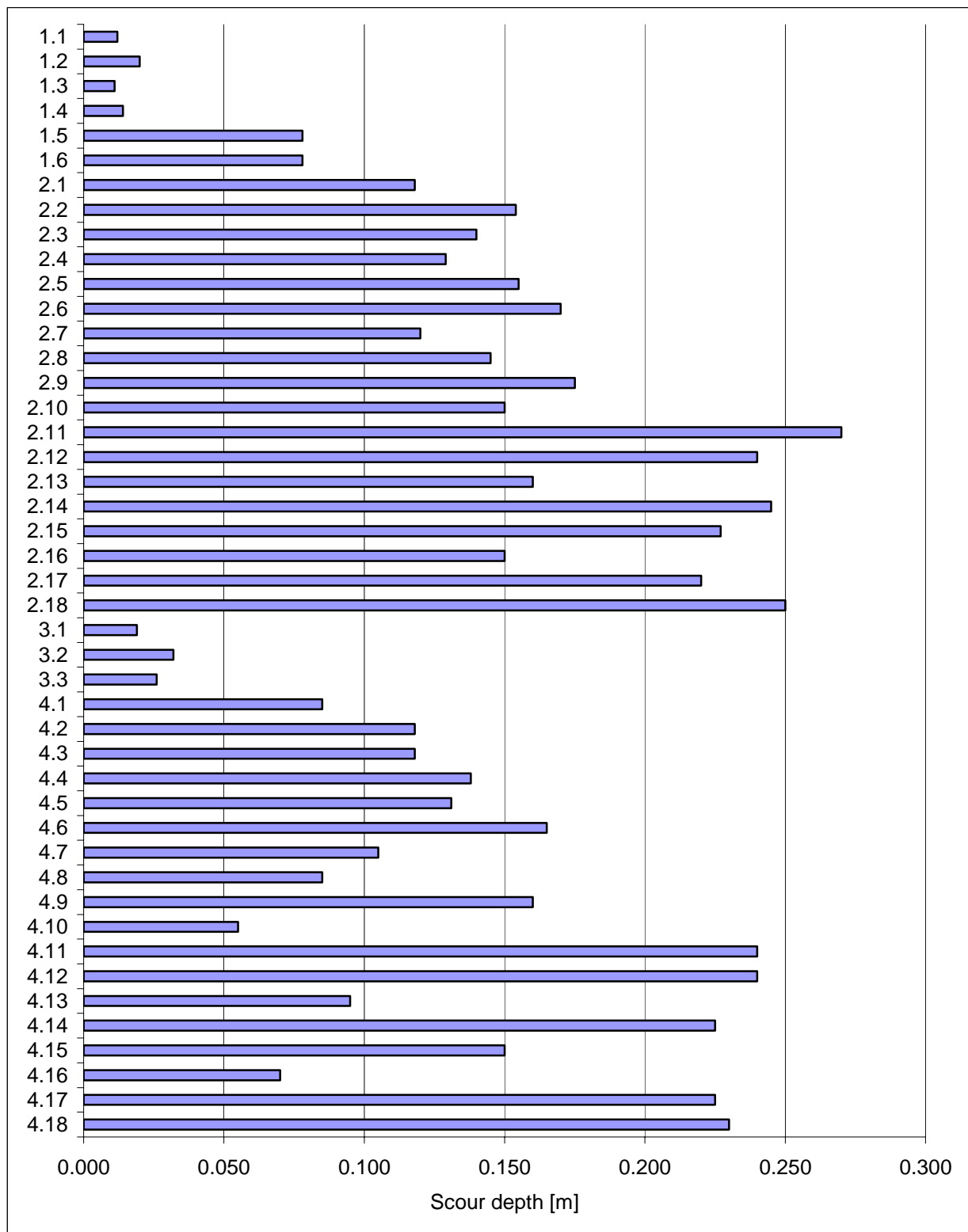


Figure 3. Maximum reached scour depths over the course of the tests.

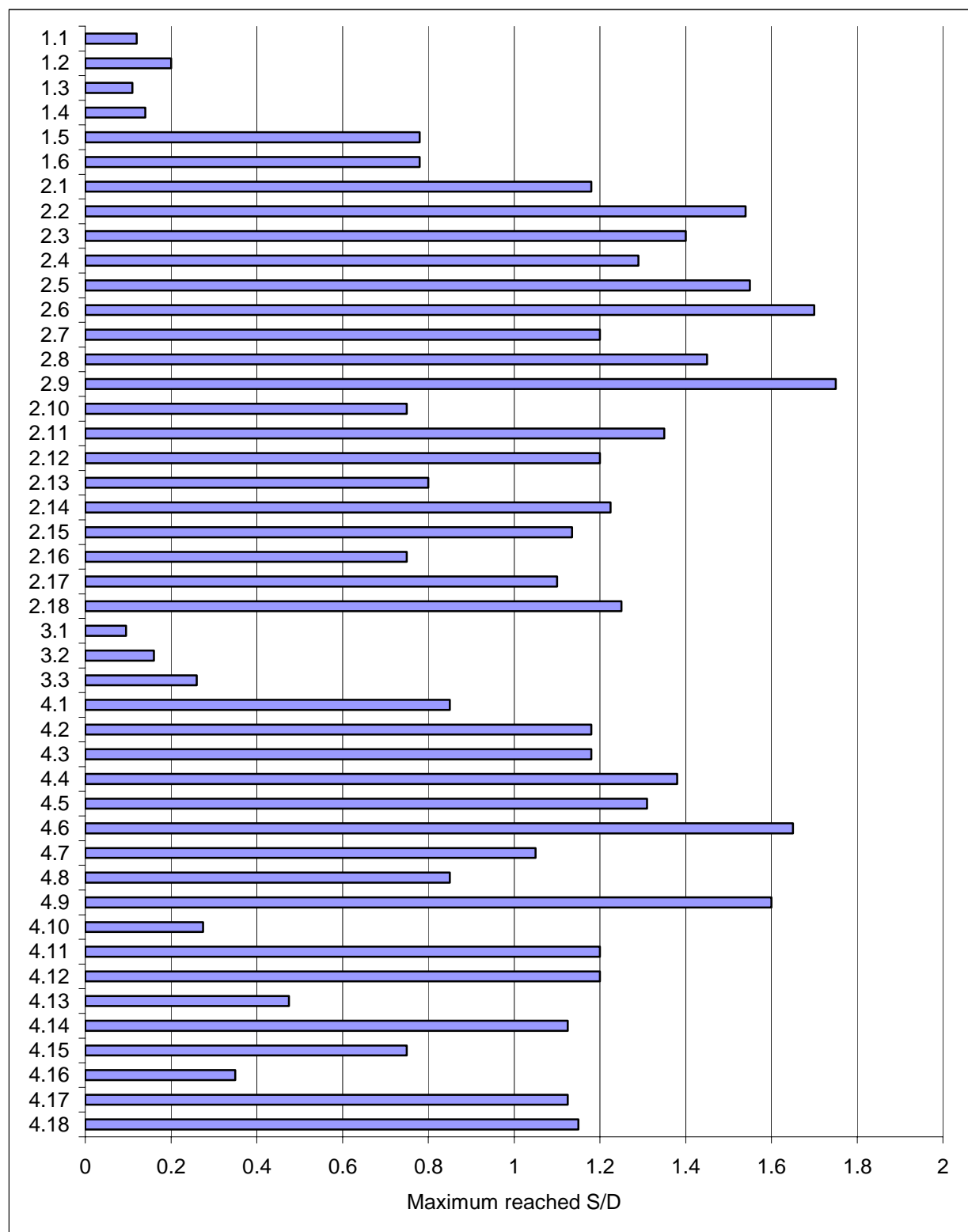


Figure 4. Maximum reached S/D over the course of the tests.

The test duration is not the same for all tests. Figure 5 show the maximum reached S/D and the test duration of every test in the test programme.

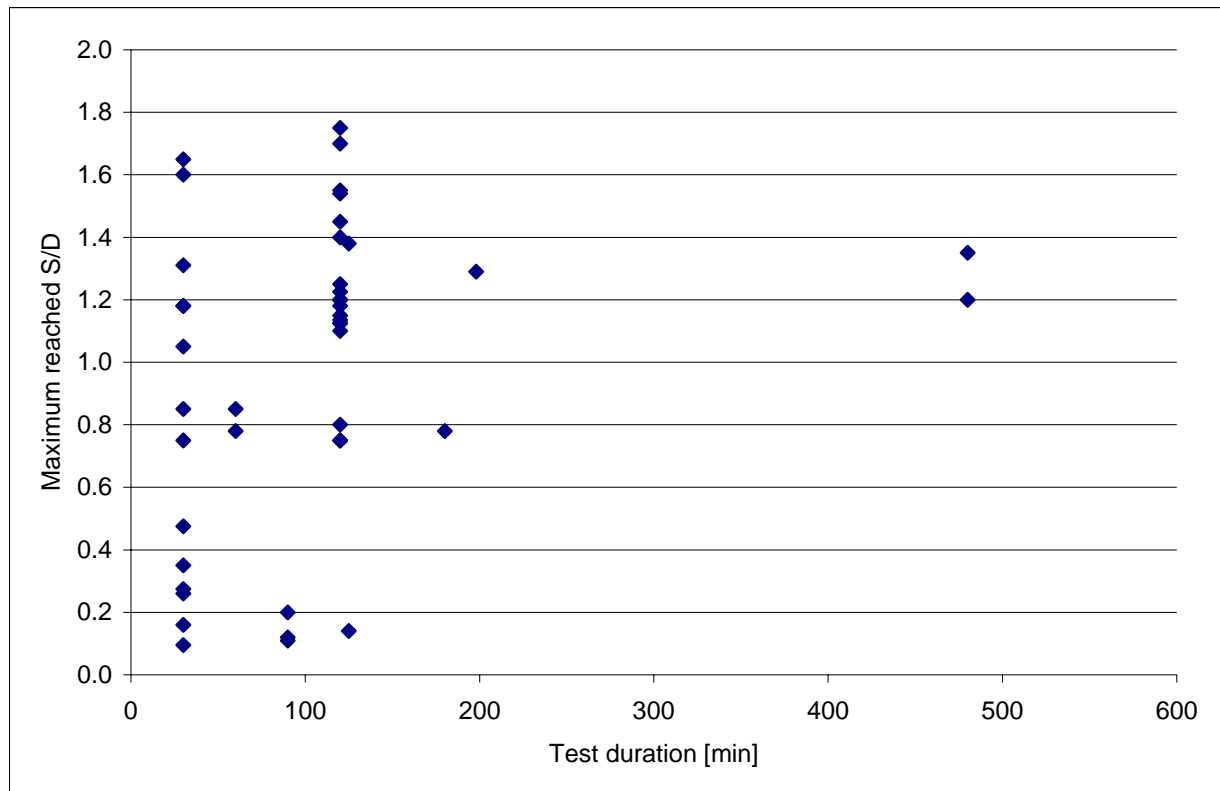


Figure 5. Maximum reached S/D and the test duration of every test in the test programme.

As it can be seen from the test results the cases with waves gives less scour compared with tests where only current is applied. In the following figures focus will be put on part 2 and 4 of the test programme with tidal and unidirectional currents.

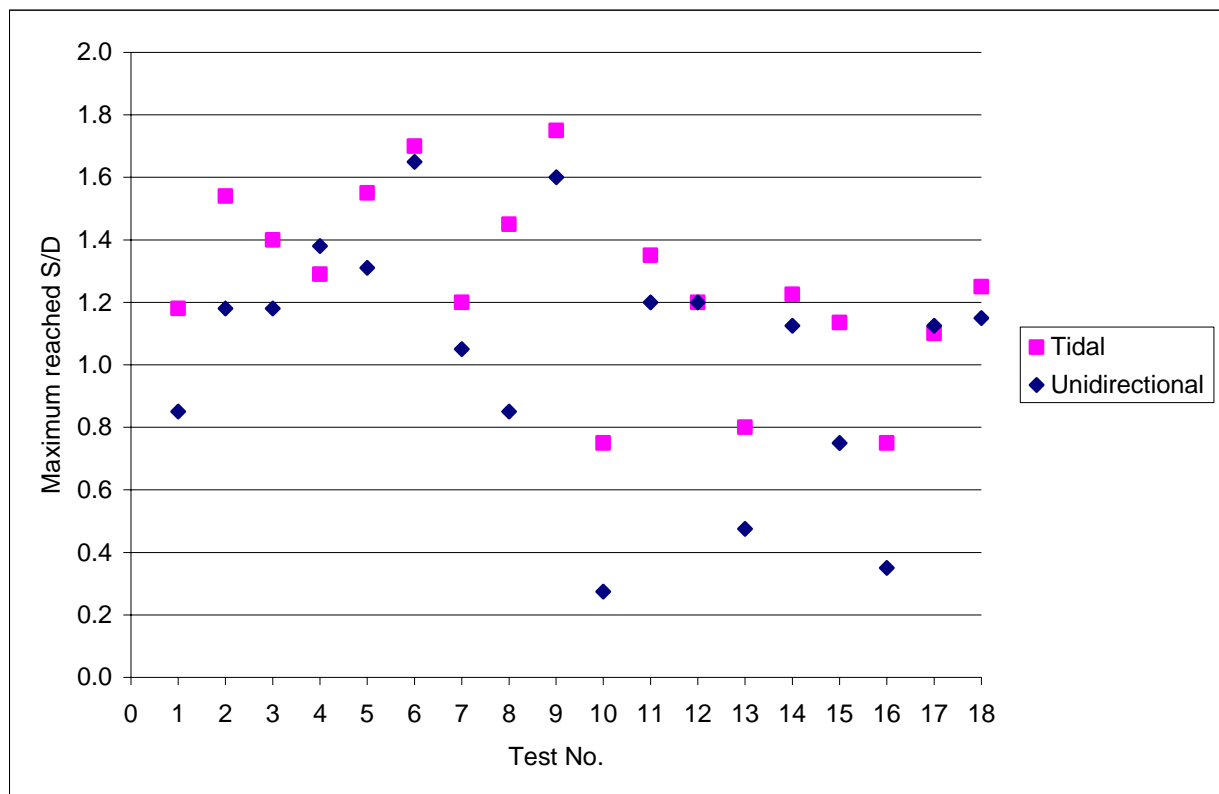


Figure 6. Comparison between test 2.* and 4.*.

With focus on pile size the tests in part 2 and 4 gives the following:

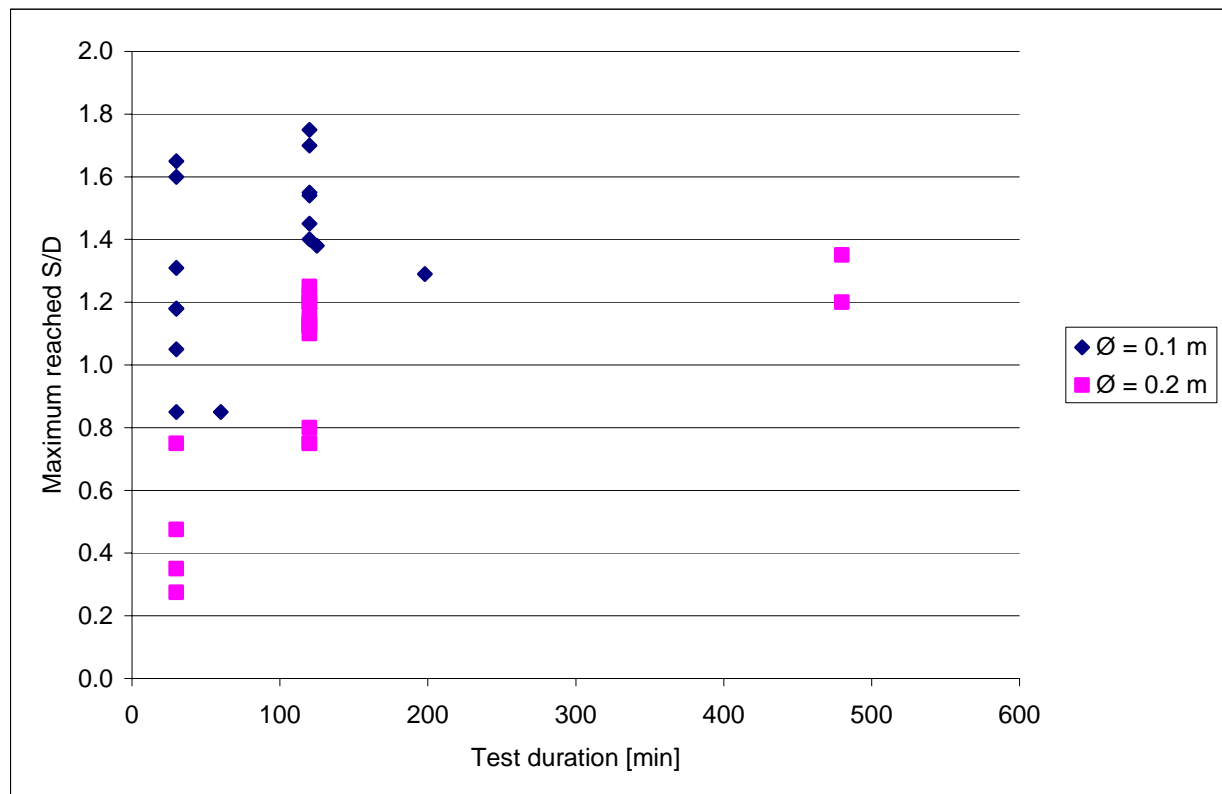


Figure 7. Comparison between pile sizes.

With focus on current velocity the tests in part 2 and 4 gives the following:

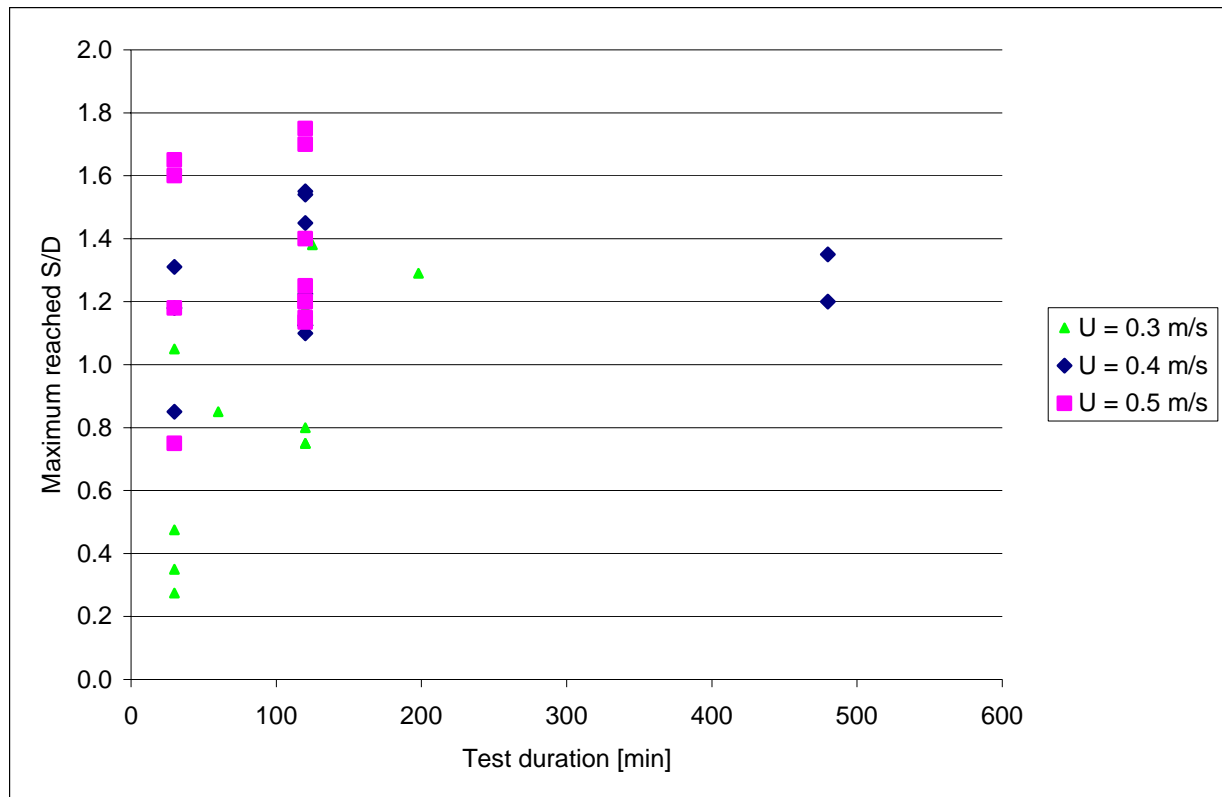


Figure 8. Comparison between current velocities.

A good part of the tests plotted in figure 8 have been measured manually some times over the course of the tests. The result of that can be seen in figure 9.

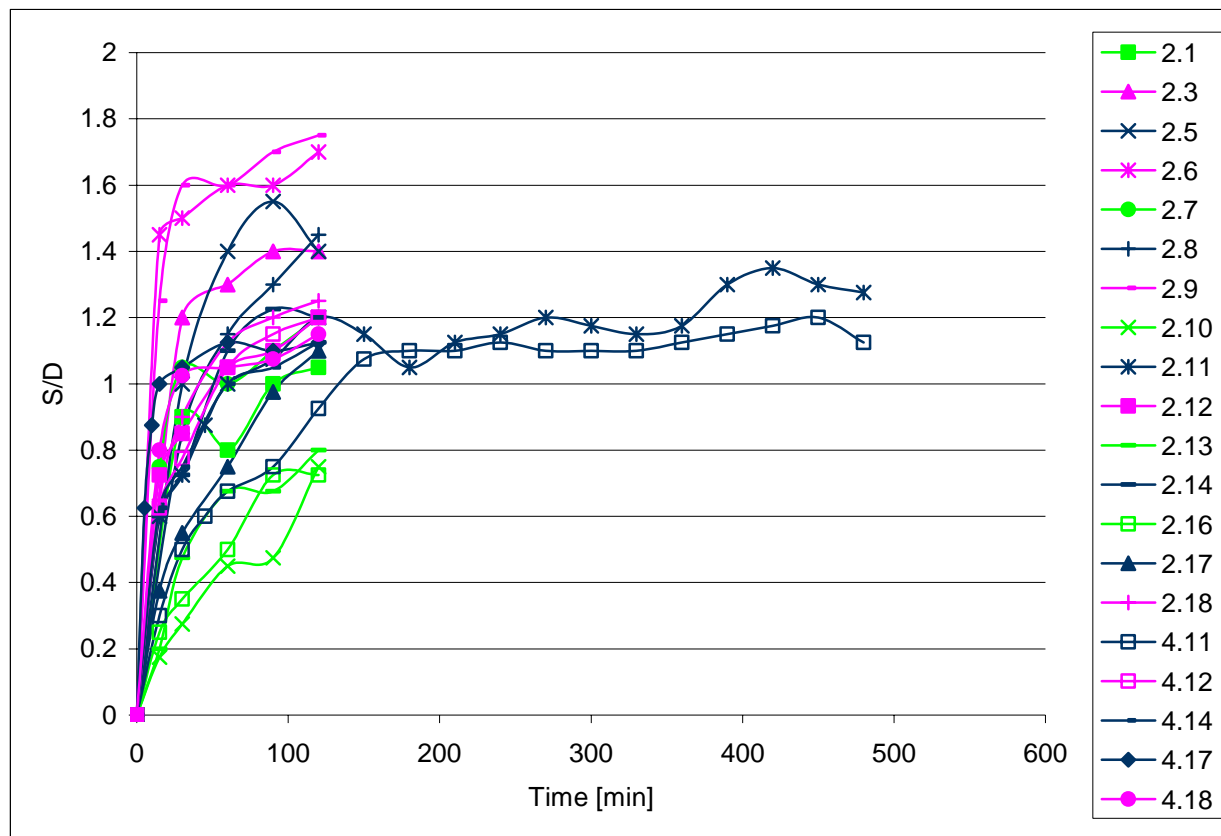


Figure 9. Comparison between current velocities.

Green: $U = 0.3$ m/s

Blue: $U = 0.4$ m/s

Pink: $U = 0.5$ m/s

As it can be seen from figure 9 an eight hour comparative study has been made on test 2.11 and 4.11. Apart from the depth the biggest stretch of the scour holes have been monitored. By use of the biggest depth and the biggest stretch and simple geometric assumptions the following conservative calculations of the volume of the scour holes have been made:

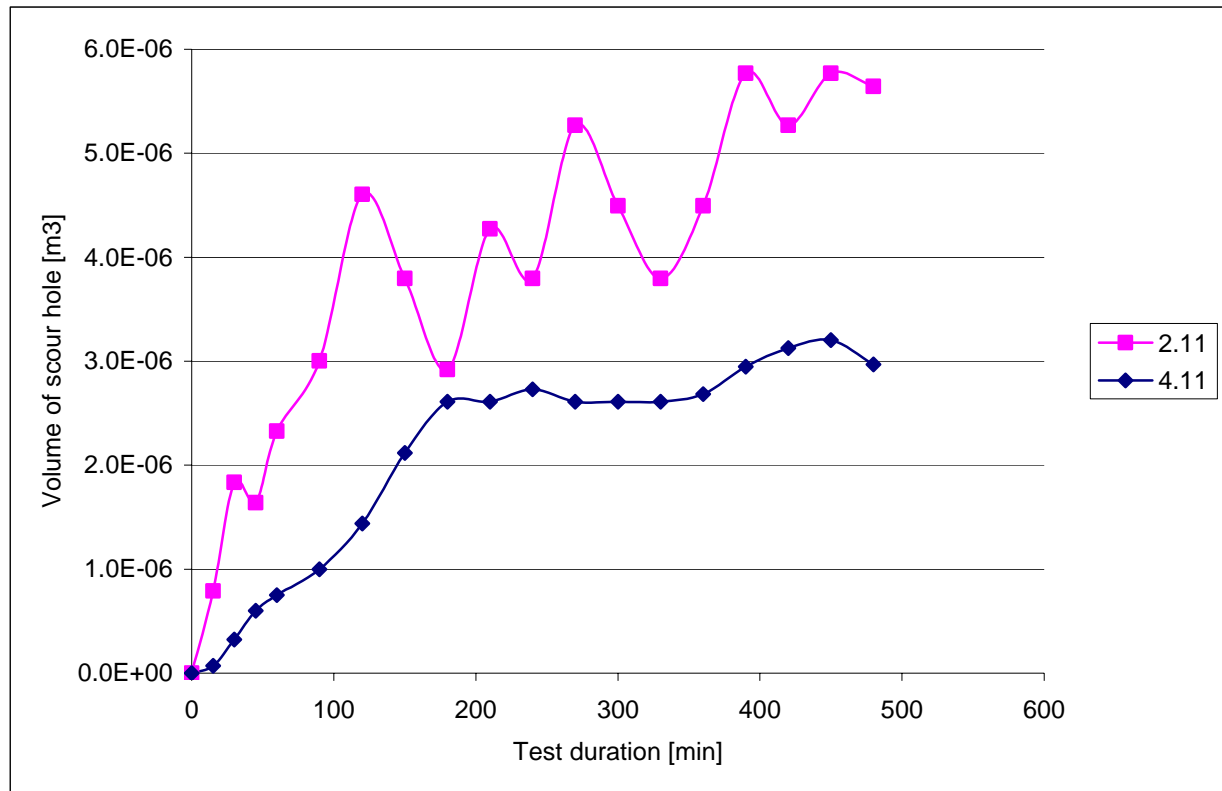


Figure 10. Variation of scour hole volume over time.

3.1. Pictures



Figure 11. The bed has been measured with a profiler. A laser measuring the bed level in a grid.

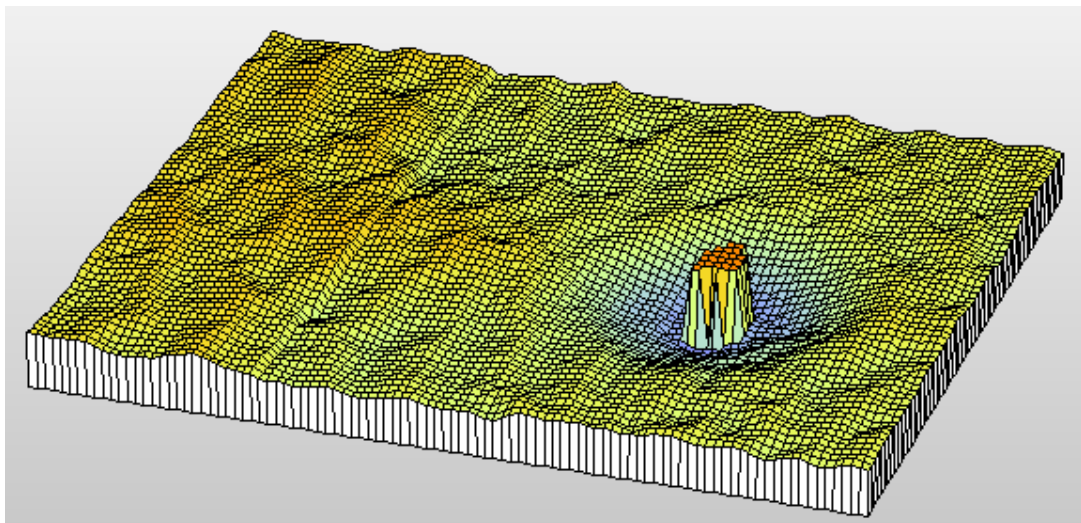


Figure 12. The outcome of a profiler measurement could look this way.

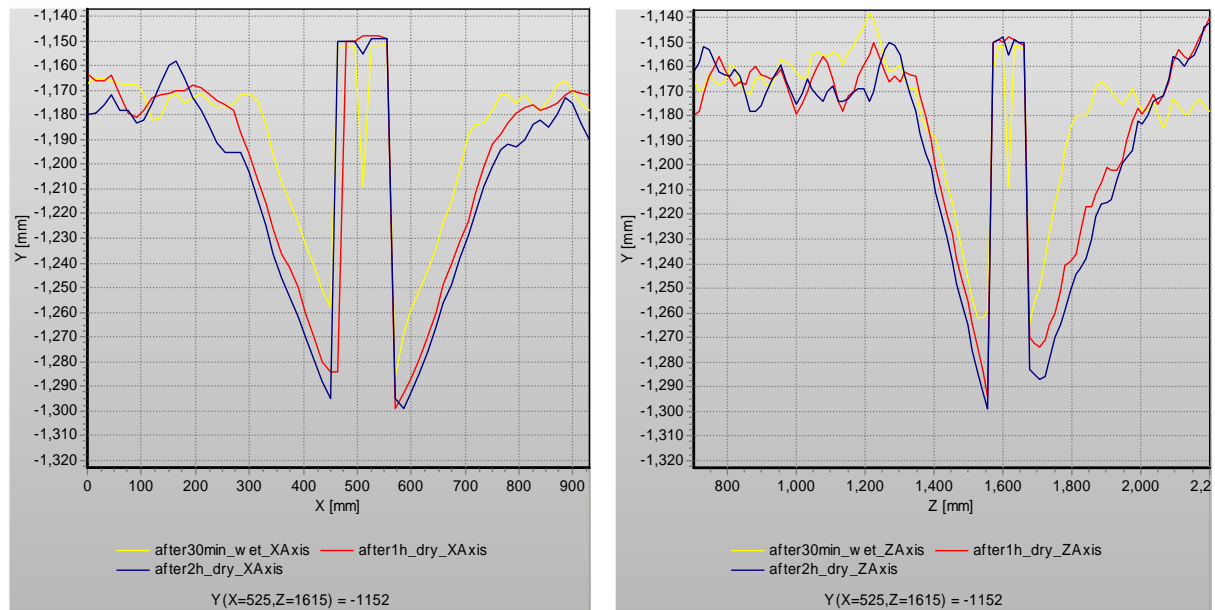


Figure 13. With several measurements over the course of the same test the development of the scour hole has been monitored.



Figure 14. The picture is from test 1.1.
In tests 1.1 – 1.4 and 3.1 – 3.3 the scour depths are mainly caused by ripples.



Figure 15. The picture is from test 1.5.
In test 1.5 and 1.6 there was both ripples and a small scour hole.

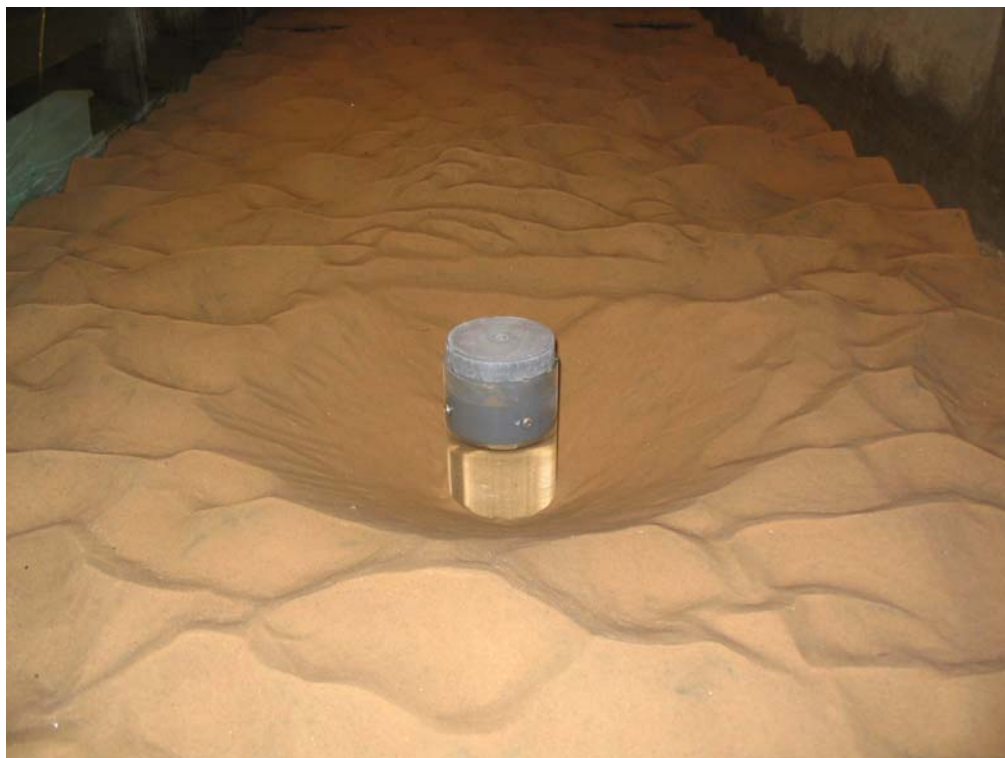


Figure 16. The picture is from test 2.2.
In tests 2.1 – 2.9 the local scour holes around the pile are of significant magnitude in comparison to the ripples and the global scour.



Figure 17. The picture is from test 2.11.

In tests 2.10 – 2.18 the stretch of the scour holes was almost as wide as the width of the flume.



Figure 18. The picture is from test 4.2.

In the tests with unidirectional current there is hump behind the scour hole. The hump on the lee side is the same width as the scour hole and up to 10 times as long.





Figure 19. The pictures are from test 4.11.

The scour holes in part 4 are circular with a tale from $\pm 45^\circ$ seen from the lee side. Inside the scour hole there is a small hump on the lee side and the circle shape is clearly marked with small ripples “pointing” towards the center of the pile.

As it can be seen from figure 14 – 19 the scour holes have certain characteristics depending on which part of the test programme they come from.

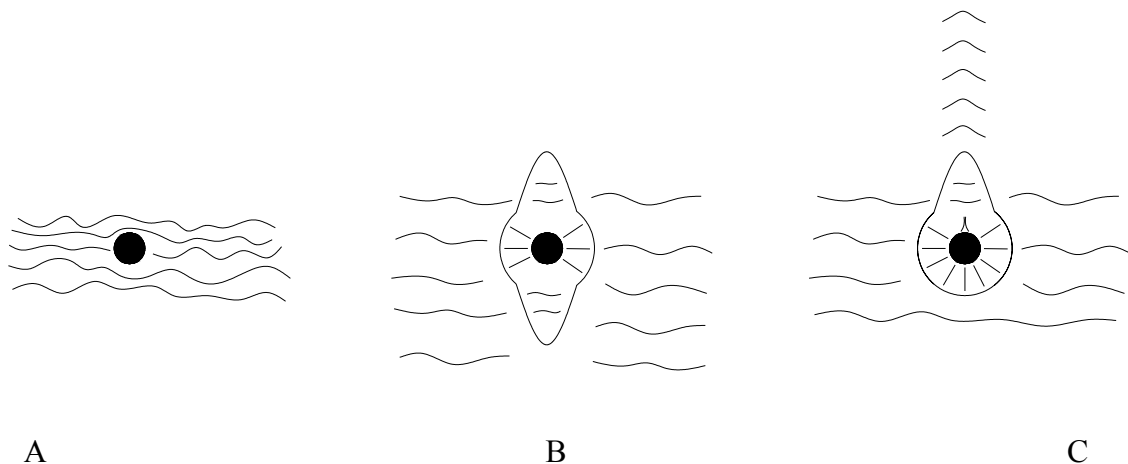


Figure 20. Typical bed contours from the tests.

- A: Part 1 and 3. Waves creating a bed dominated by ripples. Barely any scour.
- B: Part 2. Hole created by tidal current creating two tails to make the hole longer than it is wide.
- C: Part 4. Unidirectional current creates a hump both inside the hole on the lee side and a long one behind the scour hole.

4. Appendix 1 – Irregular Waves

This appendix shows the wave spectres for the tests with irregular waves – 1.1 to 1.6.

Test 1.1

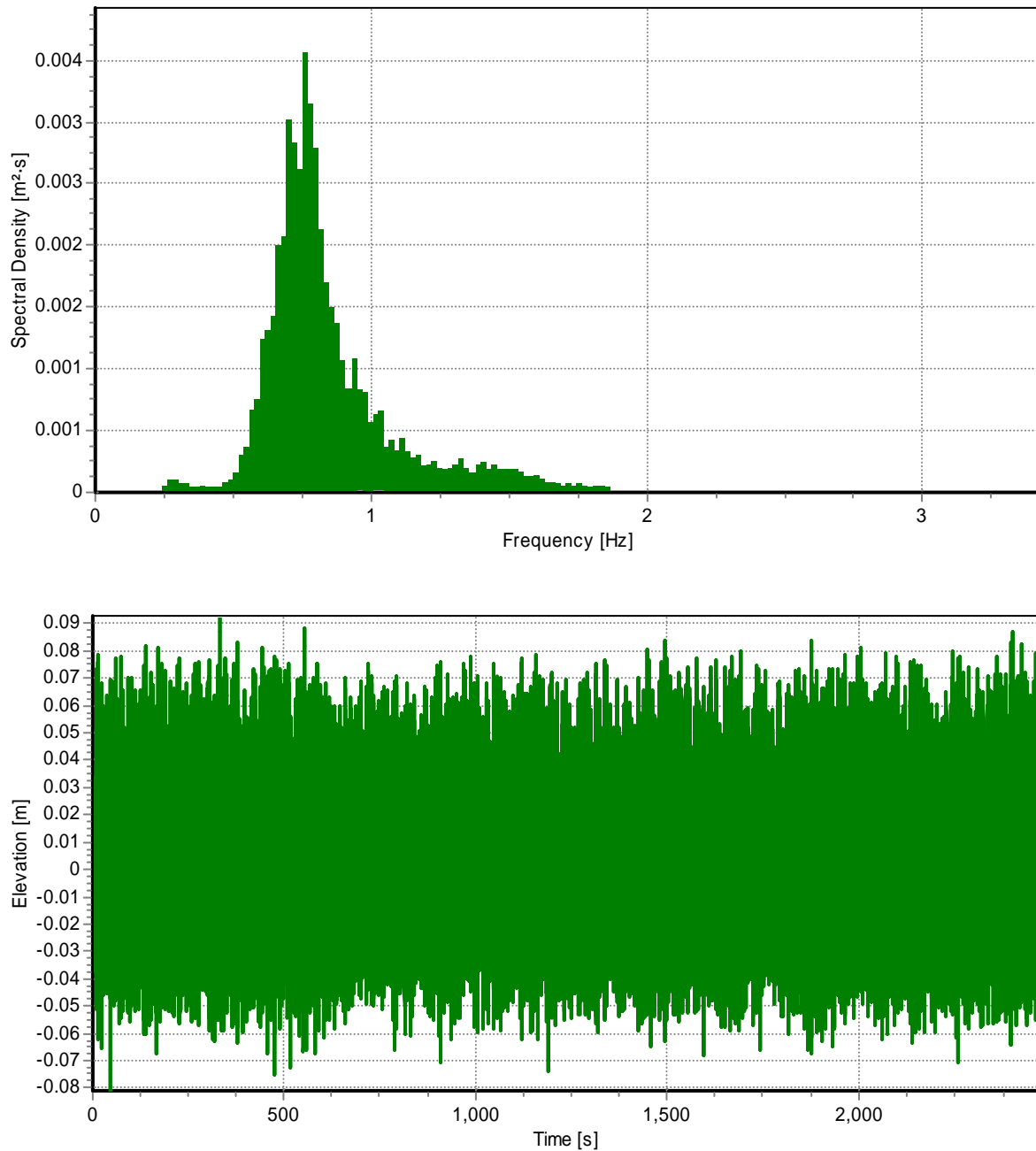


Figure 1.1. Wave spectre and elevation signal for test 1.1.

Test 1.2

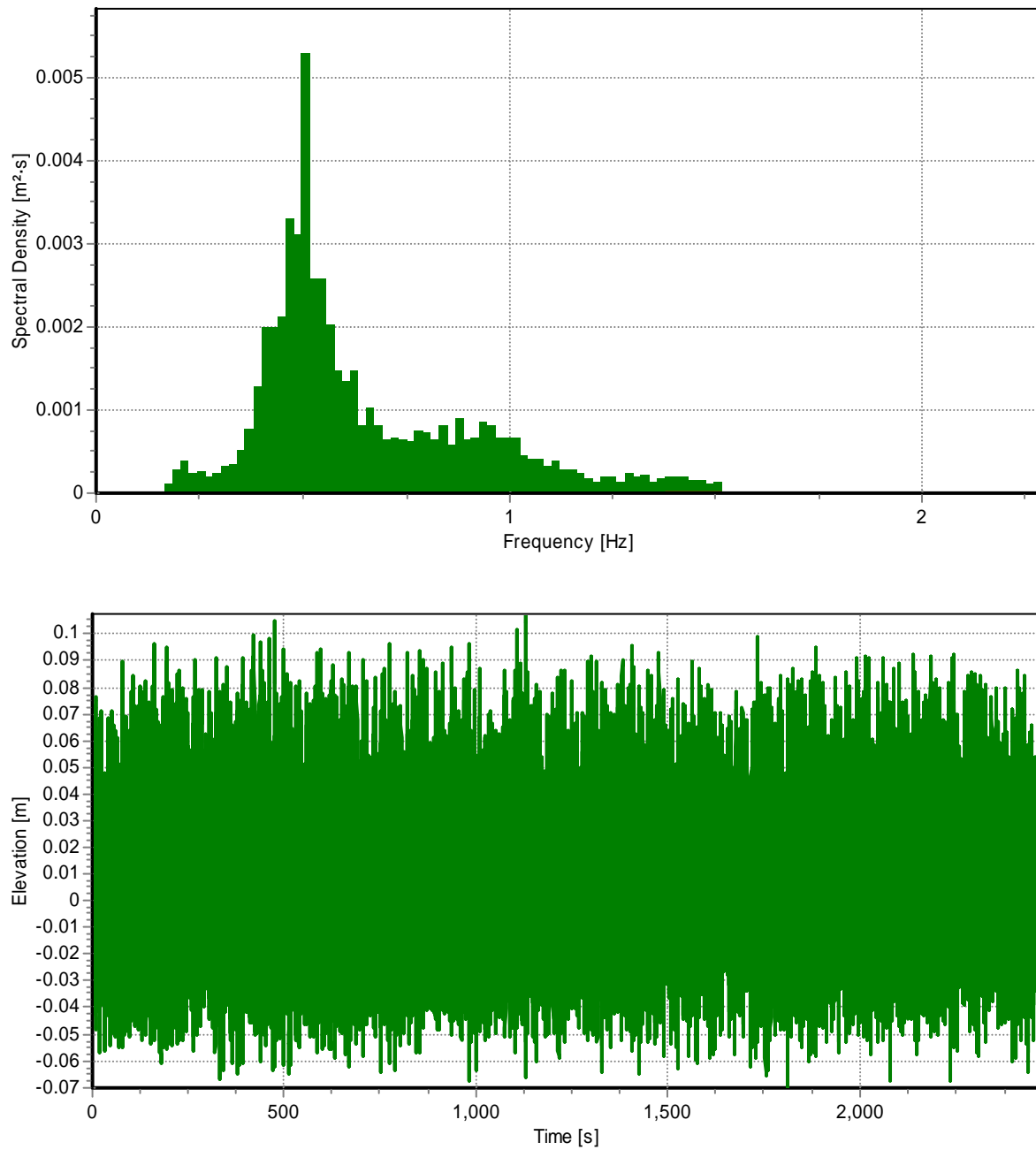


Figure 1.2. Wave spectre and elevation signal for test 1.2.

Test 1.3

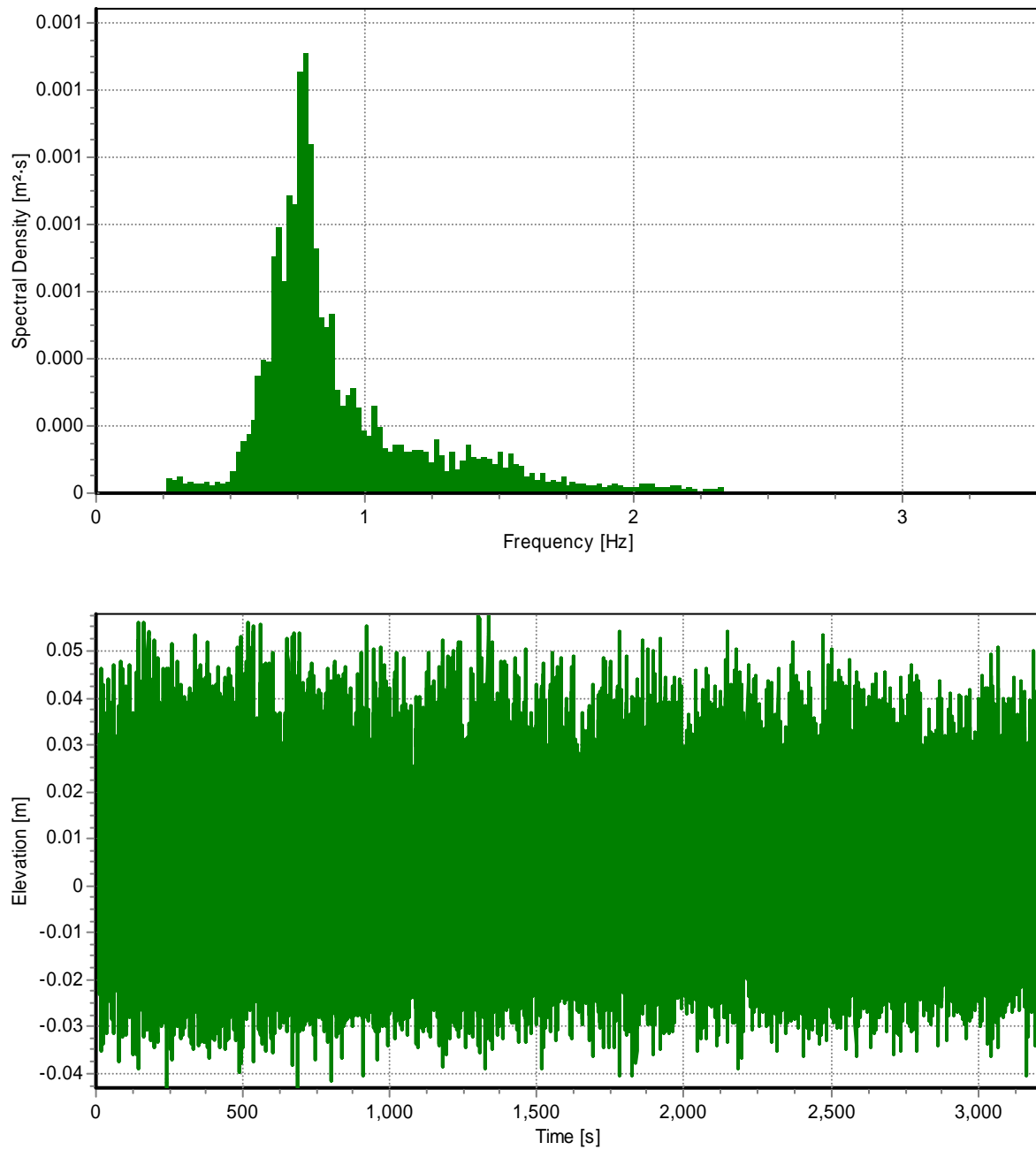


Figure 1.3. Wave spectre and elevation signal for test 1.3.

Test 1.4

Due to technical problems with the measuring device there are no result plots available for test 1.4.

Test 1.5

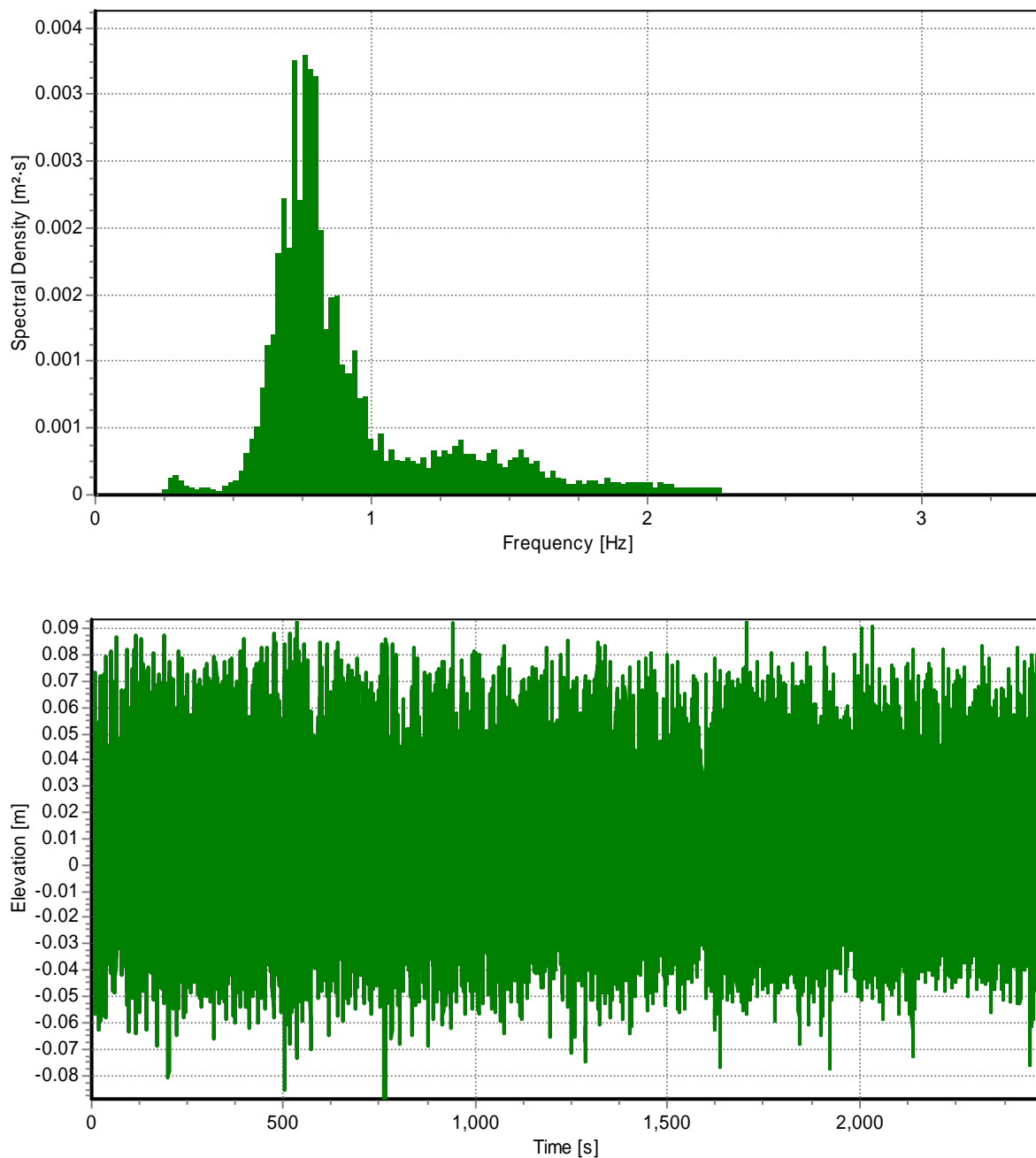


Figure 1.4. Wave spectre and elevation signal for test 1.5.

Test 1.6

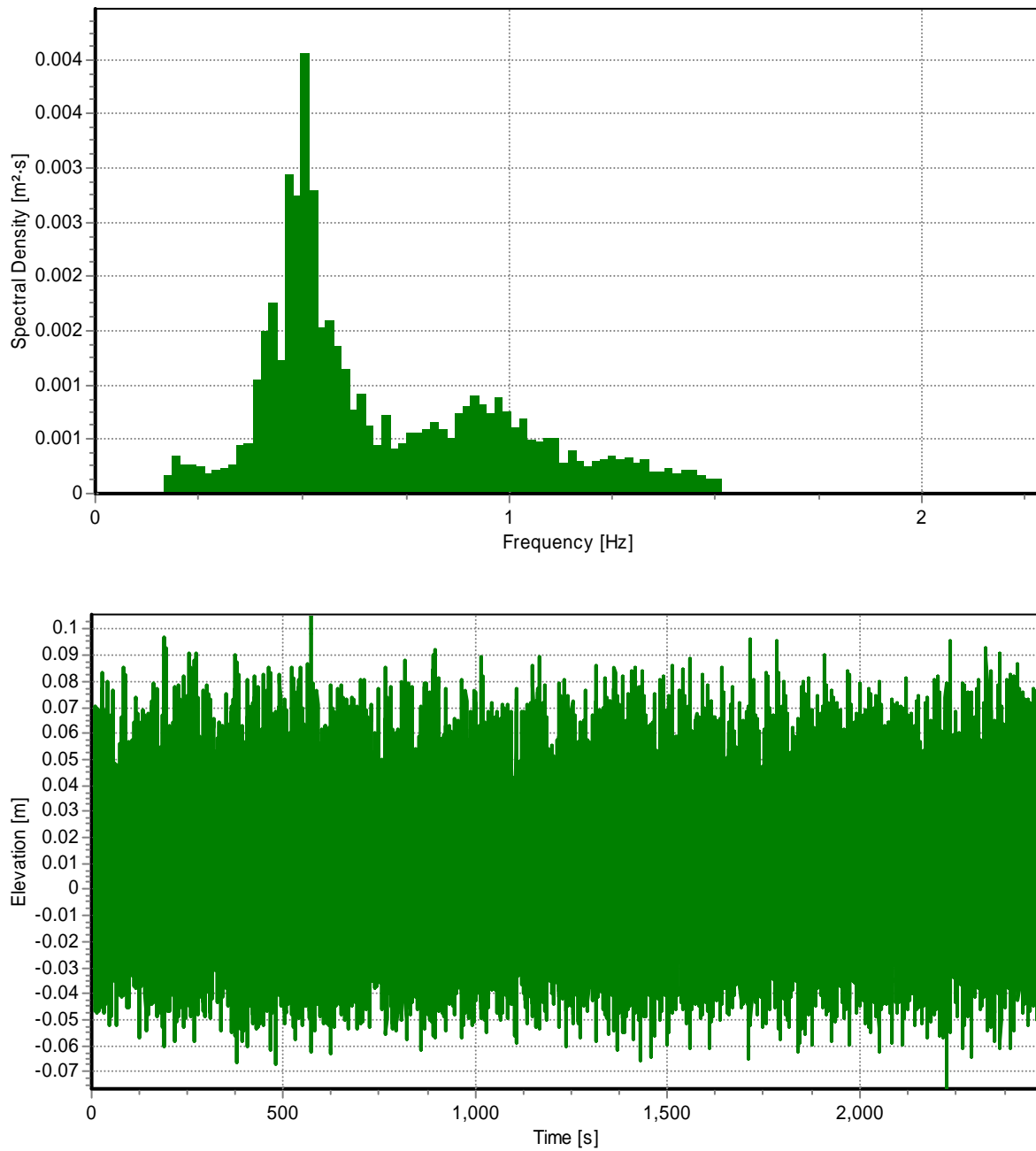


Figure 1.5. Wave spectre and elevation signal for test 1.6.

OFFSHORE WIND TURBINES SITUATED IN AREAS WITH STRONG CURRENTS

REPORT 4

Influence of breaking waves on scour processes around
circular offshore wind turbine foundations

Author

Peter Frigaard, Aalborg University
Leen De Vos, Aalborg University
Erik D. Christensen, DHI - Water & Environment
Erik Asp Hansen, DHI - Water & Environment

Work Group

Peter Frigaard, Aalborg University
Leen De Vos, Aalborg University
Erik D. Christensen, DHI - Water & Environment
Erik Asp Hansen, DHI - Water & Environment

Table of contents

1.	Introduction	109
2.	Experimental set-up	110
2.1.	Scour tests	110
2.2.	Particle image velocimetry	111
2.3.	Numerical modelling	113
3.	Experimental results	115
3.1.	Scour tests	115
3.2.	Particle image velocimetry	117
3.3.	Numerical results	121
4.	Conclusion	124
5.	References	125
6.	Notation	126

1. Introduction

Scour and scour protection are major issues to consider when constructing offshore wind farms. The majority of wind farms to be built are situated in environments characterized by strong influence of tides, wind-induced currents and waves, both breaking and non-breaking. If the turbines are placed without protection on an erodible seabed, a scour hole will develop. The engineer can either include the scour in his design, or he can place a scour protection on the seabed. Which of the two solutions is the most attractive depends on the cost of providing scour protection compared with the extra cost of making the pile stronger/longer, extra cable dredging etc. The optimal solution will depend to a large extent on the maximal scour depth an unprotected foundation will experience during its lifetime.

For many years, engineers designing bridges have been used to taking into account scour around structures exposed to steady currents. The "Manual on scour at bridges and other hydraulic structures" by CIRIA (2002) is an example of a book giving a good overview of this topic. The typical fully-developed scour depth in a uniform current is 1 to 1.5 times the pile diameter, resulting in a typical maximum scour depth in the range of 5-8 m for a typical pile with a diameter equal to 5 m.

On the other hand, wave scour has not received the same amount of attention. Nevertheless, with the development of offshore wind farms, there has been a growing focus on wave scour. Two excellent books to give an overview of wave induced scour and scour caused by combined waves and currents are "Scour at marine structures" by Whitehouse (1998) and "The mechanics of scour in the marine environment" by Sumer and Fredsøe (2002).

It is generally known and accepted that scour around a pile caused by current only is decreased when non-breaking (short) waves are superimposed on the current. So far, little knowledge on the effect of breaking waves superimposed on a current is available. Bijker and De Bruyn (1988) measured greater scour depths (up to $S_e/D = 1.9$) when breaking waves are superimposed on a current, which is considerably (up to 46%) larger than the scour in the current-only situation. They relate the increase of the scour to the observed increase of the orbital velocity under breaking waves.

Today's practice has not yet been defined, but some engineers include possible wave breaking in their design by increasing scour depth for current alone. This simply means that the design scour depth is considered to be more than 1.5 times the pile diameter. This report includes an experimental study of scour processes in physical model as well as an experimental study using particle image velocimetry (PIV) technique and numerical modelling of bed velocities, looking at the influence of non-breaking, breaking and broken waves. It is demonstrated that scour depths are only little influenced by the breaking waves.

2. Experimental set-up

2.1. Scour tests

Tests in a length scale 1:30 were performed in a wave flume at the Hydraulics and Coastal Laboratory, Aalborg University. The flume is 18.7 m long and 1.2 m wide, see figure 1. A two-way pump able to circulate 650 l/s is mounted beneath the flume. It was possible to ensure a reasonably constant velocity profile.

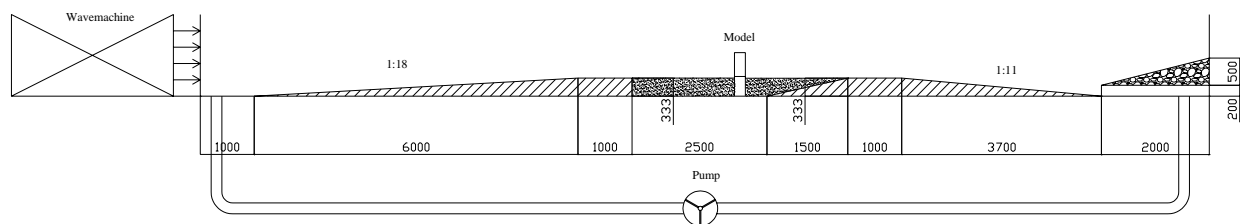


Figure 1. The wave flume. All measurements in millimetres.

The sloping bed is constructed in order to induce wave breaking. The bed slopes are made of concrete, the part in which the monopile model is built in consists of a 4 m long sand box filled with fine sand, $d_{50} = 17$ mm. Sand is also spread out in a thin layer across the slopes to simulate the natural bed sediment transport in the sandbox. A monopile model is fixed to the concrete bottom underneath the sand box. The diameter of the monopile varies between 0.10 m and 0.20 m.

In all tests a live bed condition is achieved. Scour holes are measured in a 1.5 cm by 1.5 cm grid using a laser profiler. The measured grid is 1.5 m long and 0.93 m wide. Waves and currents are measured beside the model. Waves are separated into incident and reflected waves. In Larsen et. al. (2005) a more detailed description of the test set-up can be found.

The present report focuses on the effects of breaking waves on scour. The test program described in table 1 includes both regular and irregular waves. The main purpose of the irregular tests is to study the effects of wave breaking by making comparisons with tests from literature, performed with non-breaking waves. The main purpose of the tests with regular waves is to make a comparison with the calculations in the numerical model.

Table 1. Test programme for the scour tests, irregular waves

Test no	Comments	Diameter of monopile D [m]	Significant wave height H_s [m]	Spectral peak period T_p [s]	Water depth seaward d_0 [m]	Water depth at pile h_t [-]	Current induced velocity U_c [m/s]
1.1	<i>breaking waves, with and without unidirectional current</i>	0.10	0.12	1.28	0.62	0.29	0.00
1.2		0.10	0.12	2.01	0.62	0.29	0.00
1.3		0.10	0.08	1.28	0.50	0.17	0.00
1.4		0.10	0.08	2.01	0.50	0.17	0.00
1.5		0.10	0.12	1.28	0.62	0.29	0.30
1.6		0.10	0.12	2.01	0.62	0.29	0.30
3.1	<i>Regular waves</i>	0.20	0.10	1.28	0.50	0.17	0.00
3.2		0.20	0.10	2.01	0.50	0.17	0.00
3.3		0.20	0.10	2.50	0.50	0.17	0.00

2.2. Particle image velocimetry

Particle image velocimetry is a quantitative imaging technique, which has known a rapid growth over the last two decades. It is particularly well suited for the study of wavy fluid flows which are characterized by unsteady free surfaces and internal motions, as is described by Grue et al. (2004). The main advantage of PIV is that an instantaneous 2 dimensional flow field can be quantified. This is done by adding seeding particles to the flow. The particles are lit twice in one plane by a laser in a short period (with time delay Δt). With a CCD camera these two moments are captured and the velocity field in the enlightened plane is extracted by a cross correlation analysis.

Tests were performed on a length scale of 1:100 in a wave flume of the department of civil engineering, Ghent University. The flume is 15 m long, 0.35 m wide and 0.60 m high and is made almost entirely out of glass walls, which allows taking images through the bottom plate. A piston type wave paddle is able to generate regular and irregular waves. A monopile model is built in at the end of the flume, just in front of an absorbing beach. The generated waves are measured by means of a capacitance type wave gauge just in front of the pile.

Both horizontal velocity profiles near the bottom (figure 2) as a vertical velocity profile through the centre of the pile (figure 3) were captured at different phases of a passing wave. Because of the limited space under the wave flume, a mirror is used to create the desired distance for the camera. A picture of the set-up is shown in figure 4.

The same test is repeated several times for two reasons. The first reason is to assess repeatability and an average of three tests is taken as a result; the second reason is to be able to take images at different phases of the passing wave.

A trigger was coupled to one of the wave gauges in front of the pile, in order to take a camera image at the exact same time over and over again. Due to a shift in the trigger delay, images are available with an interim of only 50 ms.

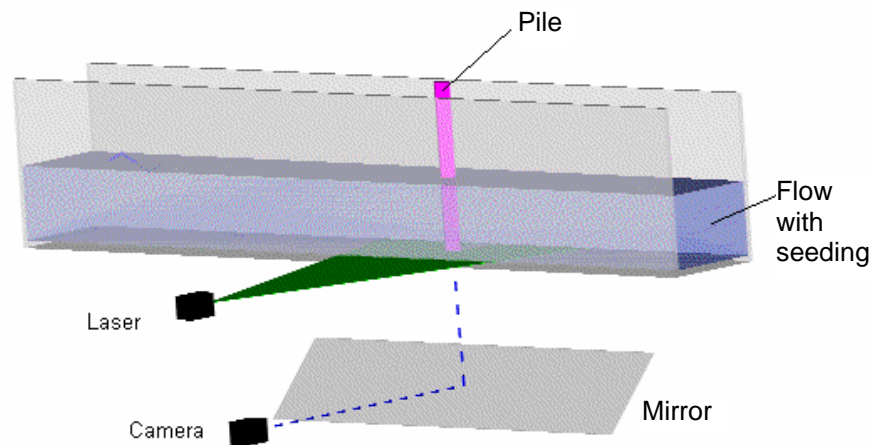


Figure 2. Principle of test set-up for velocities in a horizontal plane near the bottom.

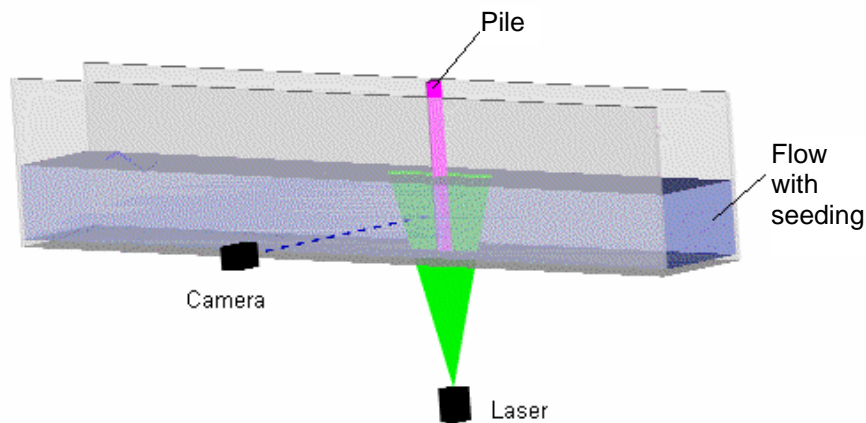


Figure 3. Principle of test set-up for velocities in a vertical plane through the centre of the pile.

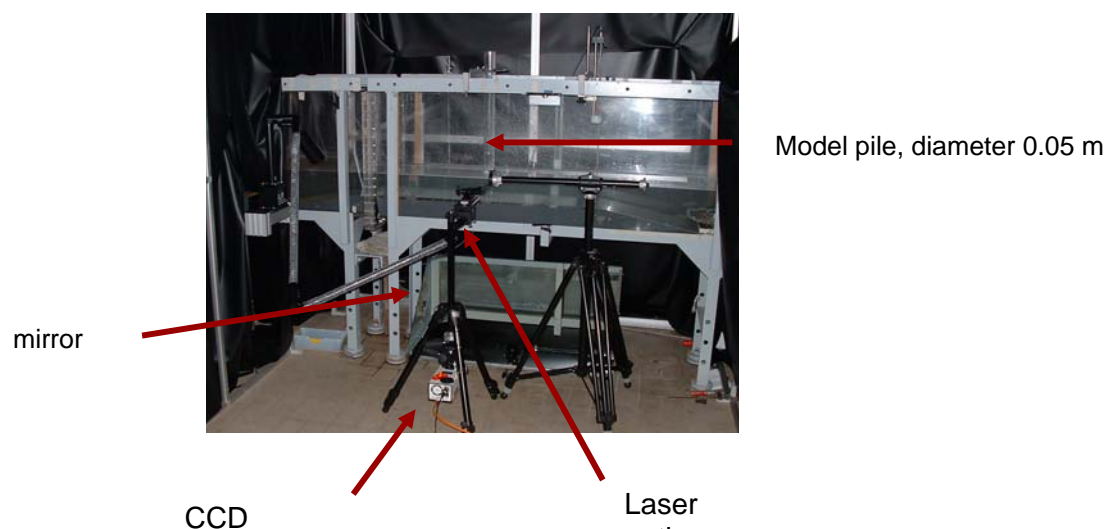


Figure 4. Picture of test set-up.

Two test series are performed, both of them with regular waves only (no current). The first tests are done with a non-breaking wave with a wave height of 0.1 m and a wave period of 1.52 s in a water depth of 0.20 m near the pile. In a second test series the velocity profiles due to a breaking wave were measured. In order to induce wave breaking, a platform was created and the pile characteristics were chosen in a way that the wave starts to break just in front of the pile: $H = 0.1\text{m}$, $T = 1.48\text{ s}$ and $d = 0.12\text{ m}$ near the pile.

The main purposes of the tests were to compare the amplification of the bed shear stress ($\tau \sim u^2$) for non-breaking and breaking waves and to compare the results with literature. After all, the sediment transport for non-cohesive sediment depends on the so called shields parameter, which expresses the ratio between the bed shear stress (driving forces) and the gravity (stabilizing

forces):
$$\theta = \frac{\tau}{gd_{50}\rho(s-1)}$$

2.3. Numerical modelling

The numerical investigations are based on the three-dimensional Navier-Stokes solver NS3. The method has been described in Mayer et al. (1998), Emarat et al. (2000), Nielsen and Mayer (2004), and Christensen et al. (2005).

The spatial discretization is based on the finite-volume approach on a multi-block grid. The time integration of the Navier-Stokes equations is performed by application of the fractional step method. Figure 5 shows an example of the multiblock grid used for the study. The grid consists of 12 blocks.

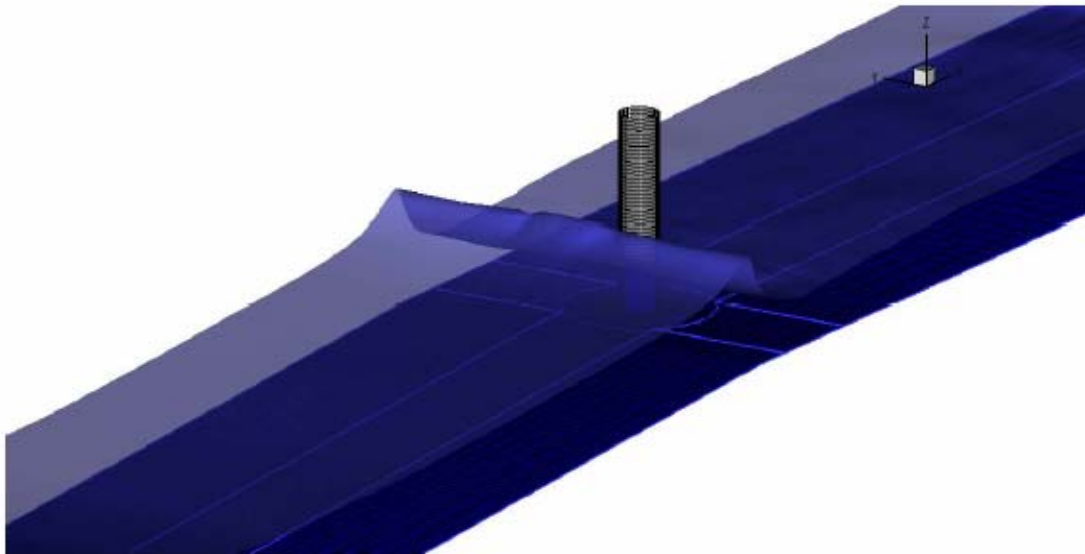


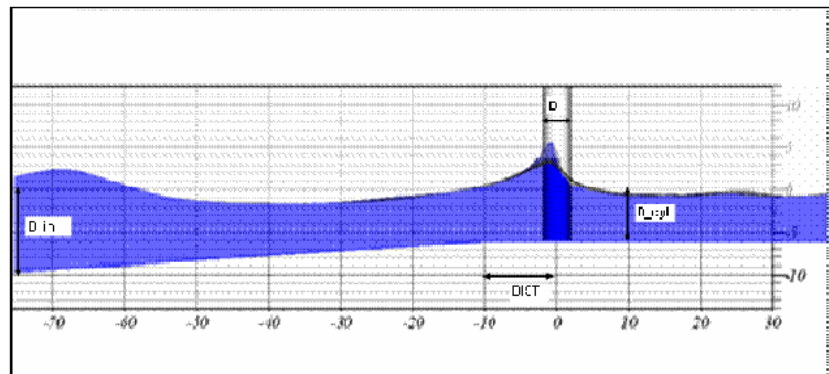
Figure 5. The multi-block structure of the computational domain shown at the bed (thick blue lines). The grid consists of twelve 3D blocks of structured data cells.

The free surface is resolved using a Volume-of-Fluid (VOF) description, with an improved scheme for the advection of the conservative quantity, F , cf. Ubbink (1997).

The scour development is mainly governed by the flow close to the seabed and the seabed properties. In order to study the influence from breaking waves, the flow is examined numerically for the same near-bed properties with and without the influence of breaking waves. The numerical model has been set up for the same near-bed flow properties as the physical scour experiments (regular waves).

The NS3 has been set up for 10 simulations (table 2) described by the parameters explained in figure 6.

D_{cyl}: Depth at the cylinder
D_{in}: Depth at inlet boundary
H_{cyl}: Shoaled wave height at the cylinder
H_{in_bound}: Wave height at inlet boundary
T: Wave period
L_{cyl}: Wave length at cylinder
K_s: Shoaling coefficient
Dia: Diameter of the cylinder
Dist: Distance from centre of



the cylinder to the beginning of the slope

Figure 6. Definition of numerical parameters.

Table 2. Numerical test parameters.

Simulation	D _{cyl}	H _{cyl}	T	Dia	KC	H _{cyl} / D _{cyl}	L _{cyl}	D _{in}	K _s	H _{in_bound}	Slope	Dist
1	6	4	8	4	4.47	0.67	57.5	10	0.9392	3.757	1:20	10
2	6	4	8	2	8.93	0.67	57.5	10	0.9392	3.757	1:20	10
3	12	5.496	9	4	4.47	0.458	87.9	16	0.9794	5.383	1:20	10
4	12	5.496	9	2	8.93	0.458	87.9	16	0.9794	5.383	1:20	10
5	6	4	8	4	4.47	0.67	57.5	10	0.9392	3.757	1:20	15
6	6	4	8	2	8.93	0.67	57.5	10	0.9392	3.757	1:20	15
7	6	4	8	4	4.47	0.67	57.5	10	0.9392	3.757	1:20	25
8	6	4	8	2	8.93	0.67	57.5	10	0.9392	3.757	1:20	25
9	6	4	8	4	4.47	0.67	57.5	10	0.9392	3.757	1:20	50
10	6	4	8	2	8.93	0.67	57.5	10	0.9392	3.757	1:20	50

The KC number is found from the near-bed orbital velocities, determined by stream function theory, assuming regular waves, a constant water depth equal to the water depth at the pile (D_{cyl}), a wave height equal to the wave height at the pile (H_{cyl}) and a wave period T.

For the numerical modelling, the main purpose was to investigate the influence of the wave breaking on the bed shear stress and to compare results with the scour experiments.

3. Experimental results

3.1. Scour tests

The largest scour depths are developed during tests 1.5 and 1.6. In figure 7 the developed scour hole in test 1.5 can be seen (picture and profile measurement at the end of the test). Please note that in the picture, the upper part of the pile has been temporarily removed in order to make the profiling.



Figure 7. Picture and profiler measurement showing scour hole after 1500 waves. Test 1.5.

All results are summarized in table 3 (irregular waves) and table 4 (regular waves). The largest scour depth that is measured is $S/D = 0.78$.

Table 3. Results from physical tests, irregular waves.

Test no	Diameter of monopile D [m]	Significant wave height H_s [m]	Spectral peak period T_p [s]	Water depth at pile h_t [-]	Current induced velocity U_c [m/s]	Scour depth S [m]	Relative scour depth S/D [-]
1.1	0.10	0.11	1.31	0.29	0.00	0.012	0.120
1.2	0.10	0.12	1.97	0.29	0.00	0.020	0.200
1.3	0.10	0.07	1.28	0.17	0.00	0.011	0.110
1.4	0.10	0.08	1.97	0.17	0.00	0.014	0.140
1.5	0.10	0.11	1.31	0.29	0.30	0.078	0.780
1.6	0.10	0.12	1.97	0.29	0.30	0.078	0.780

Table 4. Results from physical tests, regular waves.

Test no	Diameter of monopile D [m]	Wave height H [m]	Period T [s]	Water depth at pile h _t [-]	Current induced velocity U _c [m/s]	Scour depth S [m]	Relative scour depth S/D [-]
3.1	0.20	0.10	1.28	0.17	0.00	0.019	0.095
3.2	0.20	0.11	2.01	0.17	0.00	0.032	0.160
3.3	0.20	0.09	2.50	0.17	0.00	0.026	0.260

Using the methodology given by Sumer and Fredsøe (2002), it is possible to compare the results with the results for the non-breaking waves listed by Sumer and Fredsøe (2002). In table 5, the Keulegan Carpenter number KC , U_{cw} and the Shields parameter θ are listed, with

$$U_{cw} = \frac{U_c}{U_c + U_m}.$$

Table 5. Calculated KC , U_{cw} and θ values for the different test cases.

Test no	KC	U_{cw}	θ
1.1	3.1	0	0.058
1.2	6.0	0	0.108
1.3	3.1	0	0.103
1.4	5.6	0	0.164
1.5	3.1	0.61	0.186
1.6	6.0	0.51	0.241

Figure 8 shows the measured maximum scour depth S (S/D in dimensionless form) as a function of the combined wave-current velocity U_{cw} .

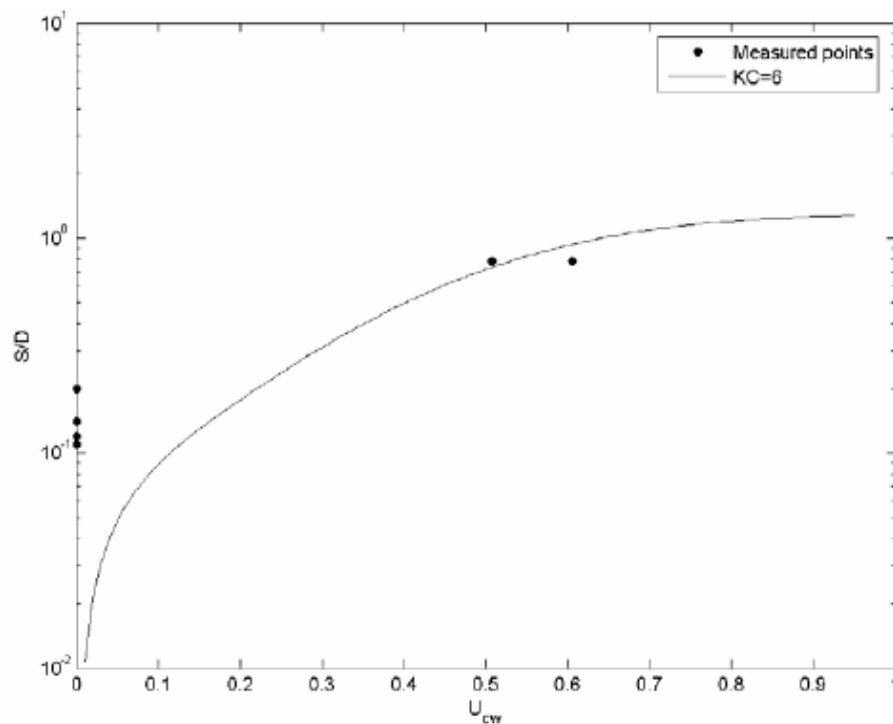


Figure 8. Comparison of predicted scour for non-breaking waves calculated according to Sumer and Fredsøe, with $KC=6$, and measured scour for breaking waves.

From figure 8, it can be deduced that the formed scour holes are comparable to those predicted by Sumer et al. (2002), which are valid for non-breaking waves. This would imply that there would be no to little influence of the wave breaking on the depth of the scour hole. It should be emphasized however that the tests are performed with irregular waves, which implies that the wave breaking does not occur for every wave, neither as it occurs at the same distance from the pile. This might influence the development of the scour hole in a less negative way than when each wave would brake at the exact same location. Irregular waves are however a much better simulation of a prototype situation.

3.2. Particle image velocimetry

In table 6, the test parameters and maximum measured velocities are reported. The KC numbers are respectively 9.4 for the non-breaking wave and 12.4 for the breaking wave. The amplification of the bed shear stress is calculated, assuming that $\tau = \frac{1}{2} \rho f_w U^2$ (or $\tau \sim U^2$), with a constant friction factor f_w .

Table 6. Results from PIV tests, regular waves.

Test no	Diameter of monopile D [m]	Significant wave height H [m]	Spectral peak period T_p [s]	Water depth at pile d [-]	Comment -	Keulegan Carpenter number KC [-]	Maximum orbital velocity away from pile U_m [m/s]	Maximum measured velocity near pile $U_{m,pile}$ [m/s]	Amplification of maximum bed shear stress $\frac{\tau_{max}}{\tau_{max0}}$
1	0.05	0.10	1.52	0.20	non breaking	9.4	0.31	0.6	3.8
2	0.05	0.10	1.48	0.12	breaking	12.4	0.42	0.85	4.1

From literature we know that for KC numbers > 7 , vortex shedding will occur (Sumer et al., 1997). This vortex shedding can indeed clearly be seen on the velocity images which are taken in the horizontal plane (figure 9 and figure 10).

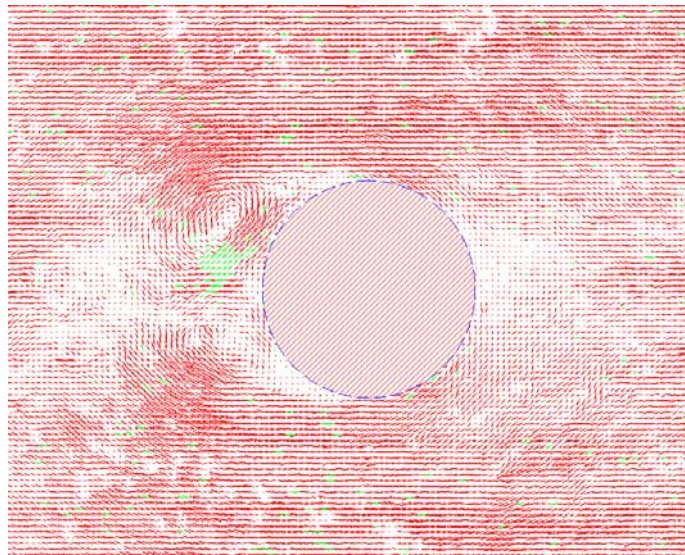


Figure 9. Velocity field around the pile, near the bottom; non-breaking wave. Average velocity: 0.1 m/s, maximum velocity 0.3 m/s (close-up around the pile).

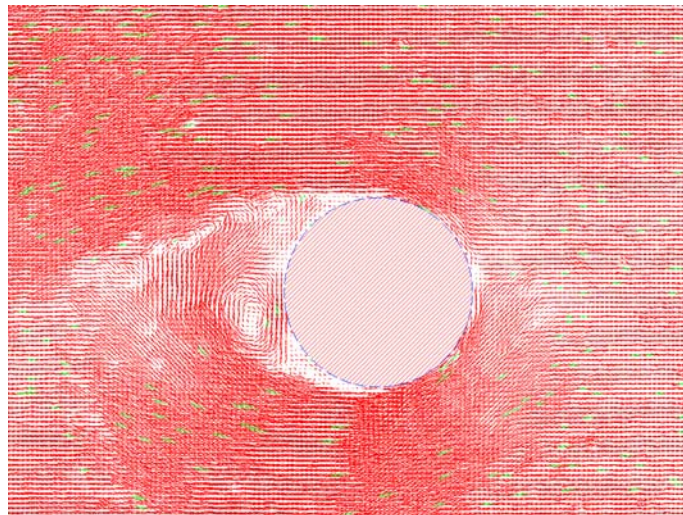


Figure 10. Velocity field around the pile, near the bottom; breaking wave.
 velocity: 0.2 m/s, maximum velocity 0.4 m/s (close-up around the pile).

Average

The amplification of the bed shear stress for two different KC numbers (non-breaking waves) is shown in figure 11. From this we can deduce that for both tests, the maximum amplification around the pile should lie around 4 (KC = 10.3 in figure 7). From table 6 we can see that for the test with the non-breaking wave, the amplification is 3.8 for the non-breaking wave and 4.1 for the breaking wave. This lies very close to the value of 4.

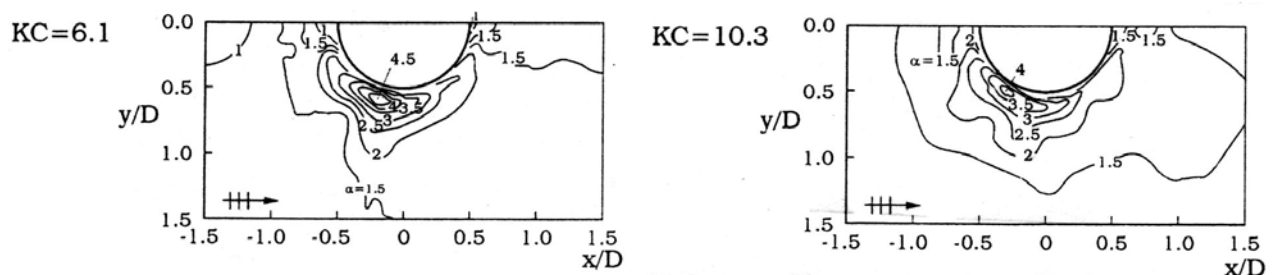


Figure 11. Amplification of bottom shear stresses around a cylindrical pile (Sumer et al, 2002)

In figure 12 and 13, the moment of maximum velocity is shown both for the non-breaking and the breaking wave. Both the vertical picture and the processed vertical and horizontal images are shown.

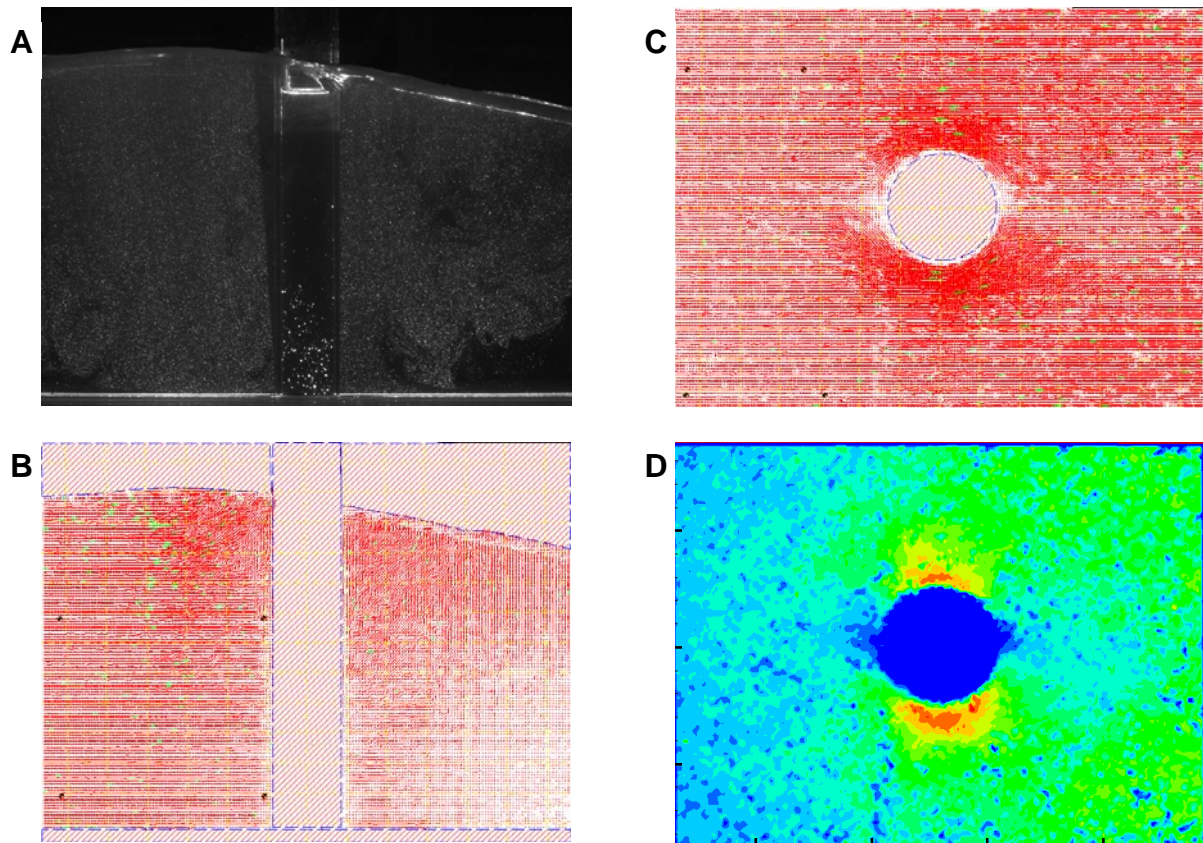


Figure 12. Snapshot of moment with maximum velocities; non-breaking wave

A: vertical picture

B: velocity vectors in vertical field

C: velocity vectors in horizontal field

D: Contour plot of velocities in horizontal field

From figure 12, it can be seen that for the non-breaking wave, the maximum bottom velocity is reached at the moment that the wave top reaches the pile. For the breaking wave (figure 13) the maximum bottom velocity occurs when the breaking crest has just passed the pile.

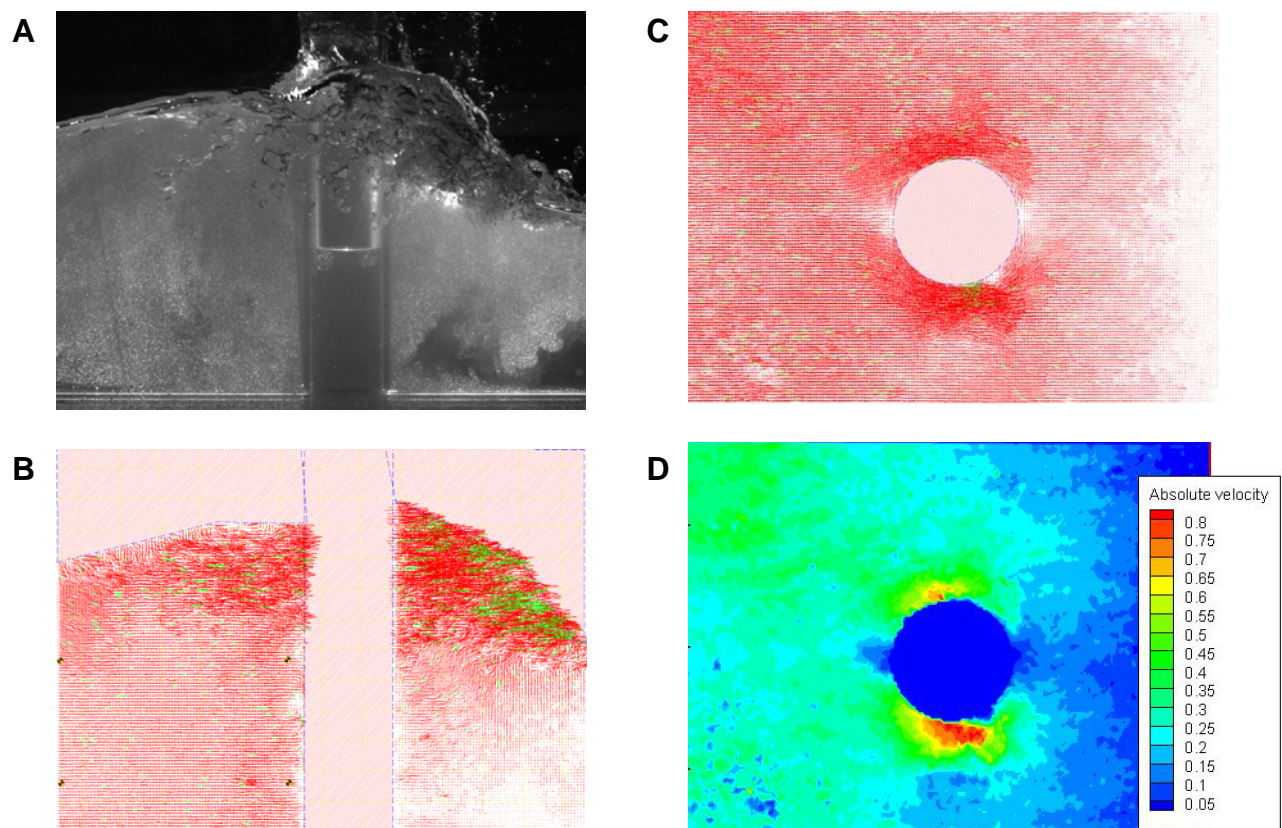


Figure 13. Snapshot of moment with maximum velocities; breaking wave

A: vertical picture

B: velocity vectors in vertical field

C: velocity vectors in horizontal field

D: Contour plot of velocities in horizontal field

Both the velocity profiles and the amplification of the bottom shear stress near the pile are comparable for non-breaking and the breaking wave. In figure 13.B it can be seen that, although velocities are very high (much higher than for the non-breaking wave) in the top part of the breaking crest (up to 1.7 m/s), the large increase in velocity is always limited to approximately two thirds of the water depth. This means that the influence of the increased turbulence and velocity due to the breaking of the wave does not reach the bottom.

3.3. Numerical results

Figure 14 shows a snapshot of a wave hitting the pile, for simulation 1 and 2. In figure 15 a snapshot of the near-bed velocities for simulation 1 and 2 are shown. The simulations show that separation does not form for the large diameter pile ($KC = 4.5$), while it does develop for the small diameter ($KC = 9$); this is in accordance with flume observations, see for example Sumer and Fredsøe (2002) and as explained above.

In order to study the influence of wave breaking, the bed friction velocities have been compared for simulation 2, where the wave is just about to break, but has not broken yet, and simulation 8,

where the breaking process is at a mature stage. A quadratic relation between the bed shear stresses and the near-bed velocities: $\tau = 0.5\rho f_w U_{bed}^2$ has been assumed. The friction velocity can be determined from this near-bed velocity U_{bed} : $U_f = \sqrt{0.5 f_w} U_{bed}$. Figure 16 shows the friction velocities, assuming a constant friction factor f equal to 0.01.

By comparing the friction velocities in the two cases, it is evident that wave breaking only has a small influence on bed shear stresses; there is even a tendency that the bed shear stresses are lower in case of wave breaking. This supports the experimental findings from the PIV measurements and the scour tests, finding that scour is only weakly dependent on wave breaking.

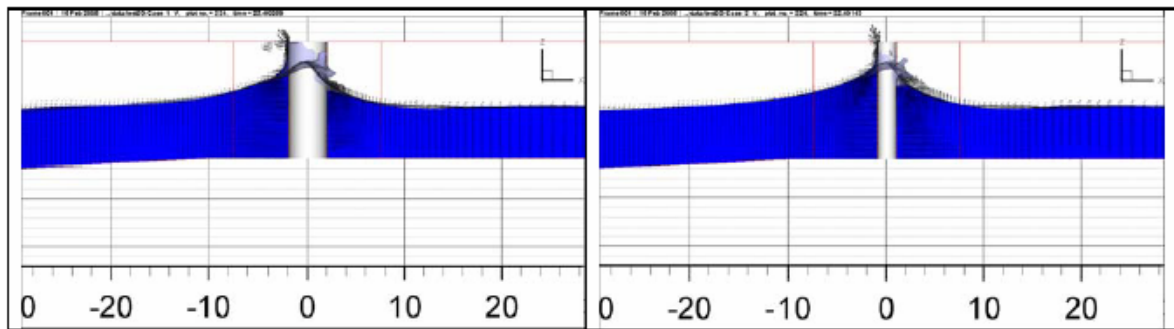


Figure 14. The wave hitting the cylinder at the same phase for simulation 1 (large pile diameter, left) and simulation 2 (small pile diameter, right).

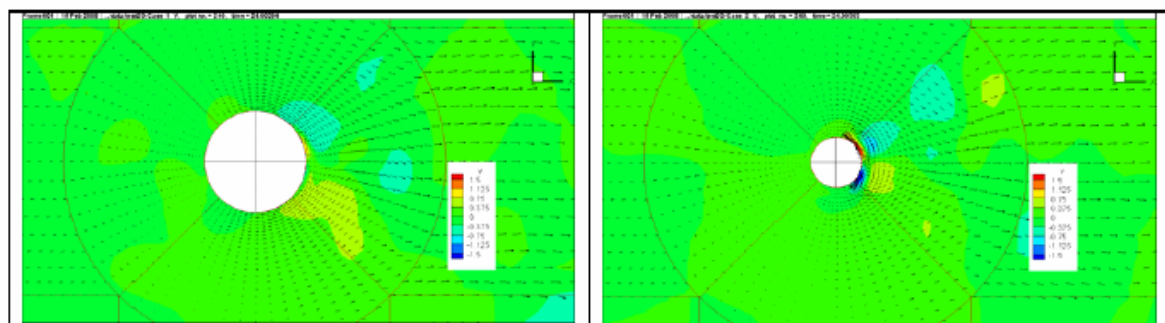


Figure 15. Snapshot of the bed velocities (m/s) for simulation 1 and 2, the colours indicate the flow velocity in the y direction (perpendicular to the wave propagation direction).

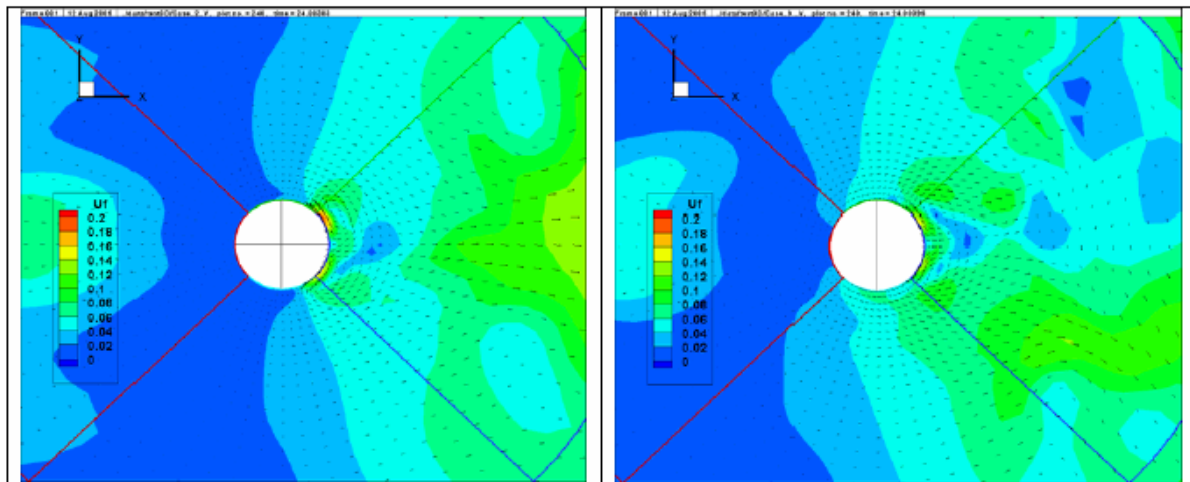


Figure 16. The friction velocity at the same phase for simulation 2 (left) and simulation 8 (right).

4. Conclusion

Normally the presence of waves will not increase but rather decrease the scour depths compared with situations where only currents are present.

In literature many equations for estimation of scour depths can be found. As a part of this project a review (Report 2) lists an overview of existing formulas. Sumer (2002) reanalyzed a lot of data from literature, and came up with the very simple equation for the maximum scour depth S , $S = 1.3 D$. Most data related to non-breaking situations.

However, knowledge on the influence of breaking waves on scour depths is limited. Bijker and Bruyn (1988) wrote: *The depth of this scour is in the order of 1.5 times the pile diameter. In case of breaking waves this value can be, however, considerably higher. The Bijker and Bruyn paper gives a large influence on the scour prediction in breaking waves.*

In the present study, no such dependency was seen. Both the physical experiments as well as the numerical study show that the effect of breaking waves only has a small influence on the scour development: both bed shear stresses and scour depths in breaking waves and in non-breaking waves were comparable. Looking closer at the figures in the Bijker and Bruyn paper, it seems that it is not the presence of the pile that causes the larger scour depths, but it is the bed itself which is subjected to large changes due to the ripple formation and dynamics. A comparable experimental study of Carreiras et al. is described in Sumer et al. (2002). Here the effect of breaking waves on scour was studied experimentally with the aid of 5 experiments in which the pile was placed at a different position related to the point of wave breaking on a 1:20 sloping beach. The study shows that, depending on the position of the pile relative to the breaking point, the ripple formation and dynamics and the formation of a bar were found to have a main influence on the evolution of scour. The final bed changes resulted from the superposition of the large scale bed evolution due to wave breaking and the small scale bed scour.

Good agreement between physical tests and numerical calculations has been shown. The numerical model seems to be able to pick up the correct physics.

In conclusion, no influence of breaking irregular waves on scour processes around circular offshore wind turbine foundations can be expected. This means, that the effect of breaking waves is comparable to the effect of non-breaking waves

5. References

- BIJKER E.W. AND DE BRUYN C.A. "Erosion around a pile due to current and breaking waves." Coastal Engineering, ASCE, 1988
- CHRISTENSEN E.D., BREDDMOSE H. AND HANSEN E.A. "Extreme wave forces and wave run-up on offshore wind-turbine foundations." Presented at Copenhagen Offshore Wind 2005
- EMARAT N., CHRISTENSEN E.D., FOREHAND D.I.M. AND MAYER S. "A study of plunging breaker mechanics by PIV measurements and a Navier-Stokes solver." Proc. Of the 27th Int. Conf. on Coastal Eng., ASCE, Sydney, Australian Vol. 1, pp 891-901, 2000
- FRIGAARD P., HANSEN A. E., CHRISTENSEN E. D. AND JENSEN M. S. "Effects of breaking waves on scour processes around circular offshore wind turbine foundations. COPENHAGEN OFFSHORE WIND 2005.
- GRUE J., LIU P.L.-F. AND PEDERSEN G.K. "PIV and water waves", World Scientific, 2004
- LARSEN B.J., FRIGAARD P. AND JENSEN M.S. "Offshore Windturbines in Areas with Strong Currents." Hydraulics and Coastal Eng. No. 19. Aalborg University. ISBN 1603-9874, 2005
- MAY R.W.P., ACKERS J.C., KIRBY A.M. "Manual on scour at bridges and other hydraulic structures" CIRIA, 2002
- MAYER S., GARAPON A. AND SØRENSEN L.S. "A fractional step method for unsteady free-surface flow with application to non-linear wave dynamics." Int. Journal for Numerical Methods in Fluids, Vol. 28, No. 2, pp. 293-315, 1998
- NIELSEN K.B., AND MAYER S. "Numerical prediction of green water incidents" Ocean Engineering, Vol 31, pp 363-399, 2004
- OFFSHORE CENTER DANMARK. Review of monopile scour, (2006). Report 2. "Offshore Wind Turbines Situated in Areas with Strong Currents". Offshore Center Danmark (OCD)
- SUMER B.M. AND FREDSE, J. "The mechanics of scour in the marine environment." World Scientific, ISBN 981-02-4930-6, 2002
- WHITEHOUSE, R. "Scour at marine structures." Thomas Telford Ltd, ISBN 0-7277-2655-2, 1998

6. Notation

d	= water depth;
D	= pile diameter;
d_{50}	= median grain diameter;
f_w	= friction factor;
g	= gravitational acceleration;
H	= wave height;
H_s	= significant wave height;
KC	= Keulegan Carpenter number, $KC = \frac{U_m T}{D}$;
s	= ratio of densities of grain and water;
S	= scour depth;
S_e	= equilibrium scour depth;
T	= wave period;
T_p	= wave peak period;
U	= velocity;
U_c	= current velocity;
U_{cw}	= velocity ratio, $U_{cw} = \frac{U_c}{U_c + U_m}$;
U_f	= friction velocity;
U_m	= amplitude of horizontal orbital velocity;
θ	= Shields parameter, $\theta = \frac{\tau}{gd_{50}\rho(s-1)}$;
ρ	= density of water;
τ	= bed shear stress, $\tau = \frac{1}{2}\rho f_w U_m^2$.

OFFSHORE WIND TURBINES SITUATED IN AREAS WITH STRONG CURRENTS

REPORT 5

CFD modelling of scour around offshore wind turbines in
areas with strong currents

Author

Tron Solberg, Aalborg University Esbjerg

Bjørn H. Hjertager, Aalborg University Esbjerg

Stefano Bove, Aalborg University Esbjerg

Work Group

Tron Solberg, Aalborg University Esbjerg

Bjørn H. Hjertager, Aalborg University Esbjerg

Stefano Bove, Aalborg University Esbjerg

Table of contents

1.	Introduction	129
2.	Mathematical formulation	131
2.1.	Flow Model	131
2.2.	Scour Model	133
2.3.	Boundary Conditions	135
3.	Numerical implementation	136
3.1.	Flow configuration	137
3.2.	Numerical mesh	138
3.3.	Numerical results	139
4.	Conclusions	153
5.	References	153

1. Introduction

Marine structures placed on an erodible sea bed are well known to introduce scour due to the interactions with currents and waves. Examples of simple marine structures are marine pipelines and offshore wind turbines. The formation of scour is an undesirable phenomenon as the forces acting on the structure will be altered, and the structure may be subjected to vibrations. Scour protection is often considered when placing marine structures on the sea bed. Such actions can, however, be expensive and intractable. A general review of scour formation can be found in the books of Whitehouse (1998) and Sumer & Fredsøe (2002). In the present report, recent CFD modelling of scour beneath pipelines and around piles is reviewed.

Brørs (1998) developed a 2D model for scour below a pipeline in steady currents. The flow model was based on a standard high-Reynolds number $k-\varepsilon$ turbulence model where turbulent production due to buoyancy was included. The scour model accounted for both suspended and bed-load sediment transport. Sediment suspension was argued only to be important in the early stage of the scouring where a sediment carrying jet exiting from the narrow gap that had formed between the pipe and the bed. The empirical expression for the bed-load sediment transport rate had a slope correction term giving an additional down-slope sediment flux whenever there is a slope and the bed shear stress was above the threshold for sediment motion. The predictions agreed very well with clear-water experiments found in the literature.

Liang et al. (2005) also developed a 2D model for scour below a pipeline in steady currents. The performance of two turbulence models, the standard $k-\varepsilon$ model and the Smagorinsky subgrid scale (SGS) model, was examined. Both suspended and bed-load sediment transports were considered in the scour model. The empirical expression for the bed-load sediment transport rate was in their case only dependent of the bed shear stress. An ad-hoc sand slide model was suggested in order to smoothen out numerical instabilities that occurred when the predicted slope of the scour hole exceeded the angle of repose of the sediment. The predictions agreed very well with both clear-water and live-bed scour experiments found in the literature. They concluded that the standard $k-\varepsilon$ model performed better than the LES model.

Dupuis and Chopard (2002) developed a lattice gas model for scour formation under submarine pipelines. The fluid-particle system was described in terms of a mesoscopic dynamic, where fictitious fluid and sediment particles move on a regular lattice synchronously at discrete time steps. An interaction is defined between particles that meet simultaneously at the same lattice site. Fluid particles obey collision rules which reproduce, in the macroscopic limit, the Navier-Stokes equation. The sediment particles move under the combined effect of the local fluid velocity field and the gravity. As they reach the ground, the sediment particles pile up and topple if necessary, changing in this way the boundary condition for the fluid. At the top of the deposition layer, erosion takes place, and if the fluid is fast enough, sediment particles are picked up and carried away. The predictions of both the equilibrium scour hole and the time evolution agreed very well with the live-bed experiments found in the literature.

Yen et al. (2001) developed a 3D CFD model for flow and scouring around circular piers. A large eddy simulation (LES) approach with Smagorinsky subgrid scale (SGS) eddy viscosity model was employed to calculate flow and bed shear fields. The scour model solved the sediment continuity equation together with an empirical expression for the bed-load sediment transport

rate. Without recalculating the flow field as the bed deforms, the flat bed shear field was modified according to the bed deformation. Gravitational effect on the sediment motion due to the sloping bed of the scour hole was included as part of the effective bed shear stress. The scour model was calibrated and verified against experimental data found in the literature. The time evolution of the scour depth and the shape of the scour were both very well predicted.

Roulund et al. (2005) and Roulund (2000) developed a 3D CFD model for flow and scour around a circular pile. The flow model was based on a standard high-Reynolds number $k - \omega$ turbulence model. The scour model solved the mass balance of sediment in which the bed load velocity was calculated from a local equilibrium of the forces acting on a sediment particle. An ad-hoc sand slide model was suggested in order to smoothen out numerical instabilities that occurred when the predicted slope of the scour hole exceeded the angle of repose of the sediment. The time evolution of the scour depth both upstream and downstream compared reasonable with their own measurements. However, the equilibrium scour depth was somewhat underpredicted. The shape of the scour hole was also well predicted.

This report covers computational fluid dynamic (CFD) modelling of scour in the project “Offshore Wind Turbines in Areas with Strong Currents” generated by Offshore Centre Denmark. The CFD model developed by Brørs (1998) for scour below pipelines is implemented in the commercial CFD code FLUENT and tested for scour around circular piles.

2. Mathematical formulation

The mathematical formulation follows closely that presented by Brørs (1999) for scour under marine pipelines.

2.1. Flow Model

The flow is governed by the incompressible Reynolds Averaged Navier-Stokes (RANS) equations and a scalar transport equation describing the suspension of sediment. The sediment concentration is assumed sufficiently low for the Boussinesq approximation to be valid. The transport equations can be expressed in Cartesian tensor notation as

$$\frac{\partial u_j}{\partial x_j} = 0 \quad (1)$$

$$\frac{\partial}{\partial t}(\rho u_i) + \frac{\partial}{\partial x_j}(\rho u_i u_j) = -\frac{\partial p^+}{\partial x_i} + \frac{\partial \tau_{ij}}{\partial x_j} + \rho(s-1)c g_i \quad (2)$$

$$\frac{\partial}{\partial t}(\rho c) + \frac{\partial}{\partial x_j}(\rho c(u_j - w_j)) = \frac{\partial J_{c,j}}{\partial x_j} \quad (3)$$

Here, x_j indicates the co-ordinate in the j -direction, and t is the time. ρ and u are the fluid density and velocity. $p^+ = p - \rho g_k x_k$ is the static pressure including the hydrostatic head. c is the sediment concentration. s is the density ratio between the sediment particle and the fluid. Finally, the gravitational acceleration is defined by the vector $g_i = (0, 0, g)$.

The sediment settling vector is defined by $w_j = (0, 0, w_s)$, where the settling velocity w_s for natural sand in clear water is taken from Whitehouse(1999) as

$$w_s = \frac{10 \cdot \nu}{d_s} \left[\left(1 + 0.01 \cdot D_*^3 \right)^{\frac{1}{2}} - 1 \right] \quad (4)$$

Here, d_s is the median sediment particle diameter and D_* is a non-dimensional particle diameter defined as

$$D_* = d_s \left(\frac{g(s-1)}{\nu^2} \right)^{\frac{1}{3}} \quad (5)$$

The turbulent Reynolds shear stresses τ_{ij} and scalar fluxes $J_{c,j}$ are modelled by the eddy viscosity and the gradient-diffusion hypothesis as

$$\tau_{ij} = -\overline{\rho u'_i u'_j} = 2\mu_T S_{ij} - \frac{2}{3}\delta_{ij}\rho k \quad (6)$$

and

$$J_{c,j} = -\overline{\rho c' u'_j} = \frac{\mu_T}{\sigma_T} \frac{\partial c}{\partial x_j} \quad (7)$$

where the mean rate of strain is defined by

$$S_{ij} = \frac{1}{2} \left(\frac{\partial u_i}{\partial x_j} + \frac{\partial u_j}{\partial x_i} \right) \quad (8)$$

The eddy viscosity μ_T is defined using a standard high-Reynolds number $k - \varepsilon$ turbulence model as

$$\mu_T = C_\mu \rho \frac{k^2}{\varepsilon} \quad (9)$$

The transport equations governing the turbulent kinetic energy k and its dissipation rate ε can be expressed as

$$\frac{\partial}{\partial t}(\rho k) + \frac{\partial}{\partial x_j}(\rho k u_j) = \frac{\partial J_{k,j}}{\partial x_j} + P + G - \rho \varepsilon \quad (10)$$

$$\frac{\partial}{\partial t}(\rho \varepsilon) + \frac{\partial}{\partial x_j}(\rho \varepsilon u_j) = \frac{\partial J_{\varepsilon,j}}{\partial x_j} + \frac{\varepsilon}{k} (C_{\varepsilon,1} P + C_{\varepsilon,3} G - C_{\varepsilon,2} \rho \varepsilon) \quad (11)$$

The production of turbulent kinetic energy consists of two parts, the production rate due to mean rate of strain

$$P = 2\mu_T S_{ij} S_{ij} \quad (12)$$

and the production rate due to buoyancy

$$G = -(s-1)g_j J_{c,j} \quad (13)$$

The modelling constant $C_{\varepsilon,3}$ for the production of turbulent kinetic energy due to buoyancy in the ε -equation is defined as

$$C_{\varepsilon,3} = \tanh \left(\sqrt{\frac{w^2}{u^2 + v^2}} \right) \quad (14)$$

Accordingly, $C_{\varepsilon,3}$ is close to zero for horizontal shear layers and close to one for vertical shear layers. The other modelling constants take standard values.

2.2. Scour Model

The development of the scour is found from a mass balance of bed sediment. Considering a unit area, the rate of change of bed level h is balanced by the net rate of sediment particles due to bed-load transport q_j , deposition D and entrainment E of sediment, i.e.

$$\frac{\partial h}{\partial t} = \frac{1}{1-n} \left[\frac{\partial q_j}{\partial x_j} + D - E \right] \quad (15)$$

Here, n is the bed porosity. The bed-load transport rate q_j is given by the expression

$$q_j = q_0 \frac{\tau_j}{|\tau|} - C q_0 \frac{\partial h}{\partial x_j} \quad (16)$$

where

$$q_0 = \begin{cases} 12 \sqrt{g(s-1)d^3\theta(\theta - \theta_{crb})} & \text{if } \theta > \theta_{crb} \\ 0 & \text{otherwise} \end{cases} \quad (17)$$

is the bed-load sediment transport rate at a horizontal bed, and τ_j is the wall or bed shear stress. The second term of the bed-load transport rate defined in Eq. (16) is a slope correction term giving an additional down-slope sediment transport whenever the bed shear stress is above the threshold for sediment motion. Following Brørs (1999), the modelling constant C is taken to be 1.5. The dimensionless bed shear stress or Shields number is defined as

$$\theta = \frac{|\tau|}{\rho g (s-1) d_s} \quad (18)$$

The critical Shields number θ_{crb} for sediment motion depend on the bed slope α following the formula

$$\theta_{crb} = \theta_{crb,0} \frac{\sin(\alpha + \phi)}{\sin(\phi)} \quad (19)$$

where ϕ is the angel of repose for the sediment. The horizontal bed threshold $\theta_{crb,0}$ is taken from Whitehouse (1998) as

$$\theta_{crb,0} = \frac{0.24}{D_*} + 0.55 \cdot [1 - \exp(-0.02 \cdot D_*)] \quad (20)$$

Accordingly, the critical Shields number is increased for sediment motion up a slope and reduced for sediment motion down a slope compared to the horizontal bed threshold.

The deposition rate of suspended sediment D is determined by the settling velocity and the near-bed sediment concentration c_0 , i.e.

$$D = w_3 c_0 \quad (21)$$

The entrainment rate of sediment E is determined by the near-bed Reynolds flux of sediment, i.e.

$$\rho E = J_{c,3} \quad (22)$$

2.3. Boundary Conditions

At the inflow boundary, a local equilibrium turbulent boundary layer flow is assumed. Accordingly, the inflow profiles for velocity $u(z)$, turbulent kinetic energy $k(z)$ and turbulent length scale $l(z)$ are specified as

$$u(z) = \min \left[\frac{u_*}{\kappa} \ln \left(\frac{z}{z_0} \right), u_0 \right] \quad (23)$$

$$k(z) = \max \left[C_\mu^{-\frac{1}{2}} \left(1 - \frac{z}{\delta} \right)^2 u_*^2, 1.5 (Tu_0)^2 \right] \quad (24)$$

$$l(z) = \min \left[\kappa z \left(1 + 1.5 \frac{z}{\delta} \right)^{-1}, C_\mu \delta \right] \quad (25)$$

Here, the free-stream velocity u_0 , the free-stream turbulence level T and the boundary layer thickness δ are input parameters. The friction velocity u_* is evaluated from the logarithmic velocity profile as

$$u_* = \frac{\kappa u_0}{\ln \left(\frac{\delta}{z_0} \right)} \quad (26)$$

The bed roughness z_0 is estimated from

$$z_0 = \frac{k_s}{30} \quad (27)$$

where the height of the roughness elements is taken to be $k_s = 2.5 \cdot d_s$.

At the inflow boundary, clear-water scour is assumed so that the concentration of sediment is assumed to be zero, i.e. $c(z) = 0$.

Along the sea bed, standard wall functions are applied. The sea bed is assumed to be rough with a height of the roughness elements taken to be $k_s = 2.5 \cdot d_s$. In the case of suspended sediment, a near-bed reference concentration c_0 is defined as

$$c_0 = \begin{cases} 0.3 & \text{if } \theta < 0.75 \\ 0.3 \frac{\theta - \theta_{crs}}{0.75 - \theta_{crs}} & \text{if } \theta_{crs} < \theta < 0.75 \\ 0 & \text{if } \theta < \theta_{crs} \end{cases} \quad (28)$$

Here, the threshold for suspended sediment transport is taken to be $\theta_{crs} = 0.25$. The actual sediment concentration in the control volume adjacent to the sea bed is taken as the maximum of the reference concentration and the concentration in the control volume just outside. This has been introduced to mimic the situation where there is a net deposition of sediment. In the case where there is no suspended sediment transport, this boundary condition implies zero flux of sediment.

Around the cylinder, standard wall functions are also used. The cylinder is assumed to be smooth. A zero flux condition is applied for the transport of suspended sediment.

3. Numerical implementation

The flow and scour models are implemented in the commercial CFD code FLUENT 6.2 applying user defined scalars UDS and user defined functions UDF.

In the flow model, the suspended sediment transport equation is implemented by solving for an extra user defined scalar (UDS). The convective flux that includes the settling velocity is defined by a `DEFINE_UDS_FLUX` macro. Finally, the transport coefficient is set by a `DEFINE_DIFFUSIVITY` macro. The buoyancy term in the momentum equations is introduced by a `DEFINE_SOURCE` macro.

The flow profiles at the inlet boundary condition are implemented through `DEFINE_ROFILE` macros. The near bed sediment concentration is set by overwriting the concentration in the control volume using a `DEFINE_SOURCE` macro.

The scour model is implemented taking advantage of the dynamic mesh capability in FLUENT using spring-based smoothing. Since the transport equation for the sea bed level, Eq. (15), is solved only on the surface mesh defining the sea bed, the user defined scalar solver in FLUENT cannot be adopted directly. Instead, the bed level transport equation is solved at the end of each time step within a `DEFINE_AT_END` macro. The sea bed level is calculated in the face centre of each face of the surface mesh. As the scouring of the sea bed takes place, the form of the sea bed will change. The vertical node movement due to scouring is introduced by the `DEFINE_GRID_MOTION` macro. The node movement is an area average of the change of bed level in the surrounding faces.

The transport equation for the sea bed level, Eq. (15), is solved adopting an Euler explicit temporal discretisation. This choice introduces a time step limitation in order to obtain stable numerical solutions. Based on the bed-load transport rate defined in Eq. (16) the following time step limitations for convection and diffusion, respectively can be estimated

$$\Delta t \leq \frac{(\Delta A)^{\frac{1}{2}}}{u_0} \quad (29)$$

$$\Delta t \leq \frac{(1-n)g(s-1)\Delta A}{24Cu_0^3} \quad (30)$$

Here, ΔA is the minimum face area.

3.1. Flow configuration

The flow configuration is that used in one of the series of model tests performed as part of the project “Offshore Wind Turbines in Areas with Strong Currents” sponsored by Offshore Centre Denmark (Larsen et al. 2005). The values chosen are shown in Table 1. Accordingly, the Reynolds number based on the freestream velocity and the pile diameter is 100 000. The physical parameters chosen for the natural sand is listed in Table 2.

Table 1 Flow configuration

Diameter of pile	D	0.2 m
Water depth at pile	h	0.5 m
Diameter of cylinder	$D[m]$	0.2
Water depth	$h[m]$	0.5
Current induced velocity	$u_c \left[\frac{m}{s} \right]$	0.46
Free stream velocity	$u_0 \left[\frac{m}{s} \right]$	0.5
Boundary layer thickness	$\delta[m]$	0.5
Free stream turbulence level	$T[\%]$	2

Table 2 Physical parameters for natural sand

Sediment diameter	$d_s [\mu m]$	250
Density	$\rho_s \left[\frac{kg}{m^3} \right]$	2655
Density ratio	s	266
Porosity	n	0.4
Angle of repose	ϕ	23

3.2. Numerical mesh

The computational domain is chosen to be 30 pile diameters long in the streamwise direction and 10 pile diameters wide in the cross-streamwise direction. The pile is located in the centre of the computational domain. The height of the domain is the same as the water depth.

The computational domain is chosen to extend 15 diameters in the streamwise direction both upstream and downstream of the pile and 5 diameters in the transverse direction on both sides. In the transverse direction, the computational domain extends 5 diameters in both directions from the pile. The computational domain is divided into an unstructured mesh comprising 27 120 hexahedral cells as shown in Figure 1. Although the mesh seems relatively coarse, the mesh is substantially refined near the pile and near the sea bed.

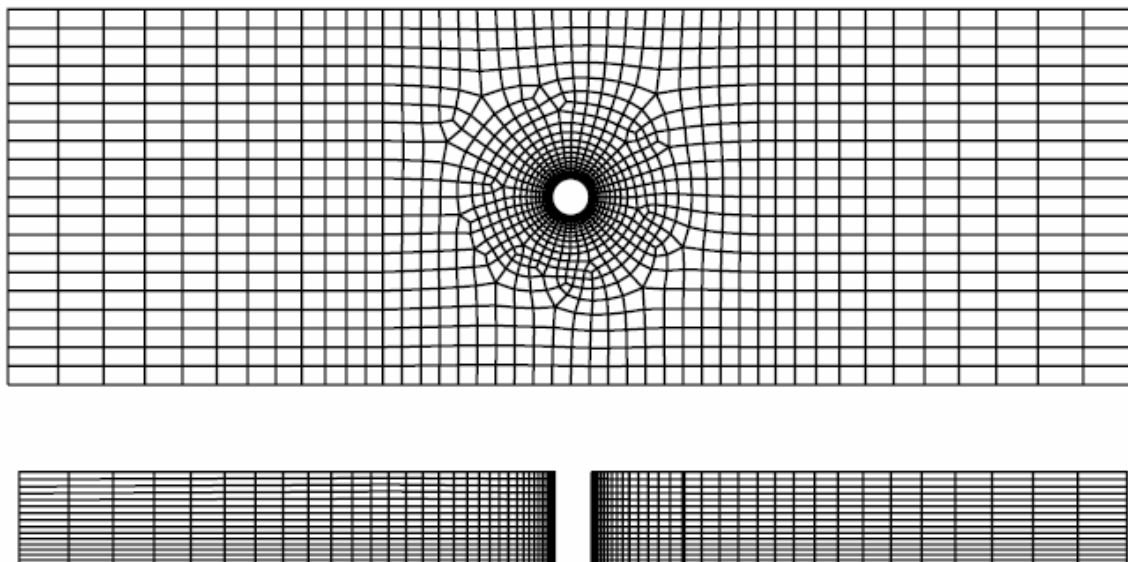


Figure 1 Numerical mesh comprising 27 120 hexahedral cells: xy-plane (top) and xz-plane (bottom).

3.3. Numerical results

All the predictions presented are transient, and second order spatial differencing is adopted for all transport equations. Based on the minimum cell volume and the freestream velocity, a time step of 23 ms is estimated from convective time stepping criteria in Eq. (29). Nevertheless, no transient large scale flow structures are recognised in the predictions. A perturbation of the flow in order to induce vortex shedding is, however, not attempted. In order to speed up the scour predictions, a time step of 0.1 s is adopted for the flow calculations.

Only, the bed-load sediment transport is included in the scour predictions. Initial calculation of the suspended sediment load indicates that a local equilibrium between sediment entrainment and deposition develops.

Due to the slope correction term in the bed load transport rate, Eq. (16), the diffusive time stepping criteria in Eq. (30) is expected to be limiting. For the present flow configuration and numerical mesh, the time step is estimated to be 0.29 ms. Accordingly, the bed level is calculated 350 times for every flow time step. The numerical mesh is updated at the end of each flow time step. Such a small time step seems odd, when the development of scour holes is known experimentally to take hours.

Scour Model for Steady Current at Lab Scale

In the first scour prediction, the sea bed is represented by a static mesh. The flow is first run to steady state. Thereafter, the rate of change of the bed level is calculated. Accordingly, there is no direct influence of the scour hole on the flow. Figure 2 shows the scour depth S/D as function of time and the bed profile h/D along the centreline in the streamwise direction at the end of the prediction. After 8 hours, the scour depth S/D approaches 0.7, which is substantial lower than the experimental value 1.3 (Sumer & Fredsøe 2002). Behind the pile, there is an accretion that reaches a maximum height h/D of 0.2.

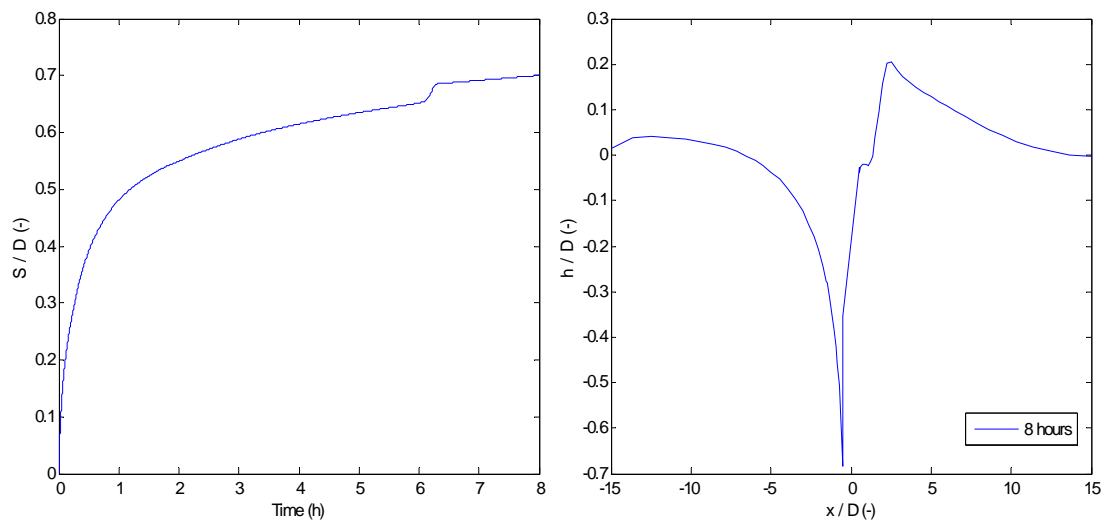


Figure 2 Scour depth as function of time (left) and bed profile along the centreline after 8 hours (right). Prediction of scour for steady current at lab scale using static bed.

Figure 3 shows contour plots of the bed shear stress or the Shields number and the sea bed level after 8 hours. The form of the scour hole does not resemble the circular ones often observed experimentally (Sumer & Fredsøe 2002).

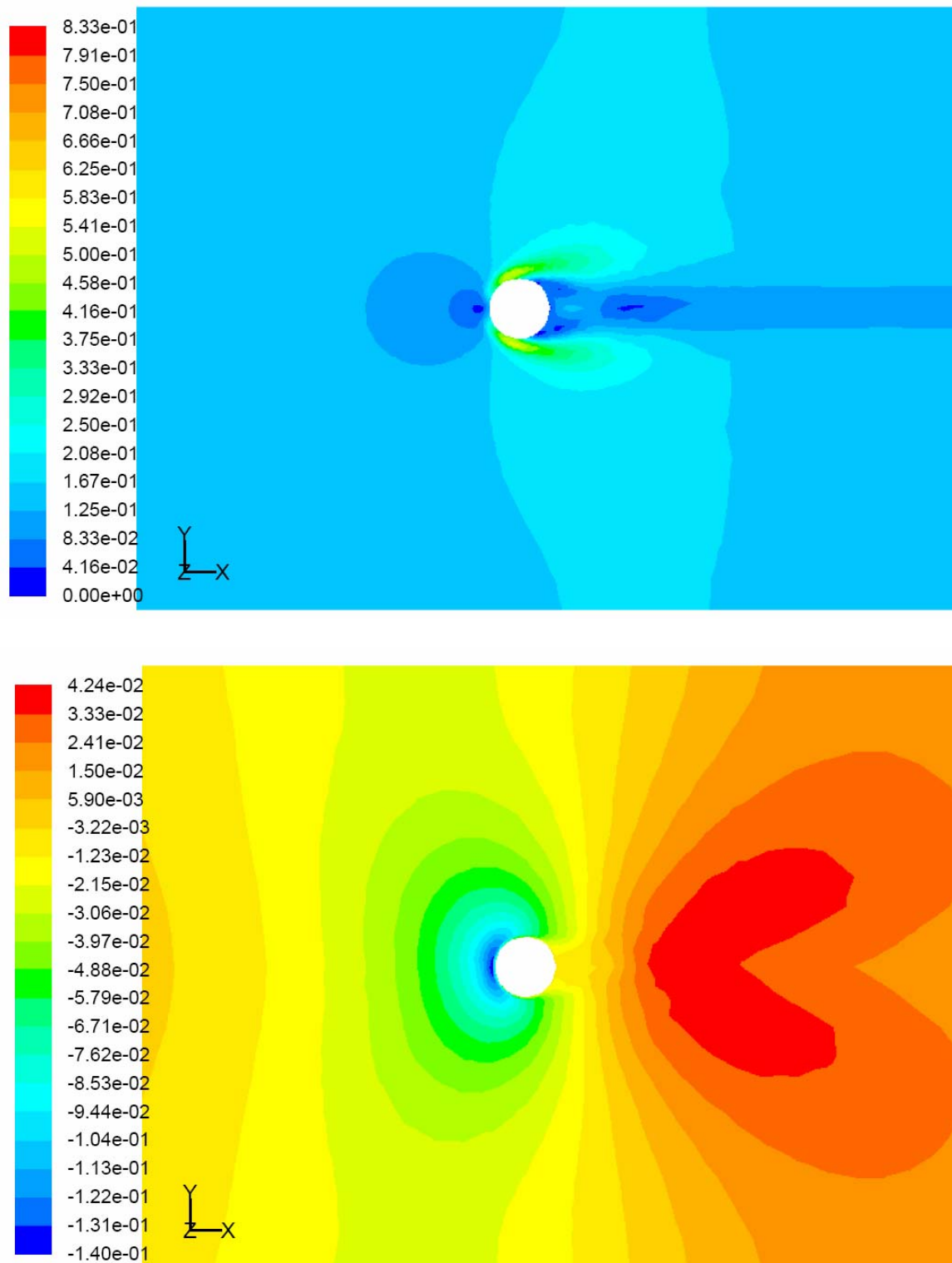


Figure 3 Contour plots of Shields number (top) and bed level (bottom). Prediction of scour for steady current at lab scale using static bed.

In the second prediction, the sea bed is represented by a dynamic mesh. Hence, there is a direct coupling between the scour hole and the flow. Figure 4 shows the scour depth S/D as function of time and the bed profile h/D along the centreline in the streamwise direction at the end of the prediction. After 4 hours, the scour depth S/D approaches 0.54 which indicates a shallower scour hole than for the static bed prediction. Some distance downstream of the pile, there is an accretion that reaches a maximum height h/D of 0.1.

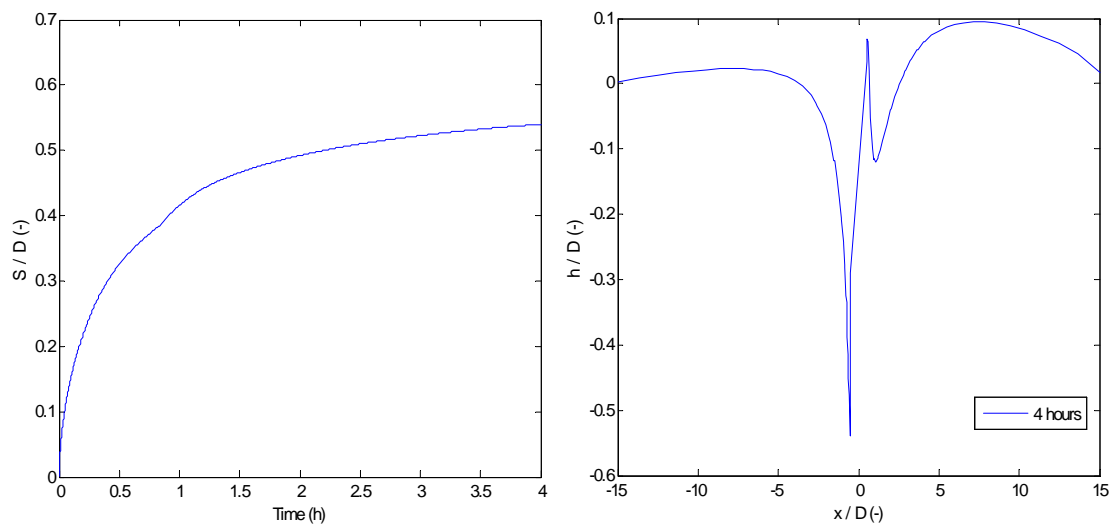


Figure 4 Scour depth as function of time (left) and bed profile along the centreline after 4 hours (right). Prediction of scour for steady current at lab scale using dynamic bed.

Figure 5 shows contour plot of the bed shear stress or the Shields number and the sea bed level after 4 hours. The form of the scour hole is this time in better agreement with the circular ones often found experimentally. Still, there is a local build up of sediment just downstream of the pile. Figure 6 shows a three-dimensional view of the scour hole also indicating the use of the dynamic mesh and a contour plot of the bed angle. As can be noticed from the figure, the bed angle tends to exceed the angle of repose for the sediment. This indicates that a sandslide model is probably essential for correct predictions of the shape and the depth of the scour hole.

Figure 7 shows the bed load transport rate in x and y-direction. As expected, there is a close relation between the shape of the scour hole and the bed load transport rates.

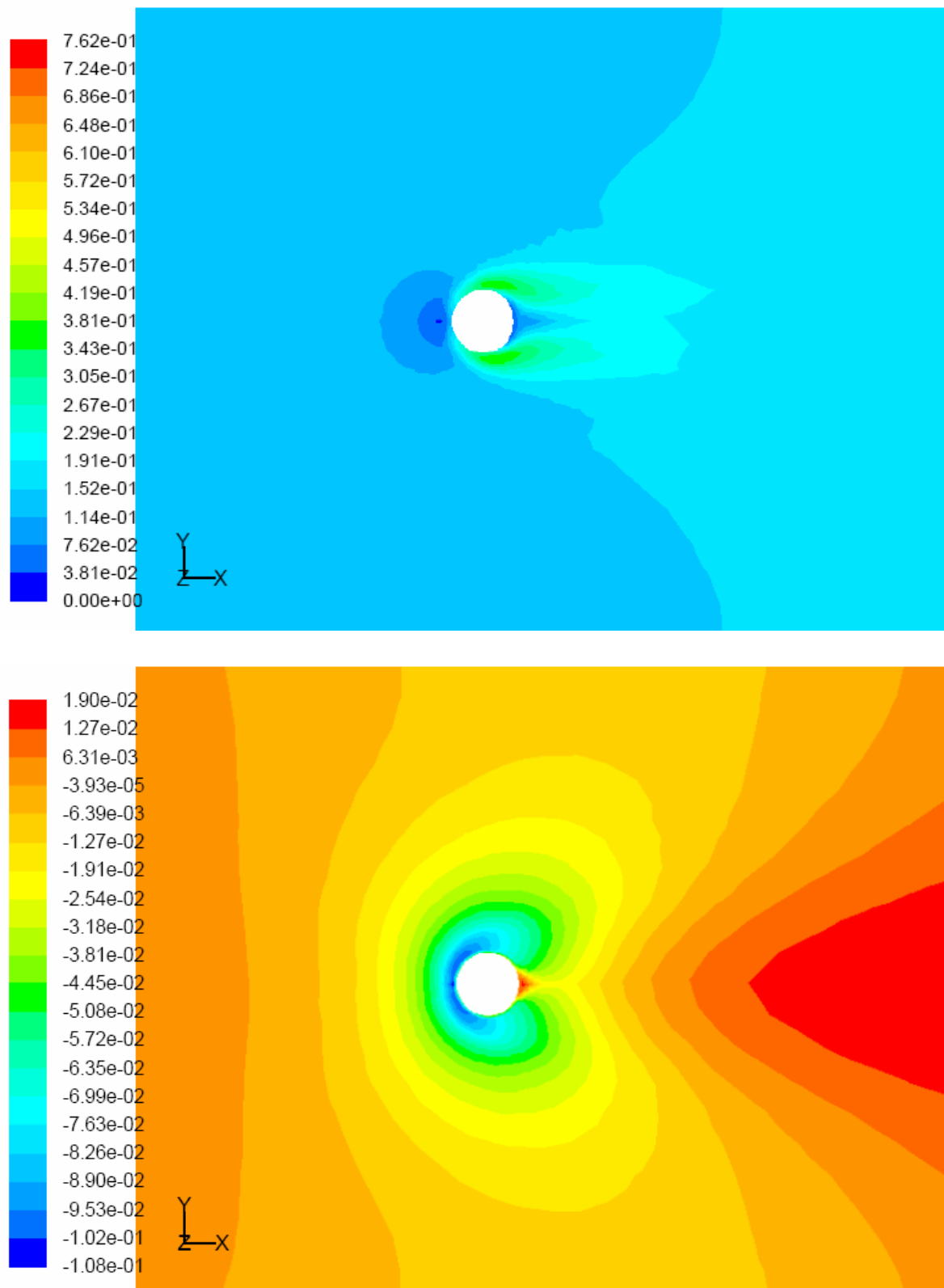


Figure 5 Contour plots of Shields number (top) and bed level (bottom). Prediction of scour for steady current at lab scale using dynamic bed.

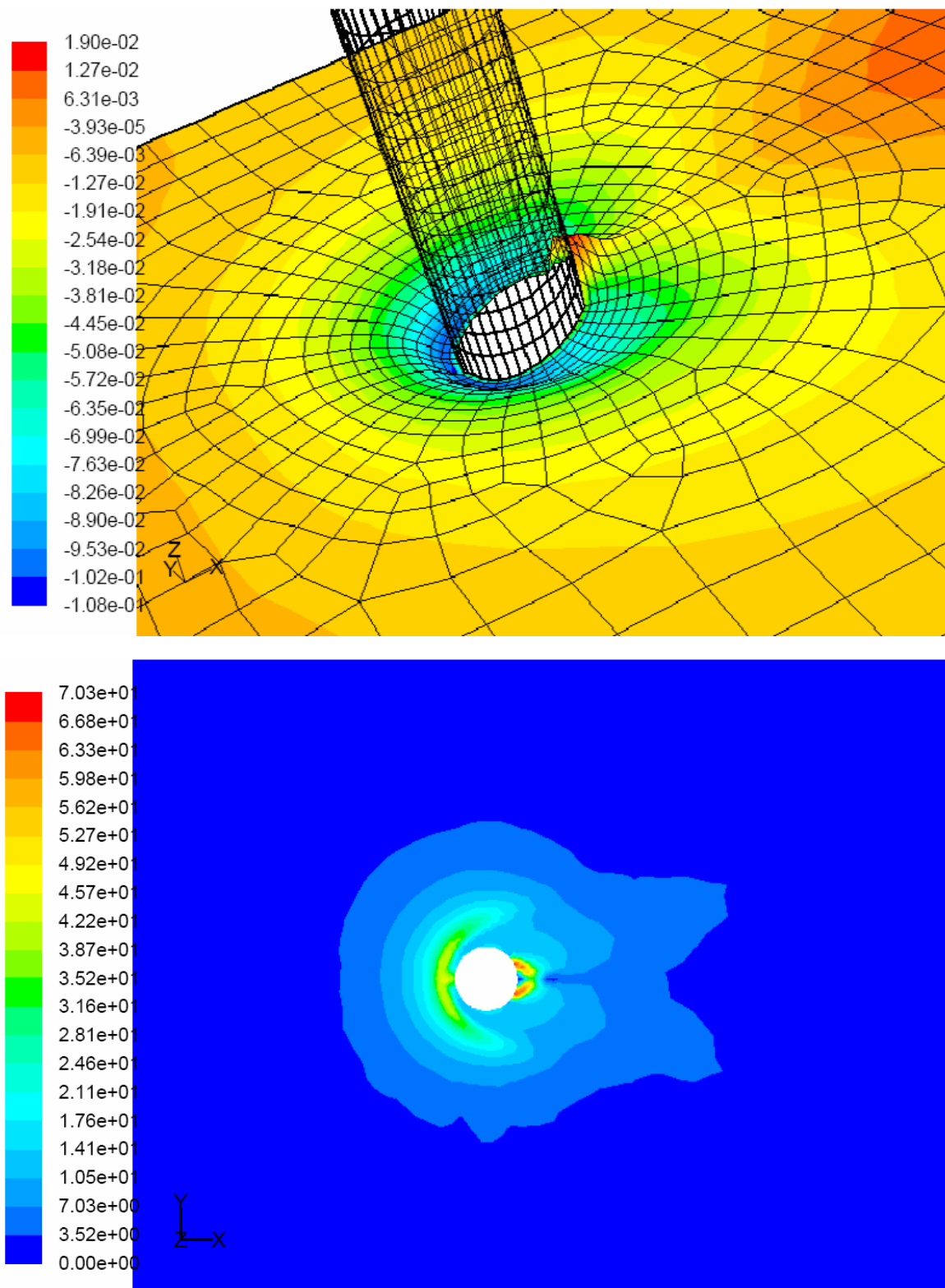


Figure 6 Contour plots of bed level (top) and bed angle (bottom). Prediction of scour for steady current at lab scale using dynamic bed.

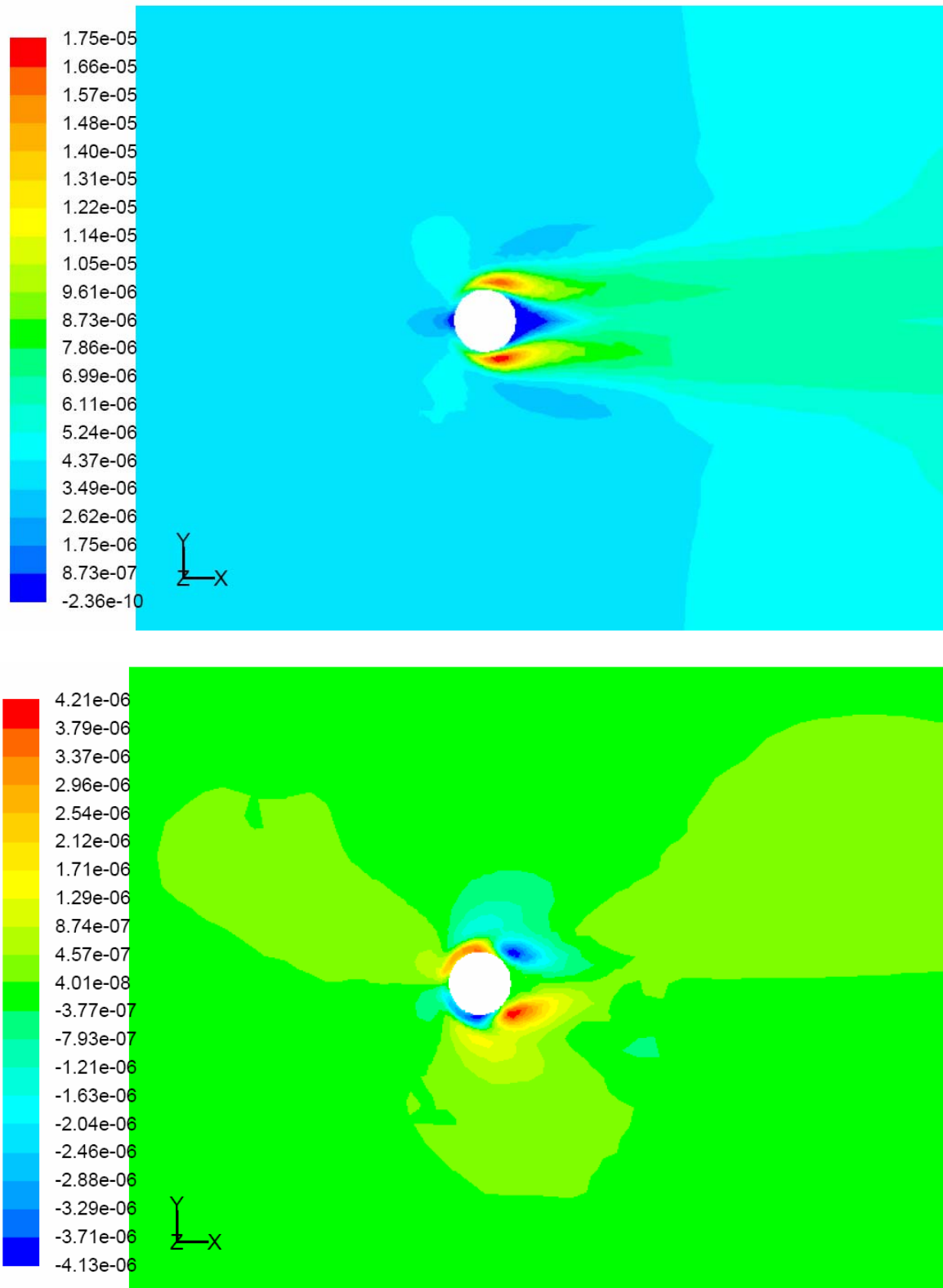


Figure 7 Contour plots of bed-load transport rate in x-direction (top) and y-direction (bottom). Prediction of scour for steady current at lab scale using dynamic bed.

Scour Model for Tidal Current at Lab Scale

A prediction of the scour for tidal current is also performed. The tidal current is simulated by turning the freestream velocity in an existing scour prediction. Figure 8 shows the scour depth S/D as function of time and the bed profile h/D along the centreline in the streamwise direction at the end of the prediction. After 3 hours, the scour depth S/D approaches 0.63, this is somewhat deeper than the corresponding case for steady current.

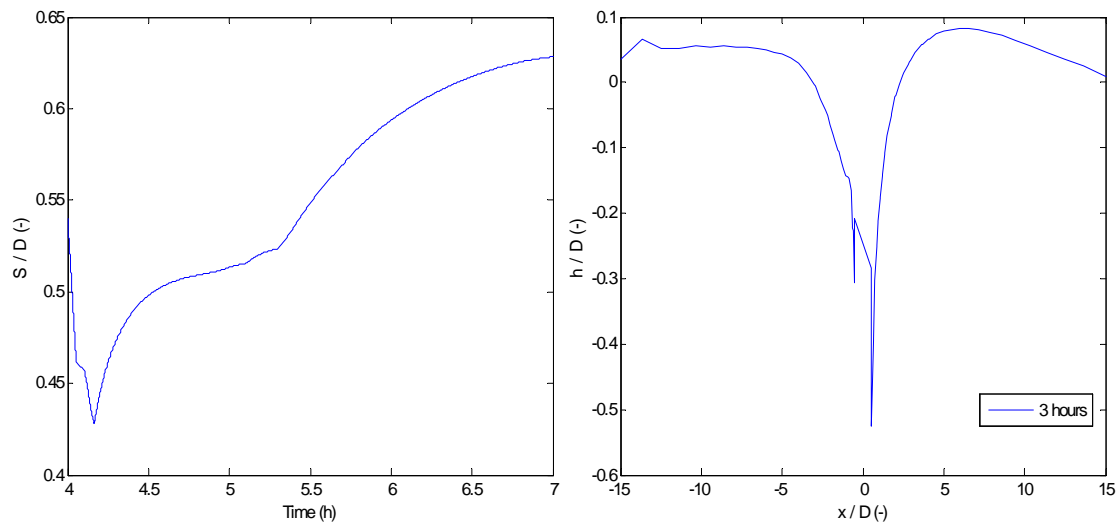


Figure 8 Scour depth as function of time (left) and bed profile along the centreline after 3 hours (right). Prediction of scour for tidal current at lab scale using dynamic bed.

Figures 8 and 9 show contour plots of bed shear stress or Shields number, bed level and the bed load transport rate in x and y-direction. Strangely enough, the model is not capable of filling the old scour hole completely. After 3 hours, two very steep holes are visible close to the pile. They exist even though the bed slope is much greater than angle of repose for the sediment. Continuing the predictions further, they even start to become deeper.

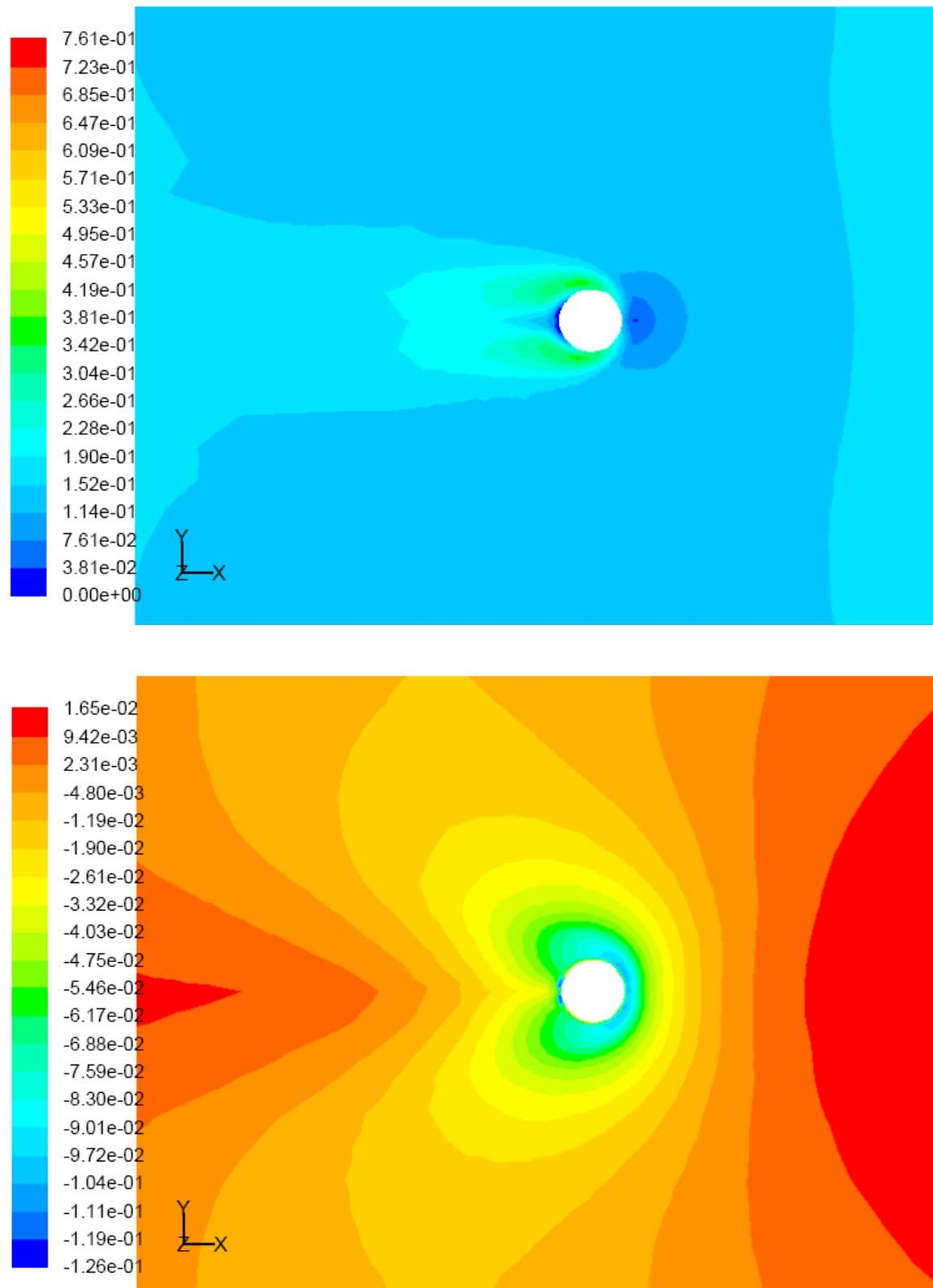


Figure 9 Contour plots of Shields number (top) and bed level (bottom). Prediction of scour for tidal current at lab scale using dynamic bed.

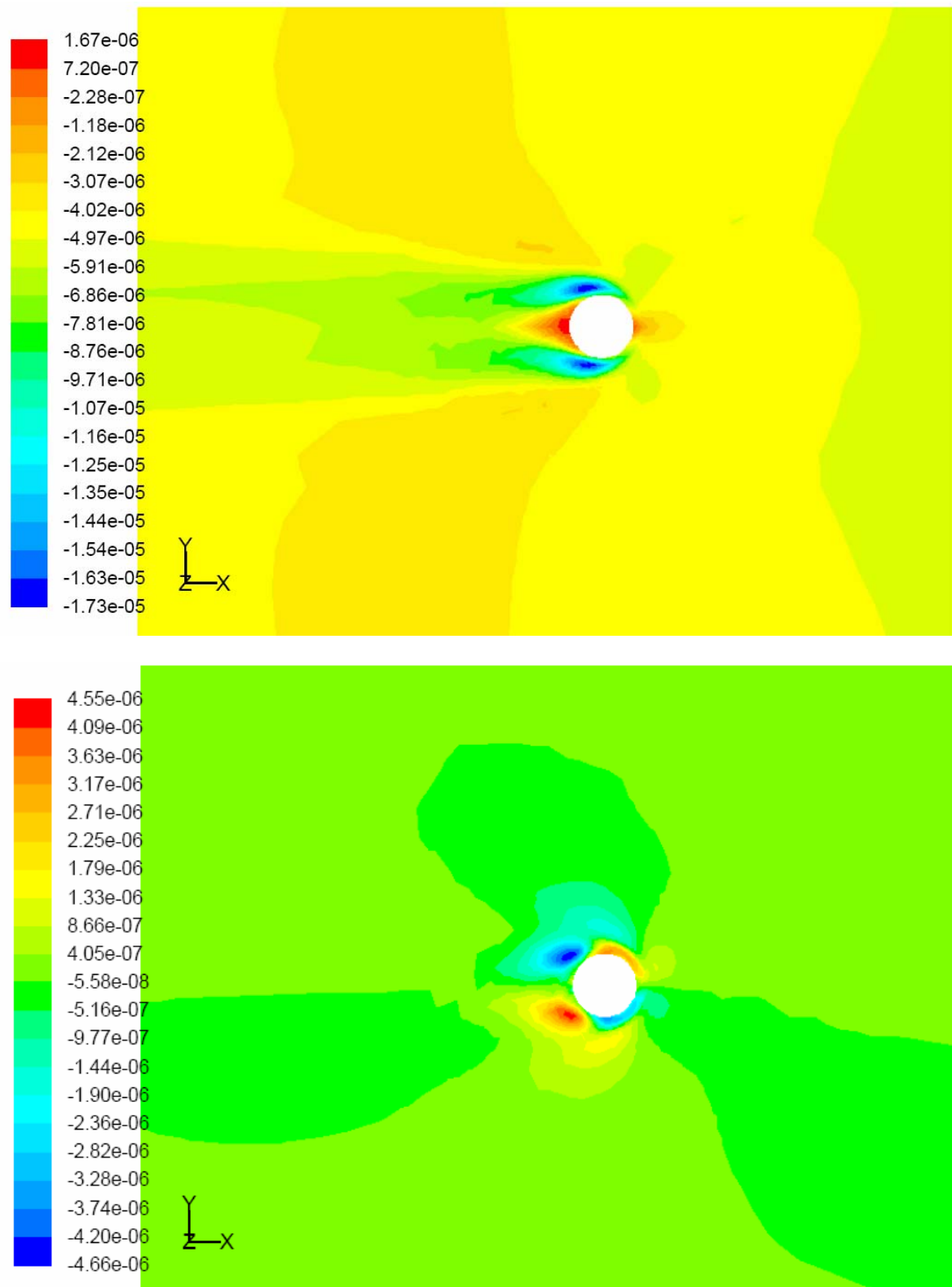


Figure 10 Contour plots of bed-load transport rate in x-direction (top) and y-direction (bottom). Prediction of scour for tidal current at lab scale using dynamic bed.

Scour Model for Steady Current at Full Scale

Finally, the scour for a wind turbine at full scale is calculated. Compared to the previous predictions at lab scale, the pile diameter and the water depth are 30 times larger. The flow conditions are calculated using Froude scaling law. Accordingly, the velocity and the time step are scaled by the square root of the length scale.

Figure 11 shows the scour depth S/D as function of time and the bed profile h/D along the centreline in the streamwise direction at the end of the prediction. After almost 22 hours, the scour depth S/D approaches 0.47 which is comparable with that predicted for the lab scale. Some distance downstream of the pile, there is an accretion that reaches a maximum height h/D of 0.15.

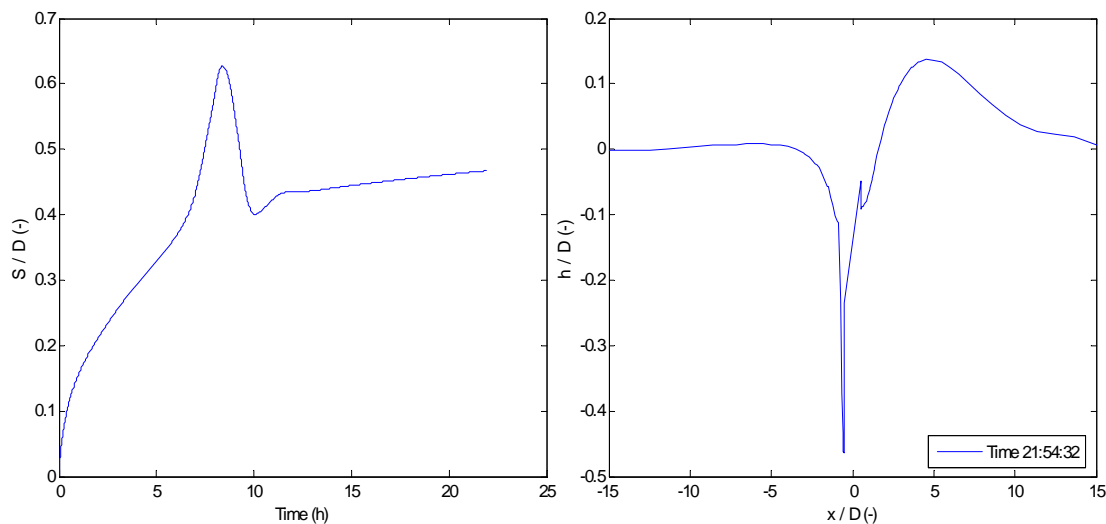


Figure 11 Scour depth as function of time (left) and bed profile along centreline after almost 22 hours. Prediction of scour for steady current at full scale using dynamic bed.

Figure 12 shows contour plot of the bed shear stress or the Shields number and the sea bed level after almost 22 hours. The form of the scour hole is similar to that predicted for the lab scale. Figure 13 shows a three-dimensional view of the scour hole also indicating the use of the dynamic mesh and a contour plot of the bed angle. As can be noticed from the figure, the bed angle tends again to exceed the angle of repose for the sediment. Hence, a sandslide model is probably essential for correct predictions of the shape and the depth of the scour hole even at full scale..

Figure 14 shows the bed load transport rate in x and y-direction.

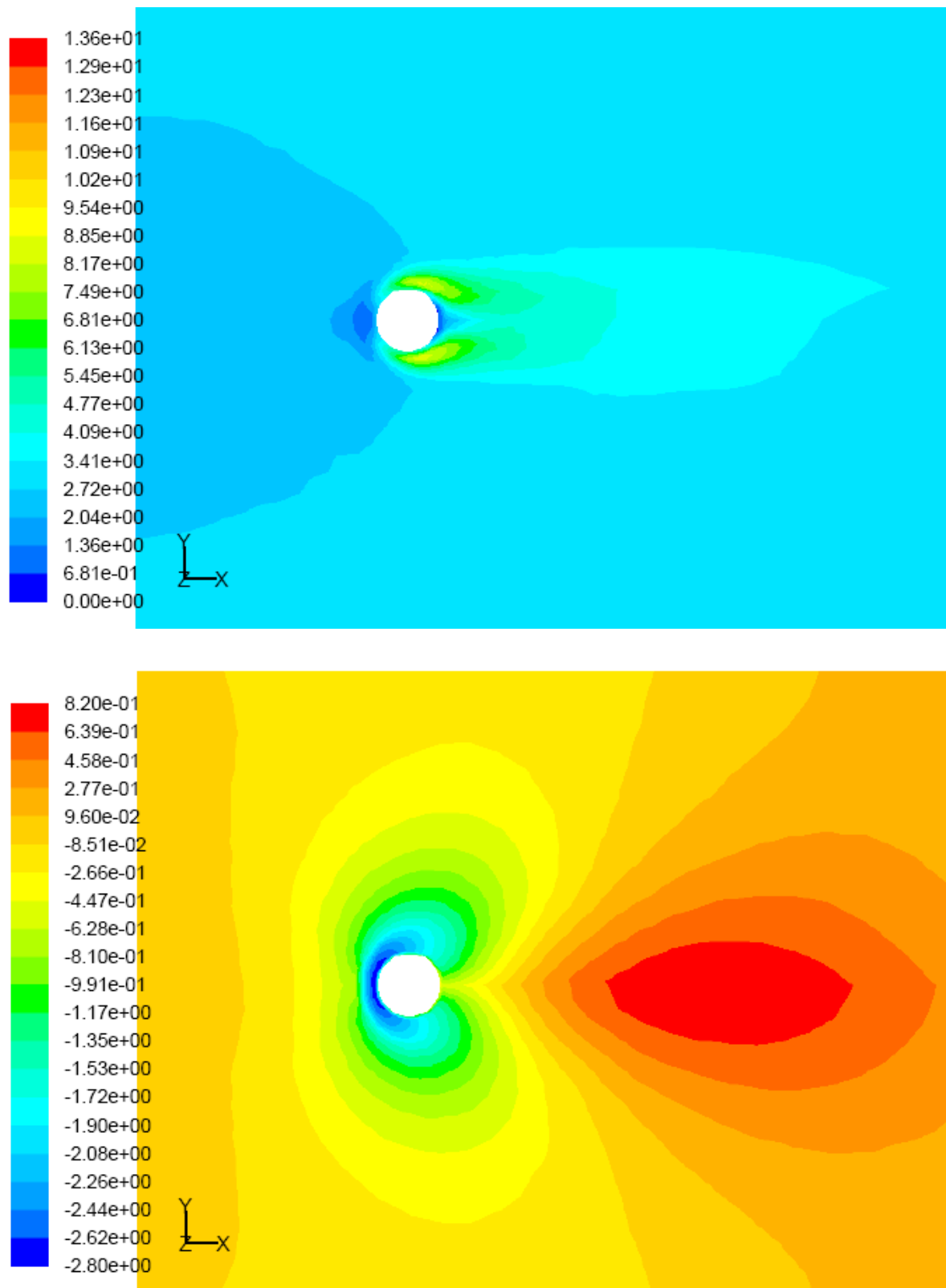


Figure 12 Contour plots of Shields number (top) and bed level (bottom). Prediction of scour for steady current at full scale using dynamic bed.

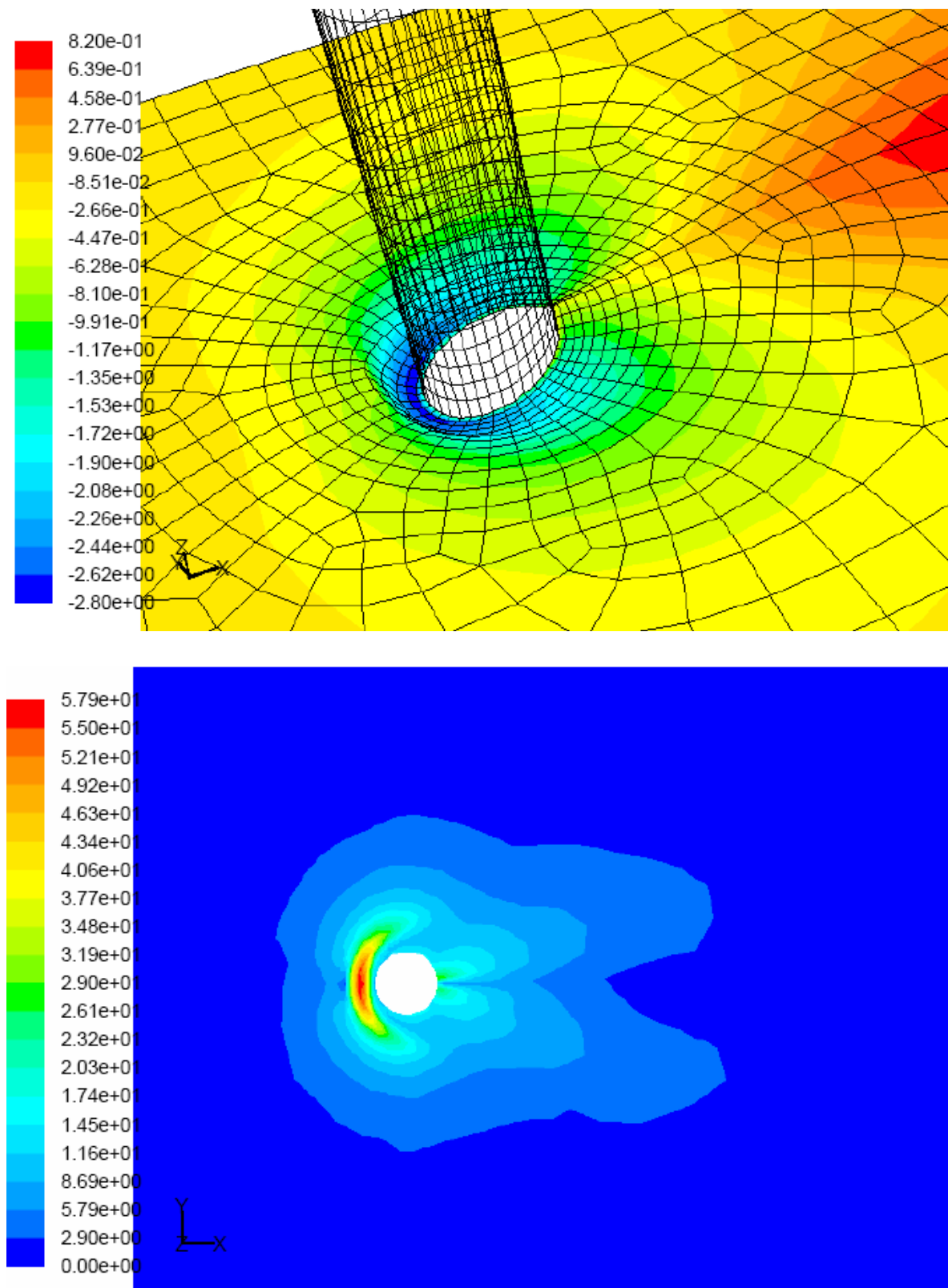


Figure 13 Contour plots of bed level (top) and bed angle (bottom). Prediction of scour for current at full scale using dynamic bed.

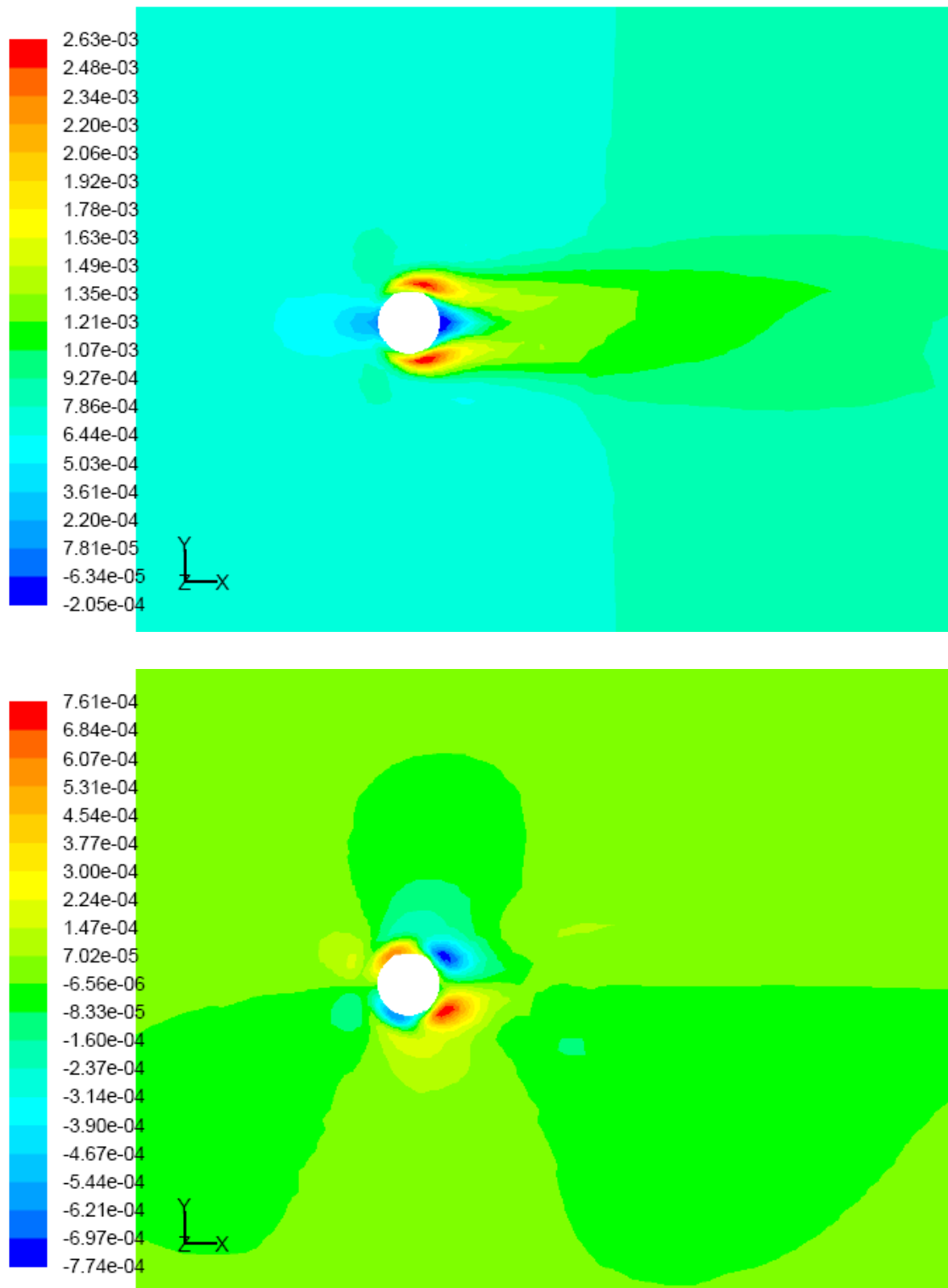


Figure 14 Contours plot of bed-load transport in x-direction (top) and y-direction (bottom). Prediction of scour for current at full scale using dynamic bed.

4. Conclusions

A scour model originally developed for scour beneath marine pipelines have been implemented in FLUENT 6.2 and tested for scour around a pile in steady current. The slope correction term in the bed load transport rate tend to impose a severe time step limitation. For the chosen flow configuration and numerical mesh, the time step required for a stable solution is found to be two orders of magnitude smaller than the time step determined from the usual Courant number criteria. As the time scale for the development of a scour hole is typically hours, such a severe time step limitation appears unphysical.

Although the mesh is refined around the pile, no transient large scale flow structures are observed. All transport equations are solved using second order spatial differencing. A LES rather than a $k-\varepsilon$ turbulence model is probably required to capture the dynamics of the large scale flow structures correctly.

All the predictions presented tend to give scour depths that are significantly smaller than the empirical relation for the equilibrium scour depth $S/D \approx 1.3$ found in the literature. The best agreement is found using a static mesh for the sea bed where there is no direct influence from the scour on the flow. For this case the predicted scour depth $S/D \approx 0.7$.

Contour plots of the bed slope indicate that the scour model allow slopes larger then the angle of repose for the sediment. Hence, a sandslide model seems to be essential to correctly predict the shape and the depth of the scour hole. No attempt is made to implement any of the ad-hoc sandslide models found in the reviewed literature.

In order to resolve the transient large scale flow structures and to get a sound physical modelling of the sediment transport including sandslide, a lattice gas model rather than a CFD model may be a better approach for predictions of scour formation.

5. References

- BRØRS, B. 1999 Numerical modeling of flow and scour at pipelines. *J. Hydr. Eng.*, **125**, 511-523.
- DUPUIS, A. & CHOPARD B. 2002 Lattice gas modeling of scour formation under submarine pipelines. *J. Comp. Phys.*, **178**, 161-174.
- LARSEN, B., J., FRIGAARD, P. & JENSEN, M.S. (2005) Offshore Wind Turbines in Areas with Strong Currents. Hydraulics and Coastal Engineering No. 19, Aalborg University, Denmark.
- LIANG, D., CHENG, L. & LI, F. 2005 Numerical modeling of flow and scour below a pipeline in currents. Part II. Scour simulation. *Coast. Eng.*, **52**, 43-62.
- ROULUND, A. 2000 *Three-dimensional numerical modelling of flow around a bottom-mounted pile and its application to scour*. Ph.D. thesis, Department of Hydrodynamics and Water Resources, Technical University of Denmark.

ROULUND, A., SUMER, B.M., FREDSE, J. & MICHELSEN, J. 2005 Numerical and experimental investigation of flow and scour around a circular pile. *J. Fluid Mech.*, **534**, 251–401.

SUMER, B.M. & FREDSE, J. 2002 *The Mechanics of Scour in the Marine Environment*. World Scientific Publishing.

WHITEHOUSE, R. 1998 *Scour at Marine Structures*. Thomas Telford Publication.

YEN, C., LAI, J.S. & CHANG, W.Y. 2001 Modeling of 3D flow and scouring around circular piers. *Proc. Natl. Sci. Counc. ROC(A)*, **25**, 17-26.

www.offshorecenter.dk



Danish offshore knowledge portal

- Development projects
- Business forums
- Virtual knowledge library
- Education offshore
- Offshore events
- Daily updated offshore news

The website is in Danish
- for English please use
www.offshorebase.dk.

www.offshorebase.dk



OffshoreBase is the new focal point for the Danish offshore companies and institutions! Here you will find potential Danish partners and suppliers whom match the exact qualifications, certifications, etc., which you are looking for.

But more than this, you may also find information about – What is written in the media? – Which conferences and seminars are being held? – Which courses may you attend in Denmark?

Within OffshoreBase.dk you will furthermore get an insight into the many technologically challenging development projects undertaken by the centre on behalf of its members.

Visit www.OffshoreBase.dk



Offshore Center Danmark